

DOCTORAL (PhD) DISSERTATION

GERGŐ LAJOS SOMODY

MOSONMAGYARÓVÁR

2025

SZÉCHENYI ISTVÁN UNIVERSITY
ALBERT KÁZMÉR FACULTY OF AGRICULTURAL AND
FOOD SCIENCES IN MOSONMAGYARÓVÁR
DEPARTMENT OF PLANT SCIENCES
WITTMANN ANTAL MULTIDISCIPLINARY DOCTORAL SCHOOL
OF PLANT, ANIMAL AND FOOD SCIENCES

HABERLANDT GOTTLIEB DOCTORAL PROGRAM FOR PLANT
SCIENCE

DOCTORAL SCHOOL LEADER:
PROF. DR. LÁSZLÓ VARGA DSc

PROGRAM LEADER:
PROF. DR. GYULA PINKA DSc

SUPERVISORS:
PROF. ZOLTÁN MOLNÁR DSc
DR. ERIKA LAKATOS, Associate Professor

**Speed Breeding as a Platform for Rapid Generation Turnover and
Recessive Phenotype Fixation in Cannabis sativa L.**

SUBMITTED BY

GERGŐ LAJOS SOMODY

MOSONMAGYARÓVÁR

2025

Speed Breeding as a Platform for Rapid Generation Turnover and Recessive
Phenotype Fixation in Cannabis sativa L.

Written by

GERGŐ LAJOS SOMODY

Made in the framework of
Széchenyi István University
Albert Kázmér Faculty of Agricultural and Food Sciences in
Mosonmagyaróvár
Wittmann Antal Multidisciplinary Doctoral School of Plant,
Animal and Food Sciences
Haberlandt Gottlieb Programme in Crop Sciences

Supervisor(s):

1. Prof. Zoltán Molnár, Professor

Albert Kázmér Faculty of Agricultural and Food Sciences in
Mosonmagyaróvár

2. Dr. Erika Lakatos, Associate Professor

Albert Kázmér Faculty of Agricultural and Food Sciences in
Mosonmagyaróvár

I recommend for acceptance (yes / no)

(signature)

**The candidate reached% during the Complex (Comprehensive) Exam,
Mosonmagyaróvár,**

.....

Chair of Complex Exam Committee

I recommend the dissertation to be accepted as a reviewer (yes / no):

First reviewer (Dr.) yes / no

(signature)

Second reviewer (Dr.) yes / no

(signature)

Maybe a third reviewer (Dr.) yes / no

(signature)

**The candidate reached% at the dissertation defense and public
debate,**

Mosonmagyaróvár,

Chair of Evaluation Committee

Doctoral (PhD) qualification:

Head of Doctoral Council

CONTENTS

CONTENT OF TABLES	9
CONTENT OF FIGURES	10
ACRONYMS	12
ABSTRACT	15
1. INTRODUCTION.....	16
2. OBJECTIVE OF THE STUDY	18
3. LITERATURE REVIEW.....	20
3.1. Taxonomy of hemp from different perspectives	20
3.2. Specialized bioactive constituents present in hemp	22
3.3. The origin of hemp and the evolutionary history of chemotypes	25
3.4. Milestones in hemp breeding	27
3.5. Contemporary challenges and future prospects in hemp breeding	31
3.6. The inheritance dynamics of morphological and developmental traits in <i>Cannabis sativa</i>	34
3.6.1. Research on hemp stem coloration.....	36
3.7. Accelerated breeding based on short generation time.....	38
3.7.1. History and rationale	38
3.7.2. Environmental factors involved in speed breeding	45
3.7.3. Effects of fertilizers, regulators and growth medium.....	48
3.7.4. Agrotechnical components	51
3.7.5. Embryo culture, genetic approaches, and the application of genetic engineering 53	
3.7.6. Practical application of speed breeding.....	54
3.7.6.1. Hybrid production	55
3.7.6.2. Selection breeding	57
3.7.6.3. Gene introgression.....	59
3.7.6.4. Genetic research	60
3.7.6.5. Biotechnological and plant physiological research.....	61
3.7.7. Prospects and limitations of speed breeding	62

3.7.8.	Speed breeding of hemp	65
4.	MATERIALS AND METHODS	69
4.1.	Characterization of the hemp genotypes used in the studies.....	69
4.2.	Characterization of the greenhouse and protected-cultivation conditions	72
4.2.1.	Morphological parameters recorded in the greenhouse	75
4.2.2.	Meteorological characteristics of the greenhouse cultivation	80
4.3.	Field trials.....	80
4.3.1.	Meteorological characteristics of the field trials	81
4.4.	Cannabinoid analysis.....	83
4.5.	Characterization of the applied breeding workflow	85
4.6.	Statistical analysis	87
5.	RESULTS.....	88
5.1.	Preliminary assessments.....	88
5.1.1.	Cannabinoid analysis for high-throughput measurements.....	88
5.1.2.	Selection of parental cultivars for breeding	89
5.1.3.	Phytopathological assessments	95
5.2.	Results for the early-maturing selection material.....	97
5.2.1.	Morphological evaluation of selection	100
5.3.	Results of the medium strain	107
5.3.1.	Morphological evaluation of selection	109
5.4.	Field Trials	114
5.4.1.	Evaluation of Stem Color Field Assessments	116
5.5.	Evaluation of Additional Distinctive Traits	117
5.6.	Evaluation of Maturity Time and Climatic Data.....	121
5.6.1.	Evaluation of phenological stages and thermal time.....	123
5.7.	Assessment of Harvestable Yield.....	129
5.8.	Evaluation of Thousand-Kernel Weight and Yield.....	130
5.9.	Comparative Evaluation of Cannabinoid Content	132
6.	DISCUSSION	138
6.1.	Integrating speed breeding into cannabis crossing.....	138

6.2.	Stabilization of the yellow-stem trait	139
6.3.	Development of phenotyping methods	140
6.4.	Cannabinoid profiling	140
6.5.	Natural versus accelerated maturation	141
6.6.	Limitations and challenges	142
6.7.	Industrial and agronomic implications	142
6.8.	Future directions.....	142
7.	CONCLUSION	144
8.	NOVEL SCIENTIFIC RESULTS OF DOCTORAL RESEARCH.....	146
9.	PUBLICATIONS	148
10.	CONFERENCE PRESENTATION AND PARTICIPATION	149
11.	ACKNOWLEDGEMENTS	150
12.	REFERENCES.....	151

CONTENT OF TABLES

Table 1. Taxonomic division of the genus Cannabis according to various sources (according to Clarke and Merlin, 2016)	22
Table 2. The varieties involved in the breeding process.	69
Table 3. Greenhouse fertilization program	75
Table 4. List of main characteristics according to CPVO methodology.....	76
Table 5. The main characteristics and examples according to CPVO	77
Table 6. The characteristics of hemp seed based on CPVO methodology.	78
Table 7. The dataframe used in the breeding process	79
Table 8. Main meteorological parameters during the last greenhouse cycles in case of early selection.....	80
Table 9. Main meteorological parameters during the last greenhouse cycles in case of medium selection.....	80
Table 10. Cannabinoid analyses performed to assess the reliability of TLC method	88
Table 11. Preliminary examination of varietal CBD and THC content	92
Table 12. Stem color observations in case of the early strain	98
Table 13. Results of the repeated stem color observation.....	99
Table 14. Chi-square test for segregation.....	100
Table 15. Stem color observations in case of the medium strain.....	109
Table 16. Comparison of VARI indices and manual observations	117
Table 17. Comparison of measured SPAD value and VARI index in case of leaf greenness	119
18. Table. Accumulated GDD and length of the main phases of Cycle-4, -5, and -6 of the speed breeding process.....	122
Table 19. Accumulated Growing Degree Day (GDD) values and key phenological observations from open-field trials in 2022 and 2023	128
Table 20. Cannabinoid analysis results in case of the cycle comparison trial. Cannabinoid content is interpreted as m/m%	133

CONTENT OF FIGURES

Figure 1. The scheme for accelerated hemp cultivation.....	73
Figure 2. Picture of the installed greenhouse	73
Figure 3. Greenhouse floor plan with LED light fixtures location	74
Figure 4. Barcoded plant for accurate data entry	78
Figure 5. The average monthly temperature and precipitation during the trial periods.....	82
Figure 6. Daylength, GDD and phenological observations in case of the open-field trials.....	83
Figure 7. TLC plates used for quick and cheap cannabinoid analysis	84
Figure 8. Well developed stigmas due to shifted, directed pollination	86
Figure 9. Illustration of rapid biomass growth.....	87
Figure 10. The total CBD m/m% of the monoecious varieties in case of the first greenhouse trial	90
Figure 11. The total CBD m/m% of the dioecious varieties in case of the first greenhouse trial	90
Figure 12. The total THC m/m% of the monoecious varieties in case of the first greenhouse trial	91
Figure 13. The total THC m/m% of the dioecious varieties in case of the first greenhouse trial	91
Figure 14. The total CBD m/m% of the progenies from the first controlled crosses and standard varieties	93
Figure 15. The total THC m/m% of the progenies from the first controlled crosses and standard varieties	94
Figure 16. Leaf morphological differences in case of Chamaeleon (left) and Eletta campana (right).....	95
Figure 17. The increasing severity of Botrytis bud rot observed in our breeding material.....	96
Figure 18. Relationship between flower density and grey mold severity scores (Punja and Ni, 2021). Marked with same letter do not significantly differ (P=.05, SNK)	96
Figure 19. Pollination with mixed pollen from selected male plants.....	97
Figure 20. Segregation of stem color in case of early selection.....	99
Figure 21. PCA biplot of the harvested plants from Cycle-4.....	101
Figure 22. PCA biplot with reduced parameters from Cycle-4.....	101
Figure 23. PCA biplot with reduced parameters from Cycle-5.....	102
Figure 24. Multivariate structure across motherplants (PCA biplot) in case of Cycle-6.....	103

Figure 25. Cycle-6 PCA of morphological and seed traits	103
Figure 26. Cycle-7 observations on PCA biplot	104
Figure 27. Motherplant of the early (B) selection	106
Figure 28. The entirely yellow-stemmed medium strain	108
Figure 29. The distribution of observations based on motherplants on PCA biplot in case of Cycle-4	110
Figure 30. Cycle-4 PCA biplot focusing only on stem color and yield data.....	111
Figure 31. Cycle-5 PCA Biplot of standardized morphological and seed traits by motherplant	111
Figure 32. Ordination of progeny trait profiles (PCA; SE-centroids by motherplant)	112
Figure 33. Cycle-7 observations visualized on PCA biplot	113
Figure 34. Cycle-8 lineage differentiation in breeding traits: PCA by motherplant	114
Figure 35. Small plot trial in case of early strain for seed multiplication in 2023.	115
Figure 36. VARI index of the open-field trial in 2023.....	116
Figure 37. Aerial image of the dense row cultural test in 2023	118
Figure 38. Correlation between VARI index and measured SPAD values.....	120
Figure 39. The generated 3D model from the aerial images	120
Figure 40. Correlation between predicted and measured plant heights	121
Figure 41. Homogenous, well developed vegetation after acclimatization	123
Figure 42. Air temperature, accumulated GDD, observed phenological stages and light control in case of early (B) strain	124
Figure 43. Air temperature, accumulated GDD, phenological observation and light control in case of the medium (E) selection	126
Figure 44. The number of seeds from individual plants in case of both selections	129
Figure 45. TKW changes across accelerated generation cycles.....	130
Figure 46. Open-field TKW observations in two growing season.....	131
Figure 47. Seed yield and germination capacity	132
Figure 48. Total CBD content comparison from the 2023 open-field trial.....	134
Figure 49. Open-field confirmation of the trend in case of Total CBD (m/m%) content	135
Figure 50. Total THC content compariosn from the 2023 open field trial	136
Figure 51. CBD and THC content during the variety registration process (Hungarian Food Safety Authority- NéBiH, 2024)	136
Figure 52. Counted CBD/THC ratio in case of the variety registration trials (NéBiH, 2024)137	

ACRONYMS

Acronym Meaning

SB	Speed Breeding
PhD	Doctor of Philosophy
DSC	Doctor of Science (a higher doctoral degree in some systems)
NLH	Narrow-Leaf Hemp
BLH	Broad-Leaf Hemp
NLD	Narrow-Leaf Drug (type)
BLD	Broad-Leaf Drug (type)
OLA	Olivetolic Acid
MEP	Methyl-D-erythritol-4-phosphate (pathway)
GPP	Geranyl Diphosphate
THCA	Δ 9-Tetrahydrocannabinolic Acid
CBDA	Cannabidiolic Acid
CBNA	Cannabinolic Acid
CBGA	Cannabigerolic Acid
CBCA	Cannabichromenic Acid
CBNDA	Cannabinodiolic Acid
THC	Δ 9-Tetrahydrocannabinol
CBD	Cannabidiol
CBC	Cannabichromene
CBN	Cannabinol
THCVA	Tetrahydrocannabivarinic Acid
CBG	Cannabigerol
GS	Genomic Selection
MAS	Marker-Assisted Selection

SSD	Single-Seed Descent
RGA	Rapid Generation Advance
PPFD	Photosynthetic Photon Flux Density
CO ₂	Carbon Dioxide
PGR	Plant Growth Regulator
DH	Doubled-Haploid
GWAS	Genome-Wide Association Study
QTL	Quantitative Trait Locus
FT	FLOWERING LOCUS T
STS	Silver Thiosulfate
RH	Relative Humidity
HPS	High-Pressure Sodium (lamp)
CPVO	Community Plant Variety Office (EU)
DUS	Distinctness, Uniformity, and Stability (testing)
TKW	Thousand-Kernel Weight
GDD	Growing Degree Day
VARI	Visible Atmospherically Resistant Index
UAV	Unmanned Aerial Vehicle
DSM	Digital Surface Model
DTM	Digital Terrain Model
SPAD	Soil-Plant Analysis Development (meter, used for leaf greenness/chlorophyll)
HPLC	High-Performance Liquid Chromatography
TLC	Thin-Layer Chromatography
SNK	Student–Newman–Keuls (post-hoc test)
PCA	Principal Component Analysis
MABC	Marker-Assisted Backcrossing

NGS	Next-Generation Sequencing
SNP	Single-Nucleotide Polymorphism
GEBV	Genomically Estimated Breeding Value
FHB	Fusarium Head Blight
AFLP	Amplified Fragment Length Polymorphism
SSR	Simple Sequence Repeat
MADC	Male-Associated DNA sequence in Cannabis (gene marker)
HLVd	Hop Latent Viroid
NIL	Near-Isogenic Line
KASP	Kompetitive Allele-Specific PCR
FISH	Fluorescence In Situ Hybridization

ABSTRACT

The development of new, adapted crop cultivars faces considerable constraints due to lengthy generation times and environmental unpredictability. This doctoral research addresses these challenges in industrial hemp (*Cannabis sativa* L.) by establishing and validating a Speed Breeding (SB) platform for rapid generation turnover and targeted genetic improvement. Hemp, a photoperiod-sensitive, dioecious species, traditionally permits only one breeding cycle per year. Using controlled environments, including light-emitting diode (LED) lighting and precise photoperiod manipulation, the established SB platform successfully compressed the seed-to-seed cycle to approximately 90 days, allowing for up to eight generations across two calendar years.

The research focused on the targeted introgression and fixation of the yellow-stem phenotype, a monogenic recessive trait associated with improved fiber quality, into genetically diverse, high-cannabidiol (CBD) founder lines exhibiting highly disparate flowering times. This was achieved through serial backcrossing and family selection within the accelerated cycles, leading to the complete fixation of the yellow-stem trait by the fifth generation. Furthermore, the selection scheme enforced a consistent reduction of Δ^9 -tetrahydrocannabinol (THC) content, ensuring compliance with legal thresholds (<0.2%), while maintaining or improving harvestable seed yield and Thousand-Kernel Weight (TKW) across cycles. The study also integrated novel high-throughput phenotyping methods, including the Visible Atmospherically Resistant Index (VARI) derived from unmanned aerial vehicle (UAV) imagery, demonstrating the efficacy of modern phenomic tools in rapid selection environments. This work confirms SB's feasibility and profound utility in accelerating the breeding pipeline for dioecious, photoperiod-sensitive crops, offering a scalable pathway to develop stable, high-value hemp varieties for industrial and pharmaceutical applications.

1. INTRODUCTION

The challenge of securing global food and industrial raw material supply under rapidly changing climatic conditions necessitates accelerated crop improvement. Traditional plant breeding, which relies on multi-year field cycles to stabilize traits, often cannot respond quickly enough to emerging market needs or environmental pressures. This time constraint is particularly acute in crops with long or photoperiod-dependent reproductive cycles, such as industrial hemp (*Cannabis sativa* L.). Hemp is an economically significant multi-purpose crop, providing fiber for textiles and construction, grain for food and oil, and specialized secondary metabolites, primarily cannabinoids like cannabidiol (CBD) and Δ^9 tetrahydrocannabinol (THC). The utility of hemp cultivars is fundamentally dictated by strict legal regulations, such as the maximum permissible THC content, which places a high premium on rapid and precise genetic manipulation.

The plant's natural reproductive biology—as a typically dioecious (separate male and female plants) and short-day species—imposes inherent bottlenecks on breeding efficiency. In temperate zones, *C. sativa* typically initiates flowering only as daylength shortens, limiting outdoor breeding to a single generation per year. This prolonged cycle hampers the necessary inbreeding to stabilize desirable quantitative traits (e.g., yield, cannabinoid profile) and qualitative traits (e.g., stem color, disease resistance).

Speed Breeding (SB) is a modern methodology that uses controlled environments, often employing optimized lighting spectra, extended photoperiods, and regulated temperature, to drastically shorten the generation time of crops. While initially proven effective in long-day cereal crops like wheat and barley, its adaptation to photoperiod-sensitive, short-day species like hemp represents a significant, yet less explored, area of research. Successful deployment of SB in hemp could condense years of traditional breeding work into a single calendar year, thereby greatly accelerating the development and registration of new, compliant cultivars.

This doctoral research was initiated to validate the application of SB as a foundational platform for industrial hemp breeding and to demonstrate its power in achieving specific genetic goals. The work focused on the successful introgression and fixation of the yellow-stem phenotype, a monogenic recessive trait. Yellow-stemmed cultivars, such as the progenitor 'Chamaeleon', are highly valued for their superior fiber processing characteristics, including a higher proportion of finer bast fibers. Achieving a homozygous state for this recessive trait across multiple generations while managing the complexity of crossing parents with divergent

flowering times ('Balaton', 'Eletta Campana', and 'Chamaeleon') demanded the precise control offered by the SB environment.

Furthermore, a critical objective was to combine this desirable morphological trait with an optimized chemical profile: high CBD concentration and non-detectable or extremely low THC content to meet regulatory requirements. The inherent challenge of maintaining seed yield and quality under the compressed physiological constraints of accelerated growth was also investigated. Finally, the research explored how modern phenotyping technologies, such as drone-based imagery, could be integrated into this rapid cycle to ensure efficient and objective selection.

The following dissertation documents the implementation, execution, and outcomes of a multi-cycle SB program, detailing the progress made in stabilizing a novel, yellow-stemmed, high-CBD, low-THC industrial hemp line, thereby providing a robust methodology for future genetic gain in *Cannabis sativa* L.

2. OBJECTIVE OF THE STUDY

The primary objective of this doctoral research was to innovate the breeding process for industrial hemp (*Cannabis sativa* L.) by integrating Speed Breeding (SB) technology with targeted genetic selection. This work aimed to establish a high-throughput platform capable of accelerating generation turnover and efficiently fixing multiple recessive traits, while simultaneously ensuring compliance with stringent regulatory standards.

Research Questions

1. Feasibility of Generation Acceleration: Can an integrated Speed Breeding (SB) protocol effectively shorten the life cycle of photoperiod-sensitive, dioecious *Cannabis sativa* lines—specifically those with highly divergent flowering times—to achieve and sustain a generation turnover of multiple cycles per year?
2. Trait Fixation and Inheritance: What is the most efficient breeding pathway (backcrossing vs. accelerated inbreeding) under SB conditions to fix the desirable recessive yellow-stem phenotype while simultaneously managing linked or associated undesirable traits, such as initial low seed yield and potential chemotype instability?
3. Phenotype-to-Chemotype Selection Efficacy: Can high-throughput, low-cost analytical methodologies (TLC) be reliably integrated into the accelerated breeding cycle for immediate selection and culling of plants to maintain strict compliance with low-THC regulatory limits without critically compromising the concurrent selection for high CBD content and yield-related traits?
4. Environmental Predictability and Yield Stability: How do the highly controlled, supra-optimal thermal and photoperiod conditions imposed by the SB environment affect the subsequent field performance (maturity time, plant height, seed yield) of the

advanced, fixed lines, and can a reliable method for phenological and morphological extrapolation be established?

Research Hypotheses

1. The application of a precisely controlled SB environment, utilizing customized photoperiod and thermal cycling, will significantly reduce the generation time of photoperiod-sensitive *Cannabis sativa* to achieve a minimum of four, and potentially up to six, generations annually, irrespective of the parental line maturity class.
2. The recessive yellow-stem phenotype can be stabilized and fixed in a homozygous state within 5 generations using a progeny-tested backcrossing strategy under SB conditions, successfully introgressing the trait from an early-maturing donor into diverse backgrounds without long-term genetic loss of vegetative vigor.
3. Rigorous selection based on high-throughput TLC screening for low-THC content will be sufficient to secure regulatory compliance in advanced lines, leading to populations where the CBD concentration stabilizes at a level significantly higher than the non-selected parental averages.
4. Advanced lines selected for compact architecture and high seed count under the high-density SB environment will demonstrate comparable or superior seed yield and Thousand-Kernel Weight (TKW) stability when subsequently validated in open-field conditions compared to their conventional parent cultivars.

3. LITERATURE REVIEW

3.1. Taxonomy of hemp from different perspectives

Hemp (*Cannabis sativa* L.) is among our earliest domesticated agricultural crops, used for recreational, medicinal, and industrial purposes (Kovalchuk et al. 2020). Its extractable fibers provide raw material for the textile and construction industries; the seed yield is rich in unsaturated fatty acids and is a valuable oil source; and the cannabinoids extracted from the inflorescence serve both recreational and medicinal purposes (Robert and Mark, 2020; Chandra et al., 2017; Small, 2017).

The genus *Cannabis* is taxonomically a member of the family *Cannabaceae*, which belongs to the order Rosales. Von Linne (1753) mentions the species *Cannabis sativa* in *Species Plantarum* as a tall, fibrous plant. Lamarck originally described the separation of two interfertile species, the Persian-origin *C. sativa* and the Indian *C. indica* (Lamarck, 1804).

De Candolle (1867) took a special approach and divided the single species *C. sativa* into four groups. The α Kif group comprised strongly psychoactive southern hemp; β *Vulgaris* denoted intermediate plants bearing characteristics of the other groups; and γ *Pedemontana* and δ *Chinensis* included northern variants suitable for fiber production.

Small and Cronquist (1976) referred to the subspecies *C. sativa subsp. sativa* and *C. sativa subsp. indica*. Since then, the taxonomic subdivision of the genus *Cannabis* has continued to vary by source. Examining plants from different geographic origins, Hillig (2005) distinguished the species *Cannabis sativa*, *Cannabis indica*, and *Cannabis ruderalis*.

Building largely on Hillig's (2005) chemotaxonomic research, Clarke and Merlin (2016) assembled a nomenclature from a geographical and cultural perspective that highlights the role of distinct gene pools in the history of hemp cultivation and selection. They identified five biotype groups. The narrow-leaf hemp (NLH), broad-leaf hemp (BLH), narrow-leaf drug (NLD), broad-leaf drug (BLD), and hybrids of narrow- and broad-leaf drug types (NLD/BLD) together encompass the four naturally occurring *Cannabis* landraces, as well as artificially produced seedless populations—the Spanish term “sin semilla” (seedless) is commonly used in the literature. It refers to the omission of pollination of female individuals (male plants are removed, or only pistillate individuals are sown), so the inflorescences ripen unfertilized, the bracts become fleshy, and cannabinoid content is many times higher than in seed-setting plants.

From the perspective of practical plant breeding, however, it is not advisable to speak of separate species. Even so, an important distinction in Hillig (2005) is the mention of East Asian NLH as *Cannabis sativa ssp. chinensis*, and European NLH as *Cannabis sativa ssp. sativa*. Heterosis, arising from a high degree of genetic divergence between parental lines, is an extremely important factor in developing industrial hemp cultivars. A single-species classification based on cannabinoid and terpenoid profiles has also been proposed (Hazekamp et al. 2016).

The genus *Cannabis* can also be divided into geographic races. Szerebrjakov mentions five races. Northern hemp (*prol. borealis*) comprises short, very early cultivars from northern Russia and Finland. The cultivation area of the Central Russian group (*prol. medioruthenica*)—Russia, Ukraine, Belarus, Germany, and Poland—is characterized by long days and cool, rainy weather. In this race, a medium vegetation period and plant height are observed, with slight branching and individuals of moderate size and leaflet number (5–9). Their stem yield is generally 5–8 t/ha, and their fibers are typically poor to medium and coarse. Male plants generally require 70–80 days to reach flowering, whereas female plants flower in 105–110 days. These cultivars have good seed-producing capacity, as natural selection and the short growing season have rendered them more generative; certain Ukrainian, French, and Polish cultivars belong here. Southern cultivars that also mature in the north are considered transitional types. These cultivars are without exception monoecious or so-called “hybrid populations.” They require 85–95 days to flower, and 115–130 days for the female plants to reach maturity. Their stem yield is 7–9 t/ha, fiber content is medium, and seed productivity is good to very good. Mediterranean hemp (*prol. australis*) is a long-season group reaching 3–4.5 m in height; seed production is feasible south of 50° N, while farther north it can only be utilized as fiber hemp. Cultivars in the southern group have the highest stem yields (12–14 t/ha) and are also the latest to reach technical maturity. These cultivars do not fully ripen north of 48–50° N. They generally have higher fiber content and finer fibers. Most cultivars in this group are dioecious. For fiber use, the vegetation period is typically measured by the timing of 50% male flowering, because technical maturity occurs then. From germination to mid male flowering, roughly 105–115 days are counted. Around 48° N, male flowering occurs in mid to late July, or possibly early August; north of 50° N, male plants flower in mid to late August. Seed productivity is generally moderate or poor, since half of the stand consists of male plants, which bear no seed. Seed production to full ripeness requires 140–170 days. East Asian hemp (*prol. asiatica*) is characterized by a short,

branching-prone stem. The leaves are large, consisting of 9–13 leaflets. They have a long vegetation period (Bócsa, 2004).

The various taxonomic classifications are summarized in Table 1.

Table 1. Taxonomic division of the genus *Cannabis* according to various sources (according to Clarke and Merlin, 2016)

Small and Cronquist (1976)	Hillig (2004)	McPartland and Guy (2004)	Clarke and Merlin (2013)	Origin	Utilization
Cultivated hemp					
<i>C. sativa</i> ssp. <i>sativa</i> var. <i>sativa</i>	<i>C. sativa</i> kender biotípus	<i>C. sativa</i> ssp. <i>sativa</i>	<i>C. sativa</i> ssp. <i>sativa</i> NLH	Europe	Fiber and seed
	<i>C. indica</i> kender biotípus	<i>C. indica</i> ssp. <i>chinensis</i>	<i>C. indica</i> ssp. <i>chinensis</i> BLH	East-Asia	Fiber and seed
<i>C. sativa</i> ssp. <i>indica</i> var. <i>indica</i>	<i>C. indica</i> NLD	<i>C. indica</i> ssp. <i>indica</i>	<i>C. sativa</i> ssp. <i>indica</i> NLD	South-Asia	Drug
	<i>C. indica</i> BLD	<i>C. sativa</i> ssp. <i>afghanica</i>	<i>C. sativa</i> ssp. <i>afghanica</i> BLD	Middle-Asia	Drug
Wild hemp					
<i>C. sativa</i> ssp. <i>sativa</i> var. <i>spontanea</i>	<i>C. sativa</i> vad változat	<i>C. sativa</i> ssp. <i>spontanea</i> + <i>C. ruderalis</i>	<i>C. sativa</i> ssp. <i>spontanea</i> + <i>C. ruderalis</i> NLHA	Europea	Feral fiber and seed
<i>C. sativa</i> ssp. <i>indica</i> var. <i>kafiristanica</i>	<i>C. ruderalis</i> + <i>C. indica</i> wild	<i>C. indica</i> ssp. <i>kafiristanica</i>	<i>C. indica</i> ssp. <i>kafiristanica</i> NLDA	South-Asia	Feral drug

3.2. Specialized bioactive constituents present in hemp

A distinctive property of hemp is the production of cannabinoids as secondary metabolites. In addition to cannabinoids, terpenes and phenolic compounds are also synthesized (Flores-Sanchez and Verpoorte, 2008). The number of cannabinoids reported in the literature exceeds 90, although some of these are degradation products ((Elsohly és Slade, 2005; Brenneisen,

2007; Radwan et al., 2009; Fishedick et al., 2010).) The most abundant cannabinoids are tetrahydrocannabinolic acid (THCA), cannabidiolic acid (CBDA), cannabinolic acid (CBNA), cannabigerolic acid (CBGA), cannabichromenic acid (CBCA), and cannabinodiolic acid (CBNDA) (Elsohly and Slade, 2005). THCA is the defining phytocannabinoid of drug-type hemp, whereas fiber-type, industrial hemp predominantly contains CBDA; CBCA is characteristic of young plants and its amount declines during maturation (de Meijer et al., 2009). The pharmacologically inactive acidic forms convert to their neutral forms via a non-enzymatic process (decarboxylation); this may already occur in the plant during ripening, or after harvest under heating (Flores-Sanches and Verpoorte, 2008). The principal sites of phytocannabinoid accumulation are the secretory cavities of glandular trichomes, which are most numerous in the inflorescences. Smaller amounts can also be detected in seeds (S. Ross et al., 2000), the root system (Stout et al., 2012), or pollen (Ross et al., 2005). Leaf cannabinoid content likewise decreases over maturation, with the highest levels found in the upper foliage (Pacifico et al., 2007). However, the levels of these compounds are strongly influenced by tissue type, age, cultivar, cultivation conditions, harvest timing, and storage method (Khan et al., 2014).

The precursors required for cannabinoid biosynthesis arise via two distinct routes. The polyketide pathway yields olivetolic acid (OLA), while the 2-C-methyl-D-erythritol-4-phosphate (MEP) pathway leads to the synthesis of geranyl diphosphate (GPP) (Sirikantaramas et al., 2005)). Geranylpyrophosphate:olivetolate geranyltransferase catalyzes the alkylation of OLA and GPP, which produces CBGA (Fellermeier and Zenk, 1998). THCA synthase, CBDA synthase, and CBCA synthase—oxidocyclase enzymes—then generate the three most common cannabinoids (Sirikantaramas et al., 2004).

Propyl cannabinoids (bearing a C3 propyl side chain instead of the C5 pentyl side chain described above), such as tetrahydrocannabivarinic acid (THCVA), are synthesized via a different route, from divarinolic acid (Flores-Sanchez and Verpoorte, 2008).

These compounds act primarily on the animal endocannabinoid system, whose main components are the CB1 and CB2 cannabinoid receptors and their endogenous ligands (anandamide and 2-arachidonoylglycerol), which are responsible for numerous physiological processes, including appetite, pain, inflammation, insulin sensitivity, fat and energy homeostasis, mood, and memory (Petrocellis et al., 2011; Piscitelli et al., 2015). The decarboxylated THC molecule, which mimics anandamide, has higher affinity for the CB1 receptor and thus produces psychoactive effects; it is also known to have anti-inflammatory, analgesic, muscle-relaxant, and anticancer roles (Petrocellis et al., 2011). By contrast,

decarboxylated CBD has markedly different pharmacological actions: among other effects, it mitigates THC's adverse effects (anxiety, immunosuppression) and has demonstrated anxiolytic, antiemetic, anti-arthritic, anti-inflammatory, and immunomodulatory activities, with good therapeutic potential in epilepsy, multiple sclerosis, schizophrenia, various neurodegenerative diseases, and appetite regulation (Burstein, 2015; Englund et al., 2012; Hill et al., 2012). CBD is also a highly promising antibacterial and antifungal compound (Appendino et al., 2008). The third most abundantly detected cannabinoid is CBC, which exhibits anti-inflammatory, sedative, analgesic, and antibacterial effects ((DeLong et al., 2010; Davis and Hatoum., 1983; Eisohly et al., 1982). CBN is a degradation product of THC; it has a much lower affinity for CB1 receptors and therefore exerts its effects not on the central nervous system but on immune system cells (McPartland and Russo, 2001).

Considering the adverse effects of cannabinoids, it can be stated that THC content correlates with short- and long-term risks. Memory impairment, reduced cognitive performance, the development of dependence, and chronic psychoses—e.g., schizophrenia—are all conditions associated with THC content, whereas CBD ameliorates these negative effects (Volkow et al., 2014; van Amsterdam et al., 2015; Iseger and Bossong, 2015).

Beyond cannabinoids, more than 100 terpenes have been identified in hemp that are responsible for aroma and flavor (Rothschild et al., 2005; Brenneisen, 2007). Monoterpenes are the defining elements of the volatile fraction; these include D-limonene, β -myrcene, α - and β -pinene, terpinolene, and linalool. Sesquiterpenes such as β -caryophyllene and α -humulene are also detectable in hemp extracts (Fischedick et al., 2010). From the roots, the triterpenes friedelin and epifriedelanol have been reported (Slatkin et al., 1971); from the fibers, β -amyirin (Gutiérrez and del Rio, 2005); and from the seed oil, cycloartenol, β -amyirin, and dammaradienol (Paz et al., 2014). The quantities of terpenes and cannabinoids are positively correlated, since mono- and sesquiterpenes are synthesized in the same glandular trichomes where cannabinoids are produced (Fischedick et al., 2010; Meier and Mediavilla, 1998).

Polyphenols—and more specifically phenylpropanoids—are common secondary metabolites in the plant kingdom. In hemp, 20 flavonoids have been detected (Flores-Sanches and Verpoorte, 2008). In the plant, these compounds function primarily as antioxidants, protecting individuals from oxidative stress. In humans, flavones and flavonols exhibit anti-inflammatory, anticancer, and neuroprotective effects (Andre et al., 2010).

The antagonistic and synergistic actions of cannabinoids, terpenes, and polyphenols can be traced across multiple authors (Wright et al., 2013; Klein et al., 2011; Smith, 2015; McPartland and Russo, 2001).

3.3. The origin of hemp and the evolutionary history of chemotypes

Because of cultural and geographical influences, the uses of hemp have diversified throughout human history. Accordingly, both the applied agronomic practices and the direction of selection have varied. These circumstances directly led, in the twentieth century, to breeding trajectories focused on fiber, seed production, or psychoactive traits (Clarke and Merlin, 2016).

Phenotypic changes are likewise evident after millennia of selection. Fiber-type cultivars (NLH and BLH) have longer internodes and fewer branches, whereas seed-type hemp shows shorter internodes and more lateral shoots. Traditional, strongly psychoactive landraces may contain up to 20% THC, while European cultivars possess scarcely ~1% (Small and Marcus, 2003). At the same time, differences of up to twenty-fold have been observed between wild and domesticated plants in thousand-seed weight (Clarke and Merlin, 2013).

Beyond morphology, physiological differences are also pronounced. Seed oil content and fatty-acid composition have been substantially modified by domestication (Mölleken and Theimer, 1997).

Significant change is likewise observed in stem fiber content and quality; in a few cultivars with exceptional genetic backgrounds, fiber content may reach 35% (Bócsa, 1994).

The morphology of the inflorescence also reflects deliberate selection. In psychoactivity-directed types—chiefly NLD/BLD “sinsemilla” hybrids—inflorescences are larger, individual flowers and upper leaves are more densely arranged, and assured seed set is irrelevant, since these plants can be maintained vegetatively (Clarke and Merlin, 2013).

In hemp, both natural and artificial bidirectional evolution can be traced. During the Pleistocene, the original genetic center of hemp fragmented; ecotypes with different photoperiod requirements emerged and stabilized owing to geographic isolation. Subsequent domestication produced two markedly divergent groups: northern, short-season NLH cultivars and late-flowering NLD variants (Colombian, Indian, Thai) (Clarke and Merlin, 2016).

The alleles responsible for THC and CBD biosynthesis exhibit high heritability; through sustained selection, populations can be separated toward one end or the other (McPartland and Guy, 2010).

Under natural selection, hemp belongs to chemotype II—that is, it shows an approximately equal, intermediate THC:CBD ratio, as in Afghan hashish-type plants. Artificial selection produced high-THC, psychoactive populations that could be identified sensorially, yielding chemotype I with high THC:CBD ratios. By contrast, in northern growing environments, long days and relatively short summers are unfavorable for achieving high THC levels because the flowering period is shortened. Consequently, natural selection kept THC content lower in East Asian BLH and European NLH landraces. Full bidirectional selection culminated with the systematic, legally mandated isolation of elite modern cultivars exhibiting extremely low THC content. The high-CBD individuals of chemotype III—since exact CBD content can only be verified analytically—are products of modern selection (Clarke and Merlin, 2016).

Inbred lines of “pure” chemotypes comprise predominantly THC-dominant (type I) or CBD-dominant (type III) individuals. Crossing such pure lines yields intermediate offspring (type II). In the second generation, following Mendelian segregation, types split in a 1:2:1 ratio into I, II, and III plants. This suggests that the genes encoding THCA and CBDA synthases are codominant at a single locus (de Meijer et. al., 2003).

Genetic investigations by Kojoma et al. (2006) as well as Bakel et al. (2011) reveal a more nuanced picture, positing multiple homologous alleles at distinct loci; linkage among these, or differences in allelic enzymatic efficiency, may explain divergent segregation in descendant generations.

Regarding the biosynthesis of the two most important cannabinoids, Weiblen et al. (2015) recognized that CBDA synthase has greater affinity for converting the CBGA precursor than does THCA synthase. When both enzymes are active, considerably more CBDA is synthesized from CBGA. Thus, industrial hemp with low levels of psychoactive cannabinoids may still possess active THCA synthase, yet CBDA synthesis predominates. Drug-type (chemotype I) plants carry a nonfunctional CBDA synthase allele; consequently, there is no competition between the two enzymes and THCA is formed exclusively from the precursor. Genetically, the marijuana-type THCA synthase allele is dominant. The otherwise recessive, nonfunctional CBDA synthase enzyme is a clear indicator that the plant is drug type.

In sum, heterozygosity at separate loci, gene duplication, selection on CBD-synthase genes (toward nonfunctional enzyme variants), the selection of phenotypes bearing larger and more numerous glandular trichomes, and hybrid vigor (NLD × BLD hybrids) led to the emergence of modern psychoactive marijuanas.

The high THC content of Asian NLD plants was secured by isolating elite individuals.

In Afghan hemp, regarded as intermediate, psychoactive hashish was collected at the stand level rather than from individual plants. This precluded elite-plant selection, so populations contain both high-THC and high-CBD individuals. This pattern resembles East Asian BLH landraces, whose active-compound content is lower because selection never prioritized large inflorescence mass or high trichome density. Modern “sinsemilla” hybrids combine the extremely high THC content inherited from the NLD parent with the barely detectable CBD content of the BLD ancestor (Clarke and Merlin, 2016).

Breeding schemes for hybrids selected on cannabinoid content begin with choosing suitable maternal plants, preferably of genetically diverse origin. These pistillate individuals are selfed by chemically inducing male flowers through manipulation of hormonal balance. This is repeated over multiple generations to attain homozygosity. Finally, the resulting line is crossed with the least-related inbred line to restore vigor (de Meijer, 2014).

3.4. Milestones in hemp breeding

Over the twentieth century, European hemp breeders sought to improve locally available landraces and, through crossing, to secure higher fiber content and seed yield. Most European cultivars share common ancestors and are less genetically differentiated than their related landraces (de Meijer, 1995; Hillig, 2004).

Hemp is naturally dioecious, with staminate and pistillate flowers borne on different plants. However, the sexual phenotype can be flexible: monoecious or hermaphroditic plants may appear. In addition to 9 pairs of autosomes, there is one pair of sex chromosomes: males are heterogametic (XY), females homogametic (XX). Environmental stress or hormonal treatments can induce flowers of the opposite sex despite the chromosomal sex (Moliterni et al., 2004).

Because hemp is fundamentally dioecious and pistillate individuals can be pollinated by many males, controlled, directed pollination poses a major challenge. Monoecious cultivars are capable of self-fertilization as well as outcrossing. Artificially constructed, all-female (unisexual) populations are suitable for producing hybrid maternal lines. Such strictly unisexual stands can be obtained by crossing monoecious and dioecious stands (Hoffmann, 1944).

Industrial hemp populations can be grouped into three main categories. The oldest domesticated are the landraces, obtained by repeated mass selection. Synthetic cultivars typically arose from crosses among selected plants of landraces. In Europe, the progenitors

derive from northern, central-Russian, southern European, and East Asian ecotype populations (de Meijer, 1995). In the early decades of the twentieth century, selection targeted time to maturity, plant height, stem girth, and vegetative mass. Stem biomass and length of the vegetation period are positively correlated, so fairly homogeneous populations could be produced quickly on that basis. Quality traits, however, are more complex. Through family selection, the first Hungarian, Romanian, and Italian cultivars were derived from the Carmagnola landrace (Ranalli, 2004).

A third category comprises cultivars obtained by crossing two synthetic cultivars. Foundational breeding methods include selection, combinational breeding, heterosis breeding, and marker-assisted selection. There are also examples of induced-mutation breeding and polyploid breeding (de Meijer et al., 2003; Di Candilo et al., 2000; Hoffmann, 1953; Mandolino et al., 2003; Parsons et al., 2019).

Among the earliest synthetic breeding results are the cultivars Kymington, Chington, and Arlington, which Dewey (1927) created from Chinese landraces.

A milestone in fiber-hemp breeding was Bredemann's work, recognizing that both parents' traits determine fiber content; therefore he evaluated male plants even before anthesis so that only the best could pollinate. Through regulated pollination, this trait could be improved far more efficiently (Bredemann, 1924, 1937, 1953; Bredemann et al., 1961).

The earliest classical crossing result is also linked to Dewey (1927), who produced a cultivar with superior fiber-yield parameters by crossing Kymington and Ferrara. The most successful heterosis-bred hybrids, however, are associated with Hungary (Bócsa and Karus, 1998).

Marker-based selection is useful for early identification of male plants and in monoecious breeding programs (Mandolino et al., 1999). Markers have also become indispensable for identifying chemotypes (de Meijer et al., 2003; Mandolino et al., 2003).

Today, most European cultivars are monoecious. The French cultivar Fibrimon was produced directly from an inbred monoecious line. This line was multiplied from a single plant bearing both staminate and pistillate inflorescences that had been isolated from a central-Russian NLH population. Pseudo-monoecious cultivars were created by crossing Fibrimon (as pollen donor) with either a high-fiber German NLH population or a late Italian or Turkish landrace, followed by backcrossing the progeny to Fibrimon. The genetic homogeneity of

monoecious cultivars must be maintained annually, since without selection subsequent generations revert toward natural dioecy (de Meijer, 1995).

Most Italian cultivars are dioecious; the best-known and oldest is Carmagnola, once the foundation of Italy's renowned textile industry (Allavena, 1967). From it, the cultivar Carmagnola Selezionata was derived. By mass selection, ecotypes suited to specific production areas were developed: Bolognese, Toscana, Ferrarese. Crossing with high-fiber German lines produced the cultivars Eletta Campana and Fibranova (Allavena, 1967; Barbieri and Tedeschi, 1968). In 1995, a new breeding program set goals of higher yield, improved fiber quality, and low THC content, resulting in the dioecious cultivars Red Petiole, Asso, and Fibrimor, and the monoecious cultivars Hermes, Carmono, Carma, and Codimono (Di Candilo et al., 2002; Ranalli, 1998).

Hungarian production likewise preferred dioecious forms, as fiber production was paramount. In Hungary, the pioneering work is attributed to Fleischmann (1931, 1934). Kompolti hemp was selected for high fiber content from an Italian-origin cultivar. The practice of producing hybrids—and therefore the field production of unisexual populations—has Hungarian roots. Uniko-B, produced by crossing Kompolti with the monoecious Fibrimor, is a unisexual hybrid with negligible pollen production; it consists largely of pistillate plants and thus has outstanding seed yield. In the second generation it loses this trait, with many truly staminate plants appearing. Kompolti Hybrid TC is a three-way hybrid; the first step was to produce the unisexual generation “Chinese Unisex” (a cross of Chinese BLH monoecious and dioecious plants). Crossing Chinese Unisex with Kompolti as pollen donor then produced the three-way hybrid with a 50% female–male ratio, hybrid vigor, and increased fiber content. Another notable outcome of domestic breeding—primarily for the paper industry—is Kompolti Sárgaszárú, a chlorophyll-deficient cultivar showing a yellow stem at flowering. The initial mutant plants were obtained by crossing an early Finnish NLH with a late Italian NLH/BLH hemp; repeated backcrossing to Kompolti fixed the new stem color in a homozygous state (Bócsa and Karus, 1998).

Polish cultivars are monoecious. ‘Białobrzegie’ is the product of successive crosses among several Russian-origin NLH lines, ultimately crossed to Fibrimor and then selected for high fiber content. Another cultivar, ‘Beniko,’ resulted from single-plant progeny selection within a Fibrimor hybrid (de Meijer, 1995).

In Romania, breeding is conducted in two research institutes: SCDA Seuieni mainly produces monoecious cultivars, whereas SCDA Lovrin produces dioecious ones. Their recent outputs include the monoecious cultivars Olivia and Successiv (Popa et al., 2022; Popa et al., 2019).

Because dual-purpose hemp is prevalent in France, French cultivars are predominantly monoecious. Some were selected directly from Fibrimon, which itself was a crossing-breeding product that von Sengbusch created in the 1950s from spontaneous monoecious plants found in a central-Russian line, high-fiber selected dioecious lines, and late Italian and Turkish landraces. True-monoecious selections include Fibrimon 21, Fibrimon 24, Fibrimon 56, and the early Ferimon 12. Pseudo-monoecious cultivars, products of crosses between Fibrimon and a dioecious cultivar, include Fedora 19, Felina 34, and Futura 77 (de Meijer, 1995). Among new-generation cultivars bred for cannabinoid profile, ‘Santhica’ represents selection for high CBG content (de Meijer, 2004).

The Finnish dioecious cultivar ‘Finola’ was registered in 1999. It is early, short, adapted to northern regions, and cultivated in Canada primarily for seed and oil (Small and Marcus, 2002).

Hemp breeding also has a long tradition in the former Soviet Union. Earlier cultivars either belonged to the southern, late-maturing group or were hybrids of central-Russian and Mediterranean hemp. The famous southern Russian ‘Kuban’ cultivar is the result of ten cycles of family selection with ‘Szegedi 9’ and ‘Krasnodarskaya 56’ as parents. ‘Szegedi 9’ is Hungarian, selected from ‘Tiborszállási’ (Serebriakova, 1940; de Meijer, 1995). The monoecious cultivar ‘USO-11’ exhibits the growth dynamics typical of the southern group; when grown in northern areas, the longer vegetative phase results in taller plants and higher fiber yield. Its name reflects this origin: the Russian abbreviation denotes “southern monoecious” (de Meijer, 1995).

Active breeding continues today in Ukraine as well—for example, the high-fiber-quality, high-seed-oil ‘Artemida’ (Mishchenko et al., 2021a) and the high-CBG ‘Vik 2020’ (Mishchenko et al., 2021b).

In Serbia, breeding was reactivated in 1992; the dioecious ‘Marina,’ the monoecious ‘Helena,’ and the hybrid ‘Diana’ were registered (Sikora and Koren, 2020).

The spread of drug-type hemp initially involved the acclimatization of South Asian NLD landraces in diverse geographic zones. In the 1960s and 1970s, NLD landraces became available in relatively large quantities in Europe and North America and provided the genetic

base. Because Colombian and Thai marijuana are equatorial, they could not mature outdoors in northern latitudes; by contrast, Mexican and Jamaican cultivars were earlier, allowing inflorescences to mature before winter. From the early 1970s, NLD hybrids combined Mexican–Jamaican material with the much more productive but later Colombian, Indian, Panamanian, and Thai lines. Initially, all male plants were removed, leaving only unpollinated females (sinsemilla), whose potential cannabinoid content far exceeds that of pollinated plants. Later, a few male plants were isolated and some mothers were pollinated to secure seed supply. Owing to the multihybrid progeny of imported NLD landraces, by the 1980s North American sinsemilla had become the most valuable drug-type hemp; early NLD lines included, for example, ‘Original Haze.’

Broad-leaf drug-type hemp (BLD) arrived in North America and Europe from Afghanistan in the 1970s. Characteristic features include high branching and a height of only 1–2 m. Compared with NLD, BLD plants are shorter and more compact, with broader, darker leaves. This underlies the common—but erroneous—habit of calling NLD strains “sativa” and Afghan hashish BLD plants “indica.” NLD × BLD hybrids matured earlier than pure NLD lines, appeared shorter and more compact, and, owing to heterosis, often displayed higher extractable cannabinoid content. Over the longer term, however, indiscriminate hybridization coupled with neglect of selection substantially degraded both active-compound content and quality.

NLD/BLD hybrids also transformed agronomy for drug-type hemp: with better cold tolerance and faster maturation, they could be grown outdoors in the cool-temperate north. Indoor cultivation spread due to increasing prohibitions, advances in lighting systems, and the expansion of shorter, more compact hybrids. This production model narrowed the accessible genetic base, and sensitivity to environmental conditions ceased to be a selection criterion (Clarke and Merlin, 2016).

3.5. Contemporary challenges and future prospects in hemp breeding

In summary, *Cannabis* plants exhibit great genetic variability due to natural and artificial selection, which is reflected in the diversity of phenotypes. Nevertheless, breeding aims have been shaped by legal regulations and prohibitions, leading to a progressive reduction in genetic diversity. Most European industrial hemp cultivars descend from a few common selection sources: dioecious forms are the result of crosses among Russian and Chinese landraces, whereas monoecious forms derive from ‘Fibrimon’. The gene pool of drug-type varieties has likewise narrowed substantially because of inbreeding, intentional or accidental selfing, and the

dominance of commercially propagated vegetative clones. If this trajectory continues, the lack of sexual recombination may increase susceptibility to animal pests and pathogens as well as climatic sensitivity.

Historical precedents illustrate similar phenomena, such as the 1845 potato blight in Ireland, where a single cultivar (“Irish Lumper”) dominated much of the acreage and proved unable to resist the new, highly virulent HERB-1 lineage of *Phytophthora infestans*, with catastrophic consequences (Kelly, 2012).

Grapevine propagation historically relied on rooted cuttings, much like modern “sinsemilla” hemp plants. In the mid-nineteenth century, the American phylloxera (*Daktulosphaira vitifoliae*) devastated large parts of Europe’s vineyards. An initial strategy crossed North American *Vitis aestivalis* with European *Vitis vinifera*, but neither pest resistance nor previous product quality was achieved. The solution proved to be the use of American rootstocks onto which European cultivars were grafted. Mysles et al. (2011) draw attention to the risks of vegetative propagation under increasing pest pressure: while effective for establishing truly homogeneous lines, this maintenance method constricts grapevine’s natural genetic diversity to an extent that threatens the long-term sustainability of viticulture.

In the mid-twentieth century, artificial selection and breeding of hemp took a new direction. Cultivation of traditional fiber, seed, or drug landraces ceased in favor of modern cultivars, or they were combined through crossing. Watson and Clarke (1997) warned that inadequate preservation of genetic resources—exacerbated by legal stipulations and anti-cannabis measures—would lead to the disappearance of landraces. Multiplication and regeneration of the diverse, high-value germplasm stored in gene banks are cumbersome. Moreover, dioecious populations must be sufficiently large (up to 2,000 individuals) for allelic diversity to be reproducible and conserved in seed (Crossa et al., 1993).

Looking ahead, challenges in hemp breeding concern both quality and quantity: the goals include higher and better-quality fiber content; appropriate cannabinoid profiles (low THC with higher CBD); improved processability; and resistance to pests and diseases. Sequencing genes responsible for stem cellulose, lignin, and pectin content could open new directions to improve suitability for textile and paper applications (Mandolino and Carboni, 2004).

Breeding for suitable protein and fatty-acid content of the grain, alongside optimization of processability, will support food-industry uses (Salentijn et al., 2014). Fiber quality is a more

complex trait; by contrast, the number of genes governing fatty-acid and protein biosynthesis in seeds is lower, so selection for these may be more efficient (Weightman and Kindred, 2005).

A new utilization pathway for traditional industrial hemp is also spreading. Cannabinoids present in threshing residues or other unused biomass are extracted and marketed as dietary supplements or medicinal auxiliaries. In response, breeders are working to produce cultivars combining high CBD with low THC. China has a long tradition of multipurpose hemp use; beyond fiber and seed, it has also been cultivated as a medicinal herb. Over the past decade, high-CBD industrial hemp cultivars have been registered (Salentijn et al., 2015).

There is growing interest in rare, otherwise low-abundance cannabinoids (e.g., CBC, CBG), and breeding efforts targeting these have also been reported (Mishchenko et al., 2021b).

Creating high-CBD populations for pharmaceutical raw material often follows the conventional “sinsemilla” approach used for drug-type hemp. First, a few promising crosses are made; selected individuals are then repeatedly selfed, or backcrossed to a parent. Hybrid vigor is restored by crossing selected, distinct inbred lines (de Meijer, 2004).

Future hemp breeding will be complemented by biotechnological advances. As an early step, Japanese researchers successfully transferred THC-synthase genes into tobacco (*Nicotiana tabacum* L.) (Sirikantaramas et al., 2005). The first hemp genome sequence was published in 2011 (van Bakel et al., 2011).

Gene editing and induced mutation likewise create opportunities for new oilseed hemp cultivars (Bielecka et al., 2014).

Genes encoding cannabinoid biosynthesis can be transferred to other organisms, such as microbes (Luo et al., 2019). Although seedless, dried hemp inflorescences can themselves accumulate ~20% THC or CBD, transgenic microbial bioreactors may nonetheless become competitors.

Extensive use of molecular markers can accelerate the breeding process. Individuals carrying desirable traits can be identified at very early phenological stages (de Meijer, 2004). Complex traits can also be developed more rapidly, and advantageous, rare mutations can be detected (Salentijn et al., 2015).

3.6. The inheritance dynamics of morphological and developmental traits in *Cannabis sativa*

The genetic makeup of hemp is predominantly heterozygous, which entails a high frequency of alternative alleles. Breeding therefore aims to fix desired traits in a homozygous state while preserving hybrid vigor.

The *Cannabis sativa* genome is complex and polymorphic, with numerous duplication and divergence events. Weiblen et al. (2015) demonstrated that part of the gene set responsible for cannabinoid biosynthesis arose through gene duplication, particularly in the cases of THCAS and CBDAS. This gene-family diversity underlies the emergence and inheritance of distinct chemotypes.

Hemp populations may be monoecious or dioecious, and this trait plays a key role in cultivar maintenance and production technology. The genetics of monoecy are not fully resolved, but the presence of a recessive allele has been proposed to promote the co-occurrence of male and female flowers on the same plant (Faux et al., 2013). Current evidence suggests polygenic control of monoecy, with variable phenotypic stability.

Sex determination is especially important for breeding monoecious hemp. In dioecious hemp, sex inheritance can be described by the Correns-type simple monofactorial model. Subdioecious hemp, upon selfing or crossing, yields female individuals in the F1 generation. An XX/XY mechanism accounts for sex inheritance in dioecious hemp; however, the inheritance of monoecy and intersex phenotypes is more complex. Neuer and Sengbusch (1943) posited a monogenic but polyallelic mode of inheritance, proposing that female-habitus intersexes are homogametic (XX), whereas male-habitus intersexes are heterogametic (XY). In contrast, Sengbusch (1952) found that female-habitus monoecious plants can also be heterogametic. In his experiments, crosses between monoecious and dioecious females produced monoecious and male offspring. Sengbusch argued that habitus is polyfactorially inherited, with frequent linkages between sex and habitus factors.

Sexual dimorphism in hemp has long been studied. The genetic basis is an XX/XY chromosome system in which the Y chromosome determines maleness (Razumova et al., 2016). Yet sex expression is modulated by environmental factors, including stress and plant hormones (Adal et al., 2021), and partial hermaphroditism occurs in some populations. Environmental factors such as light and stress also influence sex expression (Mishchenko and Laiko, 2021). During inheritance of sex-related genes, gene-segment duplications and suppression

phenomena are often observed, contributing to variability in sex stability (Injamum-Ul-Hoque et al., 2025).

Quantitative traits such as fiber content display polygenic inheritance, which likely extends to the length of the vegetation period (Crescini, 1953). In a crossing experiment, Fruwirth (1922) intercrossed plants with dark and light seed; the F1 generation showed intermediate inheritance. In F2, the progeny segregated 1:2:1 into light, gray, and dark seed. Crossing anthocyanic with green-hypocotyl plants, Crescini (1953) found that red coloration is dominant and observed a 3:1 monofactorial segregation ratio in F2; the same holds for the bronze discoloration at the base of foliage leaves. Across crosses, Crescini estimated a 30% crossover frequency. He further showed that distorted and fasciated stem forms arising under inbreeding are recessive and termed them “pinnatifidophylly” (Crescini, 1956). Seed-coat color is an important varietal character with aesthetic value and possible associations with seed chemistry and storability. Classical analyses indicate Mendelian inheritance, often governed by one or two dominant gene pairs (Faux et al., 2013). Molecular studies frequently implicate genes of the flavonoid pathway in pigmentation.

Thousand-seed weight (TSW) is a key indicator of yield quality and quantity. Evidence indicates polygenic inheritance (Amaducci et al., 2008), and genetic mapping has identified multiple QTLs that directly influence TSW (Faux et al., 2016).

Time to flowering (maturity) is a pivotal agronomic trait that strongly conditions yield and adaptation. Flowering in hemp is photoperiod-dependent and under the joint control of multiple loci, including homologs of FLOWERING LOCUS T (FT) (Toth et al., 2020). The genetic background is polygenic, but specific QTLs have already been identified, especially in northern types.

Plant height, critical for yield and harvestability, is genetically complex and polygenic, with close connections to genes involved in gibberellin synthesis and sensitivity (Faux et al., 2016). Some studies have identified distinct loci governing the upper and lower segments of plant height, which segregate independently.

Although the genetic bases of many traits are increasingly well understood, environmental factors—photoperiod, temperature, and soil type—continue to exert substantial effects on phenotypic expression (Amaducci et al., 2008). This is particularly evident for maturity time and sex expression, posing not only breeding challenges but also demands for agronomic adaptation.

Cannabinoid compounds—most notably tetrahydrocannabinol (THC) and cannabidiol (CBD)—are key elements of hemp’s chemical phenotype (chemotype). Early studies indicated Mendelian inheritance of the cannabinoid profile linked to a dominant–recessive gene pair (de Meijer et al., 2003). The THC:CBD ratio is largely determined by the presence of two alleles, Bt and Bd, which regulate production of the THCAS and CBDAS enzymes (Wenger et al., 2020).

Other cannabinoids, such as cannabigerol (CBG) and cannabichromene (CBC), are likewise under genetic control. CBG is a precursor cannabinoid from which other major compounds are synthesized and is dominant in certain cultivars (de Meijer and Hammond, 2005). Variation in CBC levels also reflects specific genetic mechanisms and has been modeled as a quantitative trait (de Meijer et al., 2009a).

3.6.1. Research on hemp stem coloration

Natural hybridization among species (Dong et al., 2021) and among cultivars with differing flowering times has been widely studied (Stetter et al., 2016; Ferwerda, 1953). Investigations of the yellow-stem hemp phenotype trace its origin to Hoffmann’s 1946 discovery of the “Hellstengeligen” trait arising from crosses between Italian and Finnish landraces (Hoffmann, 1946). This trait subsequently became a focus of hemp-breeding programs, leading to the development and registration of several yellow-stem cultivars, including ‘Carmaleonte’, ‘Ivory’, ‘Kompolti Sárgaszárú’, ‘Fibror 79’, ‘Markant’, and ‘Chamaeleon’.

The first detailed description of the yellow stem-color trait is attributed to Walther Hoffmann’s 1946 paper. The “Helle Stengel” mutant appeared in F₂ and F₃ progeny of a cross (late Italian × early Finnish hemp) in which stems turned yellow even before maturity. Based on backcrosses and F₂ generations, Hoffmann concluded a monogenic, recessive inheritance: in backcrosses the green:yellow phenotype segregated 1:1, and in F₂ it segregated 3:1. The trait showed no linkage to sex determination or to monoecious/dioecious type (“independent segregation”) (Hoffmann, 1946). The yellow stem color is thus a monogenic recessive character (Sitnik, 1981).

With respect to the relationship between yellow stem color and general pigmentation, morphological–anatomical studies have documented variability in stem color (green, yellow, purple). These differences likely reflect variation in the distribution and abundance of pigments (e.g., chlorophylls, carotenoids, anthocyanins); however, the specific molecular cause (candidate gene/variant) of yellow stems remains unidentified (Amarasinghe et al., 2022).

The yellow-stem trait is of agronomic and processing interest. Several reports note that yellow-stem cultivars may be more amenable to fiber processing than green-stem cultivars. A multi-environment study in 2023 compared a yellow ('Fibror 79') and a green ('Futura 75') cultivar to analyze the relationship between nitrogen supply and productivity/ecophysiology, advancing the working hypothesis that yellow-stem types may have lower nitrogen-uptake efficiency—potentially explaining part of the color and physiological differences (Blandinières et al., 2023).

While it has not been proven that yellow stem color is directly tied to the anthocyanin pathway, recent biochemical and gene-level elucidation of hemp pigmentation (especially purple coloration) indicates that well-defined biosynthetic and transcriptional regulatory networks underlie color traits. Results include identification of the dominant hemp anthocyanin and a regulatory model, which may provide methodological guidance for future molecular mapping of yellow stem coloration (Bassolino et al., 2023; Gagalova et al., 2024).

Studies suggest that yellow-stem hemp offers notable advantages over green-stem cultivars, including a higher proportion of long fibers relative to total fiber content (Amarasinghe et al., 2022; Musio et al., 2018; Bennett et al., 2006).

The stem color of hemp (*Cannabis sativa* L.) is not merely a morphological feature but also a trait of agronomic and technological relevance. Stem color may indicate genetic background, fiber quality, time to maturity, and even inform optimization of harvest technology (Salentijn et al., 2015). Variability in stem color—e.g., green, yellow, purple—is particularly evident in the diverse genetic materials used in industrial hemp cultivation (Kriese et al., 2004).

Multiple studies report that yellow-stem cultivars are easier to process for fiber extraction because stems may contain less lignin, facilitating retting or mechanical fiber separation (Amarasinghe et al., 2022). This can lower the energy demand of mechanical processing and increase fiber yield—clear advantages for the fiber industry.

In some cases, stem color can serve as an indicator of fiber quality. Yellow-stem genotypes often contain thinner-walled fibers that are especially suitable for textile applications, in contrast to green or purplish types, which often yield stronger but coarser fibers favored in construction (Zheljazkov et al., 2023). Thus, yellow stem color has functional as well as aesthetic value.

Stem color shows polygenic inheritance, though some studies have identified QTL associations with this phenotype. Yellow coloration frequently exhibits recessive or

intermediate inheritance; hybrid progeny often display greenish-yellow hues. Molecular-marker studies (e.g., AFLP, SSR) have linked stem color to regulation of the flavonoid-biosynthetic pathway (Bócsa, 1999).

In cultivar choice, stem colors aligned with industrial objectives are preferred. For textile processing, yellow stems are advantageous, whereas green-stem cultivars can also suit construction uses. Breeding increasingly prioritizes easily separable stem architecture and the associated yellowish stem color (McKay et al., 2019).

Although stem color is fundamentally genetic, environmental factors also modulate it. Soil pH, light intensity, and nutrient availability (e.g., N–P–K ratios) can influence pigment metabolism in stems. Consequently, the same genotype may develop differently colored stems across environments (Singh et al., 2022).

From a processing-efficiency perspective, yellow-stem cultivars often respond better to mechanical and biological retting. Owing to reduced lignin and pigment content, stems break down more quickly and fiber separation is more efficient—an especially important consideration for sustainable textiles that favor chemical-free or low-energy processing (Campbell et al., 2019).

Targeted breeding of yellow-stem types is feasible, but the molecular genetic basis is not yet fully resolved. Some studies employ genome-wide association (GWAS) to map regions governing stem color. A key challenge is that stem color often co-inherits with other agronomic traits (e.g., plant height, maturity), complicating selection (Tilkat et al., 2023). Genome-editing approaches such as CRISPR/Cas9 may enable precise modification of stem color. In the future, functional genomics and transcriptomics should pinpoint the genes influencing stem color, enabling precision breeding tailored to industrial demands (Crini and Lichtfouse, 2020).

3.7. Accelerated breeding based on short generation time

3.7.1. History and rationale

Driven by the challenges of a growing human population and changing climatic conditions, accelerated breeding (speed breeding, SB)—that is, cultivation and selection under reduced vegetative periods to shorten generation turnover—has become increasingly important. The technique began more than 150 years ago with carbon-arc lamp experiments and, with the advent of modern LED technology, has evolved into a contemporary method for compressing breeding cycles. It complements approaches such as single-plant selection and shows

considerable potential when combined with gene editing, genotyping, and genomic selection (Potts et al., 2023; Gray and Brady, 2016; Hatfield and Prueger, 2015; Hickey et al., 2017; Jighly et al., 2019).

SB optimizes environmental conditions to reduce generation times in crops such as wheat, canola, and chickpea. It is particularly advantageous for long-day species that require more than 16 hours of light for rapid flowering, whereas short-day species like soybean demand more complex protocols. As a short-day plant, hemp requires fewer than 11–15 hours of light per day to initiate flowering; this photoperiod dependence typically allows only one generation of breeding progress per year (Ghosh et al., 2018; Watson et al., 2018; Fang et al., 2021).

In its modern sense, SB did not spring from a single idea; rather, it emerged from the convergence of several cycle-shortening techniques and infrastructures. Early milestones included inserting winter greenhouse generations, *shuttle breeding* (rotating generations between two contrasting ecological zones), the SSD (single-seed descent) method, in vitro accelerators (embryo rescue, immature-seed germination), and, later, the spread of closed, photothermally controlled environments with LED lighting. Breakthrough studies demonstrated 4–6 (or more) generations per year in cereals and pulses, accompanied by practical protocols (McFadden and Brookings, 1917; Borlaug, 2007; Goulden, 1939; Watson et al., 2018; Ghosh et al., 2018).

Artificial-light cultivation of plants has a history spanning more than a century. Experiments from the late nineteenth century (carbon-arc lamps, early electric lighting) already indicated that continuous or near-continuous light can hasten flowering and shorten vegetative growth, foreshadowing the concept that targeted manipulation of daylength and light quality can buy generation time (Bailey, 1891).

The first systematized accelerators were winter greenhouse generations, used from the early twentieth century. From the 1940s onward, *shuttle breeding* grew popular: by “commuting” generations between two climates, annual cycle counts doubled, and selection pressure intensified under diverse environments. Although still far from today’s SB, these steps normalized rapid line advancement and multi-location selection (McFadden and Brookings, 1917; Magruder, 1937; Borlaug, 2007; Ortiz et al., 2007; Collard et al., 2013).

SSD (advancing one plant/one seed per generation) has been known since 1939, and toward the end of the twentieth century in vitro tools (embryo rescue) and controlled-climate chambers further accelerated turnover. Several SSD variants were developed across crops: initially

strongly in-vitro-centric (Ochatt et al., 2002; Mobini et al., 2015), then gradually shifting toward chamber-based systems, often combined with embryo-culture generation closure (Croser et al., 2016; Yao et al., 2017). These developments directly prepared the ground for the SB concept (Goulden, 1939; Ochatt et al., 2002; Mobini and Warkentin, 2016; Croser et al., 2016).

In the 1980s–1990s, NASA and Utah State University selected the dwarf wheat ‘USU-Apogee’ under closed systems with extended photoperiods and conducted spaceflight experiments spanning complete life cycles. These efforts showed that rapid growth can be sustained under long days and controlled climates—even in compact, resource-efficient systems suitable for fast generation turnover (Morrow et al., 1995; Bugbee and Koerner, 1997; Link et al., 2003; Croxdale et al., 1997).

From the 1990s, evaluation and adoption of LED technology enabled fine-tuning of light quality (red/blue/green, far-red). New fixtures improved energy efficiency, reduced heat loads, and delivered high PPF (photosynthetic photon flux density) in small spaces—preconditions for sustained 20–22-hour photoperiods. Spectrum management remains a core element of SB (Guo et al., 2023; Wu et al., 2023).

Biotron-based rapid generation advance (RGA) systems in rice (Tanaka et al., 2016) and simplified, tray-based cultivation introduced across multiple crops (Collard et al., 2017) anticipated today’s SB “logic”: high density, minimal container size, restrained inputs, and precise photothermal control. From these emerged the protocol mindset that later crystallized into SB rules (Tanaka et al., 2016; Collard et al., 2017).

Following Watson et al. (2018), it was established that six generations per year are realistic in spring wheat, barley, chickpea, and pea, and four in canola. A companion protocol (Ghosh et al., 2018) standardized photoperiod (e.g., 22 h light/2 h dark), temperature cycling, PPF, and key features of LED-chamber implementations—with more than a decade of prerelease experimentation behind the publications (Watson et al., 2018; Ghosh et al., 2018).

Commercial adaptations appeared in the early 2010s: in peanut, greenhouse- and chamber-based SB solutions were deployed (O’Connor et al., 2013). Species-specific procedures soon followed: near-seven generations/year in canola (Yao et al., 2016), eight to nine/year in wheat/barley (Zheng et al., 2013), and cycle shortening in winter wheat despite vernalization requirements (Schoen et al., 2023) (O’Connor et al., 2013; Yao et al., 2016; Zheng et al., 2013; Schoen et al., 2023).

For a long time SB was successful mainly in long-day species, but LEDs have made floral induction reliably programmable in short-day crops as well. In amaranths, rapidly segregating populations were developed (Stetter et al., 2016), and in soybean, five generations/year were demonstrated with LEDs and timed harvest. A milestone paper formalized photoperiod-management principles for short-day species (Jähne et al., 2020; Stetter et al., 2016).

In winter cereals (winter wheat, triticale), cold requirement remained a bottleneck. *Speed vernalization* protocols were designed to compress cold treatment and, embedded within SB, to accelerate the full cycle; tailored SB schemes (e.g., triticale under long days with photoperiod control) followed (Cha et al., 2022; Cha et al., 2021; Vikas et al., 2021).

By the early 2020s, “comprehensive SB” denoted multivariable optimization of the entire system. Photothermal greenhouses (sunlight plus supplemental lamps) and modular shelving scaled high-throughput cultivation to economically viable levels, while quality assurance matured for field/operational transfer (Song et al., 2021; Jamali et al., 2020; Watson et al., 2019).

SB has expanded rapidly: in rice, a community-validated protocol is now available (Kabade et al., 2024); “SpeedyPaddy” enabled large-scale advancement at low cost (Sandhu et al., 2024); in finger millet (*Eleusine coracana* Gaertn.), “Rapid Ragi” standardized procedures (Sajja et al., 2025); and in hemp, SB procedures have been described for research and agronomic aims (Schilling et al., 2023).

The last steps of the cycle became another arena for acceleration: early harvest of immature seed, forced drying, and germination save days to weeks (Yao et al., 2016; Tanaka et al., 2016; Rogo et al., 2023; Saxena et al., 2017).

A subset of phenotypes validated under SB correlates well with field observations (e.g., leaf-rust resistance, root phenotypes). In the same setting, multivariate genomic selection (GS) and marker-assisted introgression (e.g., *Glu-B1i* allele) can run markedly faster (Richard et al., 2015; Riaz et al., 2016; Cha et al., 2024; Watson et al., 2019).

By the mid-2020s it became clear that SB is not a standalone method but a switching module within modern breeding pipelines. It is suitable for refreshing GS training populations, purging transformed/edited candidates, speeding backcross culling, and enabling high-throughput phenotyping. Industry and academic reports converge: SB is the bridge between “classical” and “digital” plant breeding (Watson et al., 2019; Chiurugwi et al., 2019; Li et al., 2024).

From the artificial-lighting trials of the late nineteenth century, through NASA's closed systems and SSD/in vitro accelerators, to the 2018 standardizations, the history of SB shows that technological infrastructure (LEDs, climate, CO₂, density), experimental design, and methodological integration together make industrial-scale cycle acceleration possible. A photoperiod- and spectrum-controlled environment alone is insufficient: SB becomes a sustainable method only if the entire pipeline—from sowing to official plant variety protection—can be tuned to short cycles (Wellensiek, 1962; Jamali et al., 2020; Watson et al., 2018; Cha et al., 2022).

Generation time is the critical point in plant breeding. Stabilizing a line and field-validating candidates takes years, while climate extremes, biotic/abiotic stresses, and global demand shift rapidly. SB is justified on two grounds: time—more generations can be run per year—and risk reduction—the selection pressure and measurements are maintainable under controlled conditions. From the earliest trials, SB visibly shortened cycle time and directly accelerated genetic gain (Watson et al., 2018; Li et al., 2018; Borlaug, 2007).

Crop breeding is time-consuming not only because of a single long generation but also because, to create pure lines, hybridization is followed by 4–6 years of inbreeding. In self-pollinated crops, resulting lines must be evaluated over multiple years to judge suitability. In cross-pollinated species—where heterosis-based hybrid breeding predominates—advanced lines serve merely as starting material for combining-ability tests. Without modern cycle-shortening methods, release of varieties or F1 hybrids in annual crops such as wheat or sunflower can take up to 15 years (Watson et al., 2018; Jamali et al., 2020). Creating varieties or F1 hybrids in biennial and perennial species is an even greater challenge (Van Nocker and Gardiner, 2014; D'Angelo and Goldman, 2019).

The practical metric validating SB is generations per year. In cereals, 4–6 (or more) generations have been realized: near-seven per year in canola (Yao et al., 2016), eight to nine per year in wheat and barley (Zheng et al., 2013), and marked cycle reductions in winter wheat despite vernalization constraints (Schoen et al., 2023). In cotton, five generations per year were recently demonstrated (Wang et al., 2025). These figures suggest that multiyear line-development phases can be compressed to 1–2 years—a strategic advantage in breeding programs (Watson et al., 2018).

SB dovetails especially well with SSD/SPS (single-seed descent/single-plant selection) and RGA (rapid generation advance), because generations can be cycled at high density in small

spaces under standardized conditions. In rice, rapid advancement was shown early in biotron systems (Tanaka et al., 2016); in peanut, commercial SB programs appeared in the 2010s (O'Connor et al., 2013); and in oat, a cost-effective SSD+SB combination was developed (“Single-Seed-Speed Bulks,” Kigoni et al., 2023).

Environmental control in SB renders complex traits measurable and repeatable that would be unwieldy in open fields. It has been used for rapid prescreening of root phenotypes (Richard et al., 2015) and for confirming leaf-rust resistance (Riaz et al., 2016), with several early-generation traits showing good field transfer. A recent study on the genetic control of spring barley development under SB conditions (Rossi et al., 2024) underscores that accelerated cycles not only save time but also yield new scientific insight (Blinkov et al., 2025).

SB shortens the cycle time of genomic selection (GS) and marker-assisted selection (MAS): training populations can be refreshed and backcross (BC) generations advanced more rapidly. In spring wheat, a multivariate GS approach has been integrated with SB (Watson et al., 2019). Gene-edited event “clean-up” and transformation platforms (e.g., maize: Ishida et al., 2007; wild rice: Shimizu-Sato et al., 2020) gain explicit time savings when combined with SB. As a practical example, SB + MAS + BC synergy has been reported in wheat (Cha et al., 2024).

In winter-hardy types, cold requirement is the classic time constraint. *Speed vernalization* protocols (Cha et al., 2022) intentionally shorten cold treatment and, when coupled with SB, compress the full cycle. Fresh experimental examples document reduced generation time in winter wheat (Schoen et al., 2023). The idea of “cycle shortening” dates back to the 1960s (Wellensiek, 1962), but only with today’s LED-based photothermal systems has industrial application become feasible.

Targeted manipulation of light quality justifies SB: wavelength-dependent responses have been shown in soybean (Harrison et al., 2021); LED-controlled flowering time has been documented in short-day species (Jähne et al., 2020); and far-red supplementation shortened generation time in triticale (Blinkov et al., 2025). Spectrum optimization is rightly considered part of SB in order to accelerate cycles without degrading agronomic performance (Song et al., 2021).

Daylength manipulation is central to SB: extending daylength accelerates flowering in many species (Ji et al., 2022), whereas, in short-day crops, the timing of long-day/short-day switches governs the vegetative-to-reproductive transition (Jähne et al., 2020). The detailed rice

protocol (Kabade et al., 2024) integrates not only photoperiod but also temperature and scheduled early harvest to make generation shortening reliable. Photoperiod induction becomes predictable and reproducible—one of SB’s fundamental justifications.

Under controlled environments, elevating CO₂ and fine-tuning light cycles further reduce generation time: in soybean, CO₂ supplementation provided acceleration (Nagatoshi and Fujita, 2019), and in legumes, optimizing light/dark cycles directly improved generational throughput (Mitache et al., 2023; 2024). Such environmental configurations are scarcely feasible in the field, so SB is a justified platform for experimentally dissecting and routinely applying environment–development parameters (Blinkov et al., 2025).

Cycle closure is another lever: early removal of immature seed, forced drying, and embryo rescue provide immediate time savings. In canola, a protocol based on detailed comparative experiments is available (Yao et al., 2016), and in accelerated systems, precise logging of environmental parameters is a key step (Tanaka et al., 2016). Embryo rescue as a generation-shortening tool has been comprehensively reviewed (Rogo et al., 2023). In legumes, even germinating immature seed shortened the cycle by three weeks (Saxena et al., 2017).

Lighting and cooling are among SB’s major cost drivers (O’Connor et al., 2013). Even so, increasing LED efficiency, hybrid (sunlight + LED) greenhouses, and rack-based tray cultivation make systems scalable and cheaper. Historically, the NASA line (USU-Apogee) demonstrated that high generational tempo is sustainable even in compact, closed systems (Bugbee and Koerner, 1997). The investment is therefore justified because it can be converted into time savings—direct financial value in breeding.

SB’s pace raises new questions for variety registration and quality assurance: legal–administrative mechanisms must keep up with rapid cycles (Jamali et al., 2020). Programs employing SB should enforce strict standard operating procedures (SOPs—sampling, barcoding, phenotyping standards) so speed does not cause documentation or identification errors (Blinkov et al., 2025).

SB platforms also enable application in species with limited conventional infrastructure. In hemp, for example, artificial light control allows flowering synchronization and rapid generation rotation (Somody and Molnár, 2025; Somody et al., 2024), strongly motivating the use of controlled environments. The same applies to “orphan” or emerging crops: targeted photoperiod management and spectrum tuning enable rapid prototyping.

The specific effects of thermal and light extremes can be reliably studied—and selected for tolerance—under controlled conditions; in soybean, for instance, wavelength influenced development under SB (Harrison et al., 2021). Detailed SB protocols in soybean and rice show that yield and quality components (e.g., timed induction, nutrient regulation) can be deliberately tuned (Kabade et al., 2024), and a fresh, standardized SB procedure has appeared in finger millet (“Rapid Ragi,” Sajja et al., 2025). All of this underpins the use of SB for rapid validation of target phenotypes.

In certain species, growth-regulator treatments (cytokinin, cold shock, GA) can be used within SB to shorten generation time. In faba bean and lentil, both *in vitro* and *in vivo* approaches have confirmed the feasibility of acceleration (Mobini et al., 2015; 2016; 2020), and in pea, a simple, efficient SB procedure has been developed (Cazzola et al., 2020). These examples support the conclusion that where species- or genotype-specific bottlenecks remain, physiological and hormonal modules can bolster acceleration.

Taken together, experimentally substantiated examples justify SB on three grounds. Time: measurably more generations per year. Quality: controlled, standardized phenotyping and photothermal regulation. Integration: synergy among GS/MAS/GE and modern greenhouse—LED infrastructure. Across many species, the achievement of 4–9 generations/year, shortened vernalization, spectrum and daylength control, CO₂ supplementation, and cycle-closure techniques all indicate that SB is not only fast but also learnable, reproducible, and economically rational as a module of modern breeding (Watson et al., 2018; Zheng et al., 2013; Cha et al., 2022; O’Connor et al., 2013).

3.7.2. Environmental factors involved in speed breeding

The essence of speed breeding (SB) is to accelerate key stages of plant development by environmental control: optimizing photoperiod and light quality; managing temperature, CO₂ concentration, nutrient and water supply; tailoring substrate/pot size; applying growth regulators; and employing simple agronomic tactics. Originally developed for cereals, SB has since been extended to vegetables, legumes, thermophilic species, and short-day crops, using LED light control, greenhouses, and low-cost yet precisely regulated growth-cabinet systems (Watson et al., 2018; Bhatta et al., 2021; Cha et al., 2023).

In long-day species, 20–22 hours of light most effectively shortens time to flowering and maturity; classic protocols pair the “22/2” cycle with mild night cooling and use “sunrise–sunset” dimming at switching to reduce stress. Under such settings, wheat and barley can reach

6–8 generations per year; triticale and durum wheat respond similarly. However, excessively long or continuous light can stress certain genotypes, causing stomatal and assimilation disorders; accordingly, cyclic SB-I lighting (rather than 24/0) has become the industrial standard (Watson et al., 2018; Cha et al., 2021; Ji et al., 2022).

Successful cereal SB protocols typically use a photosynthetically active photon flux density (PPFD) of ~440–650 $\mu\text{mol m}^{-2} \text{s}^{-1}$ measured at a canopy height of 45 cm; within this range, vegetative biomass accumulation and the reproductive transition are both rapid. Too little PPFD induces etiolation and delayed flowering; too much risks leaf scorch, wilting, and poor seed set—especially in legumes, which require finer light-intensity tuning (Watson et al., 2018; Mitache et al., 2024a; Liu et al., 2022).

The red:blue ratio is generally adjusted to balance rapid biomass building (red) with compact habit (blue). Excess blue curbs elongation but may delay flowering, while far-red—by mimicking “dusk” signaling—accelerates heading/flowering in several long-day species. In triticale, increasing far-red substantially shortened generation time; in soybean, a blue–red-dominant spectrum paired with targeted temperatures enabled five generations per year (Blinkov et al., 2025; Harrison et al., 2021; Liu et al., 2022).

For short-day species, SB is a matter of strategic timing: build vegetative biomass under long days (LD), trigger induction under short days (SD), then—if needed—re-extend daylength to hasten seed fill. With LED programs, flowering time control is reliable even in short-day crops (Jähne et al., 2020). Because longer daylength can advance flowering in many species, precise photoperiod control is warranted (Ji et al., 2022).

In short-day crops (e.g., certain soybean maturity groups, hemp, pepper), flowering is hastened by preserving an uninterrupted dark phase and timing light pulses carefully: late-night light constitutes night interruption and can delay flowering, whereas disciplined short days accelerate it. With well-programmed photoperiods, annual generation number can approach five (Jähne et al., 2020; Harrison et al., 2021).

Temperature governs germination rate, the vegetative-to-reproductive transition, meiotic quality, and pollen/embryo viability. In long-day cereals, common daytime optima are ~22–25 °C with modest night cooling; in warm-season species (rice, soybean, cotton), daytime 28–32 °C can accelerate development. Large diurnal swings, however, induce stress and slow growth, so gradual transitions are preferable (Watson et al., 2018; Ficht et al., 2023; Kabade et al., 2024; Nagatoshi & Fujita, 2019).

Excess heat impairs pollen quality and embryo development, sharply reducing seed set in sensitive species (documented in strawberry model systems and multiple field crops). To avoid this, maintain stable temperatures and moderate peaks around flowering/pollination (Pipattanawong et al., 2009; Hatfield et al., 2011).

The key to shortening generation time in winter cereals is compressed vernalization. Germinating seeds surface-placed at 10 °C under a 22/2 photoperiod were vernalized in 28 days; isolated embryos allow further acceleration. The method is not universal across genotypes but marks an important step toward broad application (Cha et al., 2022; Zheng et al., 2023; Schoen et al., 2023).

In biennial onion, 12 weeks at 10 °C effectively induce floral primordia; aligning vernalization length with the subsequent photoperiod is crucial for accelerated cycles (D'Angelo and Goldman, 2019).

High stand density—via competition—can hasten flowering in several crops; cereals, pea, and soybean respond particularly well in tray systems. Although per-plant yield diminishes, generation turnover increases (Ghosh et al., 2018; Lee et al., 2023; Mobini and Warkentin, 2016).

In some species, physiologically mature green seed can be used with seed treatment and hygienic germination, though risks of fungal infection and weaker early growth rise; in onion, bulb dormancy can be broken with 15% H₂O₂ (Samineni et al., 2020; Mescouto et al., 2024; D'Angelo & Goldman, 2019).

Legumes are sensitive to excessive light intensity and heat spikes; reducing the blue fraction and holding PPFD in the mid-range often helps. In vitro/in vivo RGA can be combined with regulators (GA, 6-BAP) for rapid turnover (Cazzola et al., 2020; Mobini et al., 2015; Samineni et al., 2020).

A typical side-effect of SB acceleration is smaller plants with reduced per-plant seed production—compatible with SSD, but it must be anticipated in phenotyping. Forcing flowering via extreme nitrogen restriction or excessive density can compromise seed set (Ghosh et al., 2018; Kabade et al., 2024; Marenkova et al., 2024).

Because flowering–pollination–fertilization are heat-sensitive, peak PPFD and temperature control during the reproductive phase are critical in SB systems (Pipattanawong et al., 2009; Watson et al., 2018).

In green-seed/early-harvest cycles, high humidity elevates mold risk; strict hygiene during germination, dormancy breaking with H₂O₂ or GA when needed, shallow sowing, and avoiding overly deep covering are recommended (D'Angelo & Goldman, 2019; Kabade et al., 2024; Samineni et al., 2020).

Optimizing an SB environment is never about a single parameter. Stable short cycles arise from coordinated tuning of conditions. The primary literature above shows that modest, purposeful stress (competition, moderated N supply, controlled far-red) combined with protection of reproductive windows (stable heat/PPFD, hygiene) yields the most effective practice—calibrated by species and genotype (Watson et al., 2018; Cha et al., 2022; Blinkov et al., 2025; Kabade et al., 2024).

3.7.3. Effects of fertilizers, regulators and growth medium

The efficiency of speed breeding (SB) is strongly shaped by nutrient supply, the choice of growth regulators, and the physico-chemical properties of the growth medium. By targeted management of macronutrients (nitrogen, N; phosphorus, P; potassium, K) one can modulate the pace of the vegetative–reproductive transition, while micronutrients and complete fertilizers help sustain photosynthetic performance and seed quality during rapid cycles. Alongside these factors, the mode of nutrient delivery (root-zone vs. foliar feeding), use of hydroponic systems, pot size, and medium composition directly influence floral initiation, seed set, and total cycle length under SB (Zhang et al., 2022; Ghosh et al., 2018; Cazzola et al., 2020).

Nitrogen supplied as nitrate or ammonium accelerates vegetative growth but—depending on species and cultivar—can delay flowering. To mitigate this, N top-up should be curtailed once signs of reproductive transition appear; otherwise surplus N shifts source–sink relations and lengthens the cycle. Conversely, extreme N deficiency may trigger stress-induced early flowering that shortens the generation at the cost of yield and quality; thus both “too little” and “too much” N are to be avoided in SB (Zhang et al., 2022; Kabade et al., 2024).

Adequate—but not excessive—P and K can hasten phase change, whereas their deficiency elicits stress responses that often induce premature yet unfavorable reproduction. In rice, foliar P+K supplementation speeds development; in tomato, elevating root-zone K shortened time to ripening. Both examples indicate that targeted P/K intervention can shorten SB cycles (Kabade et al., 2024; Gimeno-Páez et al., 2025; Zhang et al., 2022).

During accelerated cycles, micronutrients (e.g., Fe, Zn, B) can become limiting for vegetative growth, photosynthesis, and seed development. Consequently, balanced complete

fertilizers and routine leaf analysis/soil-solution monitoring are recommended. Under SB conditions, deficiency symptoms manifest faster, so continuous supplementation and timely correction are critical to maintain growth rate and seed quality (Marenkova et al., 2024; Sandhu et al., 2024; Taku et al., 2024; Sajja et al., 2025; Ghosh et al., 2018).

Root-zone fertilization (in solid media) and foliar feeding differentially affect uptake and physiology; in SB, phase-adjusted combinations generally perform best. In hydroponics, fine-tuning electrical conductivity (EC), pH, and ion ratios allows more stable nutrient delivery for accelerated development and reduces the risk of over- or under-supply (Sandhu et al., 2024; Cazzola et al., 2020).

High-density tray culture (≤ 100 mL per cell) induces competitive stress that advances flowering in several cereals, pea, and soybean, while reducing seeds per plant—an acceptable trade-off with SSD. Yet overly small cells raise desiccation risk, and species-specific responses occur: in hemp and tomato, smaller pots have delayed flowering. Cell counts are often aligned with DNA-extraction plate formats to streamline genotyping workflows (Ghosh et al., 2018; Mobini and Warkentin, 2016; Zheng et al., 2023; Lee et al., 2023; Schilling et al., 2023; Gimeno-Páez et al., 2025; Marenkova et al., 2024; Jähne et al., 2020).

Chamber-controlled CO₂ enrichment typically accelerates biomass accumulation and, in several species, progression through phenophases; in soybean, five generations per year have been reported with CO₂ supplementation, and in rice, heading can be advanced. Effects are species- and genotype-specific, however: in some legumes (e.g., soybean, chickpea) the impact on flowering date is weak or absent. CO₂ should therefore be optimized alongside, not instead of, light and temperature (Nagatoshi and Fujita, 2019; Tanaka et al., 2016; Ghosh et al., 2018).

Regardless of form (NO₃⁻/NH₄⁺), nitrogen drives vigorous vegetative growth and may delay flowering; thus, after the onset of reproductive transition, throttling N supply is advisable. By contrast, potassium and phosphorus generally accelerate flowering and maturation—both deficiency (stress-induced flowering) and adequate supply can shorten the cycle. In rice, foliar K/P feeding is part of the “SpeedFlower” protocol (Zhang et al., 2022; Kabade et al., 2024; Ghosh et al., 2018).

Hidden micronutrient deficiencies are more likely under accelerated development; continuous monitoring and comprehensive micronutrient supplementation prevent physiological disorders and growth slowdowns. Root-zone and foliar application are especially

important in SB, and hydroponics offers precise nutrient control—even for legumes (Cazzola et al., 2020; Sandhu et al., 2024; Marenkova et al., 2024).

In rice, a high-density tray system designed for rapid turnover achieved stable 95–100% emergence and 90–105-day harvests with “minimalist” fertilization—the keys were density and disciplined nutrient/water management, not over-fertilization (Collard et al., 2017).

Shallow, low-volume cells can precipitate faster phenophase advancement—competition and moderated nutrient/water limitation hasten floral induction—while reducing per-plant seed production, again compatible with SSD. Cells that are too small, however, dry quickly and curb growth; cell volume and irrigation frequency must therefore be harmonized (Ghosh et al., 2018; Mobini and Warkentin, 2016; Marenkova et al., 2024).

Nutrient-poorer media (e.g., sand) may accelerate flowering in some species, whereas adding coconut coir delayed germination in rice. Practical recommendations on medium volume and mineral composition are now included in several protocol appendices (Kigoni et al., 2023; Sandhu et al., 2024).

Tray dimensions are often matched to DNA-extraction plate layouts, accelerating marker-assisted selection and logistics (Jähne et al., 2020).

The chemical–physical traits of the medium also modulate vegetative phase length in SB. In sand—serving as a nutrient-poor medium—the vegetative period has often shortened, whereas coconut coir has delayed germination. These observations point to the fine regulatory role of medium-induced nutrient and water stress; given cultivar- and species-specific response curves, local pilot tests should precede full deployment (Kigoni et al., 2023; Sandhu et al., 2024).

Gibberellic acid (GA) is the most widely used agent in SB for rapidly breaking seed dormancy; excessive use, however, can cause hypocotyl/epicotyl elongation that complicates seedling logistics. In pea, GA-biosynthesis inhibitors produced compact stands better suited to high density without yield loss. Under accelerated conditions, cytokinins promoted pollen germination and earlier seed set—direct advantages for cycle shortening (Lulsdorf and Banniza, 2018; Watson et al., 2018; Mobini and Warkentin, 2016; Mobini et al., 2020; Kabade et al., 2024; Marenkova et al., 2024; Jähne et al., 2020).

In faba bean (*Vicia faba* L.), cytokinin (6-BAP) treatment hastened fertilization; in pea, the GA-biosynthesis inhibitor flurprimidol yielded compact plants without yield penalty—

especially useful where headroom and light distribution are limited (Mobini et al., 2015; Mobini et al., 2020; Mobini and Warkentin, 2016).

In hemp, fast cycling often results in a predominance of pistillate flowers, which complicates selfing; silver nitrate/sodium thiosulfate treatment can induce stable staminate flowers within ~14 days, enabling SB-compatible selfing and hybrid production (Schilling et al., 2023).

Although SB is fundamentally an *in vivo*, environment-driven technique, in certain cases *in vitro* PGR combinations and trace-element supplements (e.g., daminozide, CuSO₄) have improved developmental tempo in cereals—especially useful in embryo-culture-based shortening when seed-maturation phases must also be compressed (Miroshnichenko et al., 2021; Mobini et al., 2020; Mobini and Warkentin, 2016).

Under extended photoperiods and higher light intensity, CO₂ enrichment is commonly applied, particularly in soybean; while this accelerates biomass accumulation and the generative transition, it simultaneously raises nutrient demand and the risk of relative deficiencies. Hence, in CO₂-enriched SB systems, even tighter, cycle-by-cycle tuning of solution EC/pH and leaf/tissue analytics is warranted (Nagatoshi and Fujita, 2019; Gamage et al., 2018).

Medium and nutrient settings do not generalize readily across species and genotypes. The same pot size or medium composition that is beneficial in cereals may delay development in tomato and hemp. Therefore, in SB, local pilot testing and iterative fine-tuning of environmental, nutritional, and PGR parameters are essential to achieve genuinely short cycles with stable seed yield (Ghosh et al., 2018; Schilling et al., 2023; Gimeno-Páez et al., 2025).

3.7.4. Agrotechnical components

In speed breeding (SB) cycles, agrotechnical interventions aim to control the timing of phenophases and enhance stand uniformity: synchronizing flowering and maturation with crossing windows, accelerating generation closure (early harvest, forced drying), and breaking post-harvest seed dormancy for prompt resowing. In practice, these measures are paired with high-density tray culture and targeted morphological manipulations (e.g., removal of lateral shoots), which integrate well with SSD and have been shown across several species to shorten the cycle—especially when seed is harvested before full maturity and forcibly dried, then the next round is initiated as needed by embryo rescue or dormancy breaking (González-Barrios et al., 2021; O'Connor et al., 2013; Samineni et al., 2020).

Removing lateral shoots while retaining the main stem advances flowering by a few days (on average $\leq \sim 5$ days) in several cereals, yielding more uniform and earlier maturity; however, seeds per plant decline, and at large scale the operation is labor-intensive (Tanaka et al., 2016; Song et al., 2021; Marenkova et al., 2024; Rana et al., 2019).

In tomato, agronomic treatments (e.g., truss management, stand density, water and nutrient profiling) combined with embryo rescue have demonstrably shortened generation time under SB; the strategy centers on rapidly concluding the reproductive phase and finishing seed maturation *ex situ* under laboratory conditions (Gimeno-Páez et al., 2025).

One of the most effective agrotechnical accelerators is the gentle forced drying of seed/fruit harvested typically 10–20 days after flowering: in oat, combining “early panicle harvest” with SB significantly reduced generation time; in cowpea, new generations were successfully initiated from seeds obtained from oven-dried, immature pods (González-Barrios et al., 2021; Edet and Ishii, 2022).

When forced drying entails viability risks (species/cultivar dependent), isolating embryos and growing them on nutrient media can yield transplantable seedlings within 10–20 days; this has been validated in several species—pea, cereals, sunflower, and safflower—though the approach is equipment-intensive (Mobini and Warkentin, 2016; Gimeno-Páez et al., 2025; Zheng et al., 2023; Rogo et al., 2023).

Post-harvest seed dormancy is a frequent issue in SB. It can be shortened by stratification, seed warming, GA treatment, or CaCl_2 priming. In onion, 15% H_2O_2 effectively breaks bulb dormancy. Sowing green (but fully developed) seed has accelerated turnover in chickpea and soybean; however, germination may be weaker due to fungal infection, and early growth slower because of smaller seed reserves; overly deep sowing further delays establishment (Finch-Savage and Leubner-Metzger, 2006; Samineni et al., 2020; Mescouto et al., 2024; D’Angelo and Goldman, 2019; Kabade et al., 2024).

One of the most effective means of hastening maturation is variance reduction. Lateral-shoot removal, high plant density, and disciplined timing of water and nutrient supply together bring earlier and more homogeneous ripening. The trade-offs are reduced seeds per plant and increased labor; these methods are therefore most appropriate where the goal is rapid generation turnover rather than maximizing per-plant seed yield (Tanaka et al., 2016; Ghosh et al., 2018; Marenkova et al., 2024; Lee et al., 2023).

3.7.5. Embryo culture, genetic approaches, and the application of genetic engineering

Speed breeding is not solely about environmental control of phenophases: further cycle compression and accelerated genetic gain are achieved by integrating embryo culture (early harvest, embryo rescue), in vitro–assisted SSD/RGA procedures, doubled-haploid (DH) technology, as well as MAS/GS and gene-technology modules (CRISPR/TALEN). By reducing genotype \times environment noise and tightening generation turnover, time is saved in line development, backcrossing, and rapid validation of target genes (Watson et al., 2019; Prasanna et al., 2012; Li et al., 2018; Shan et al., 2013; Liu et al., 2021).

Cycles can be shortened by weeks when plants are regenerated in vitro from embryos of seed harvested early—particularly at stages where forced drying carries high viability risk. Embryo rescue is a classical tool in several legumes and oilseed crops (e.g., lentil, sunflower) and works reliably under SB provided sterile technique, medium composition, and timing are rigorously controlled (Rogo et al., 2023; Bermejo et al., 2016).

In vitro–assisted single-seed descent (iv-SSD)—laboratory germination and miniaturized cultivation—can “seamlessly” advance successive generations; in chickpea, rapid generation advance (RGA) has enabled as many as seven generations per year. These approaches are especially effective in SB when environmental accelerators are combined with a laboratory closure module (Pazos-Navarro et al., 2017; Samineni et al., 2020).

DH platforms (e.g., in maize) offer “one-step” production of homozygous lines; coupled with SB, they permit rapid rotation of donor and recurrent backgrounds, fast pre-advancement of DH donors, and cycle-by-cycle intensification of backcrossing. Scalability is species- and genotype-dependent (Prasanna et al., 2012; Rogo et al., 2023).

Marker-assisted selection (MAS) delivers immediate time savings by culling unwanted allele carriers early. In rice, SNP-based MAS + SB produced salt-tolerant lines (*hst1*); in wheat, targeted introgression of the *Glu-B1i* allele was accelerated on SB + MABC platforms; in canola, haplotype-level introgression and gene pyramids have been implemented under accelerated conditions (Rana et al., 2019; Cha et al., 2024; Song et al., 2021; Baloch et al., 2024).

Genomic selection (GS) estimates breeding values (GEBVs) from genome-wide marker profiles and predictive models. The largest time savings arise when both the training population and candidates are phenotyped under SB in a uniform, rapid environment. In wheat, SB was

shown to shorten the F_2 – F_8 phase, and GS-based selection delivered faster genetic gain (e.g., yield, FHB resistance) than classical phenotypic selection (Watson et al., 2019; Nannuru et al., 2025; Voss-Fels et al., 2019).

A controlled SB environment reduces environmental variance, increasing the power of QTL mapping and GWAS; in wheat, high-throughput root phenotyping (root angle, root mass) and rapid assessment of adult leaf-rust resistance have been reported. Developmental-genetics studies in spring barley under SB conditions have identified new candidates governing flowering and growth (Richard et al., 2015; Riaz et al., 2016; Rossi et al., 2024).

SB cycles also enable rapid “clean-up” of transformed/edited events (removal of helper constructs, background homogenization). CRISPR/Cas9 and TALEN case studies (rice: resistance to bacterial leaf blight; tomato: reduced ethylene for improved shelf life) show that practical deployment of gene targets is shortened when paired with SB. Recent reviews explicitly highlight SB \times GE (gene editing) synergy as an industrial-scale solution (Shan et al., 2013; Liu et al., 2021).

The regulatory status of gene-edited crops varies by jurisdiction (e.g., in some cases classified as non-GMO, elsewhere subject to stricter authorization), which affects the practical pace of SB \times GE integration. Streamlined procedures can hasten market entry, but country-specific compliance remains necessary (Waltz, 2016; Bogatyreva et al., 2021).

3.7.6. Practical application of speed breeding

Speed breeding (SB) is an acceleration module that saves time across the pipeline—from crosses, through SSD and backcrossing, to MAS/GS cycles, and even the “clean-up” of gene-edited lines. A controlled photothermal environment—photoperiod, spectrum, PPFD, temperature, CO_2 —both synchronizes flowering and seed set for hybridization and creates a standardizable phenotyping background for early selection and genetic/physiological experiments. In practice, this yields 4–9 generations per year (species-dependent), shorter BC cycles, and orders-of-magnitude cheaper “pre-screening” prior to field deployment (Ghosh et al., 2018; Samineni et al., 2020; Watson et al., 2018).

Under SB conditions, synchronization of flowering can be ensured uniquely both within and across genotypes (Watson et al., 2018; Chiurugwi et al., 2019). This is particularly important in dioecious species such as hemp (Schilling et al., 2023). Synchronization enables a large number of crosses—even among distantly related parents; seed set is typically high, and F_1 seed shows good germinability (Watson et al., 2018; Marenkova et al., 2024). From

generation to generation, germination and the timing of phenological phases remain stable under SB (Watson et al., 2018).

In short-day species (soybean, pepper, hemp), LED-programmed LD–SD–LD staging reliably times floral induction and seed set, allowing alignment of parental flowering; in rice, a detailed, large-scale protocol demonstrated the same in greenhouses. Avoiding heat and light peaks during the reproductive window protects pollen and embryo viability, which is especially critical for targeted crosses (Jähne et al., 2020; Kabade et al., 2024; Pipattanawong et al., 2009).

SB is an ideal framework for SSD/SPS: in high-density trays, segregating generations can be advanced rapidly, so inbred parents required for hybridization can be produced within 1–2 years. Backcross (MABC) generations can likewise be “compressed,” as shown for targeted introgression of the *Glu-B1i* allele; a whole-genome “speed introgression” platform has been described for *Aegilops tauschii*–wheat transfers (Samineni et al., 2020; Cha et al., 2024; Li et al., 2024).

3.7.6.1. Hybrid production

When crossing encounters biological constraints (weak or unpredictable flowering), hybrid production can be aided by floral-induction methods; for example, in cassava, grafting was used to induce inflorescences, opening a crossing “window” under SB. After fertilization, early seed harvest plus embryo rescue saves days to weeks to the next generation and has become routine in several crops (Ceballos et al., 2017; Rogo et al., 2023; Gimeno-Páez et al., 2025).

In hybridization, SB times events (flowering windows, shortened vernalization, sex manipulation); in selection, it stabilizes conditions (uniform environment, early phenotyping); in genetic studies, it improves quality (larger samples, less noise); and in biotechnology, it expedites clean-up (rapid BC cycling, segregation). The greatest gains arise when environment and workflow are both “time-optimized”—especially true for MAS/GS and GE integration and LED-controlled photoperiod strategies (Watson et al., 2018; Cha et al., 2024; Li et al., 2024; Rogo et al., 2023; Jähne et al., 2020).

In hemp, integrating silver-ion treatments into the SB cycle induces stable staminate flowers on pistillate genotypes within a few weeks, enabling selfing and controlled hybridization in small spaces with rapid cycles (Schilling et al., 2023).

The hybridity of F₁S can be verified with molecular markers (Mobini and Warkentin, 2016; Stetter et al., 2016; Edet and Ishii, 2022) or with biochemical (protein) markers (Aydin et al., 2024). In some crops, DNA can be obtained from part of the seed while preserving the embryo,

allowing culling of undesired lots before sowing (Gangashetty et al., 2024). Phenotypic confirmation is also possible when crossing a maternal genotype carrying a recessive trait with a paternal genotype carrying the dominant allele (Edet and Ishii, 2022). Hybrid verification is especially important in small-flowered species with uncertain crossing efficiency, such as amaranth (Stetter et al., 2016) and soybean (Nagatoshi and Fujita, 2019).

For segregating hybrids to pure lines, SSD is ideal under SB. A typical schedule is: following hybridization, produce a large quantity of F₁ seed in cycle 2; in cycle 3, sow all seed (250–1000); then for 3–4 further cycles, resow one seed per plant. This rapidly generates lines at scale for breeding evaluation and genetic studies (Watson et al., 2018; Ficht et al., 2023; Aydin et al., 2024).

When creating recombinant inbred lines (RILs) for genetic purposes, parallel selection is avoided to prevent bottlenecks (Mobini and Warkentin, 2016). For breeding-oriented line development, by contrast, phenotypic selection is feasible for traits that show strong SB–field correlation. Alongside classical visual/manual phenotyping, modern digital phenotyping can be applied (Alahmad et al., 2018; Watson et al., 2018). Selection in segregating populations can also be supported by genetic typing (Watson et al., 2018). To facilitate this, it is practical to sow into 96-cell trays that align with 96-well plates used for DNA extraction and PCR. Selection may target single traits or combinations (Alahmad et al., 2018). Certain traits—e.g., yield, abiotic-stress tolerance—cannot be assessed reliably under SB and must ultimately be tested in the field (Watson et al., 2018).

Line development can be conducted entirely under SB from hybridization to the final generation (Mobini and Warkentin, 2016; Somody and Molnár, 2025), or partially—for example, accelerating only early generations (Alahmad et al., 2018), or performing hybridization under conventional conditions followed by SB-based inbreeding (Mitache et al., 2024b; Sandhu et al., 2024). SB can also be used for cultivation outside the natural growing season (Batista et al., 2024).

To date, rapid production of breeding and RIL lines has been demonstrated in bread wheat (Hickey et al., 2010, 2012; Cha et al., 2022; Batista et al., 2024), durum wheat (Alahmad et al., 2018), lentil (Lulsdorf and Banniza, 2018; Mitache et al., 2024b), peanut (O’Connor et al., 2013), hemp (Somody and Molnár, 2025), rice (Sandhu et al., 2024), chickpea (Croser et al., 2021), and pea (Mobini and Warkentin, 2016; Cazzola et al., 2020).

3.7.6.2. Selection breeding

Genomic selection is among the most promising strategies compared with conventional methods. Today, high-throughput SNP and NGS-based platforms enable cost-effective genotyping of large, segregating populations (Li et al., 2018). Its advantages include effectiveness for quantitative traits controlled by many loci of small individual effect (e.g., yield, resistance to certain diseases)—traits whose phenotyping is often deferred to later stages (Watson et al., 2019; Pandey et al., 2022; C eran et al., 2024; Nannuru et al., 2025). Additional benefits are the rapid identification of high breeding-value lines, shorter breeding cycles, and savings in resources (Watson et al., 2019; Pandey et al., 2022; C eran et al., 2024).

The method hinges on comprehensive phenotyping and genotyping of a large training population with genome-wide DNA markers, followed by the computation of genomically estimated breeding values (GEBVs) for complex traits. Predictive models fitted to the phenotype and genotype data can capture the trait’s full genetic variance. Using these models, candidate populations—once genotyped—are evaluated, and the highest-GEBV lines are selected (Watson et al., 2019; Pandey et al., 2022; C eran et al., 2024).

In wheat, high-throughput root phenotyping and rapid assessment of adult leaf rust resistance have been described under SB (Richard et al., 2015; Riaz et al., 2016; Richard et al., 2018). In rice, combining SNP-based MAS with SB improved salt tolerance efficiently, demonstrating that marker screening saves internal cycle time and focuses phenotyping capacity on truly promising candidates. In peanut, SB was implemented in an industrial setting, where MAS and accelerated generation turnover together enabled a shortened pipeline (Rana et al., 2019; O’Connor et al., 2013).

Both theoretical and empirical studies show that coupling rapid generation advance with GS accelerates genetic gain; in tropical rice, GWAS-informed prediction models were linked to selection, while simulations in wheat for FHB resistance showed advantages for SB+GS schemes (Spindel et al., 2016; Voss-Fels et al., 2019; Nannuru et al., 2025). The combination increased genetic gain in bread wheat for yield (Watson et al., 2019) and for resistance to Fusarium head blight (Nannuru et al., 2025), outperforming purely phenotypic selection (Nannuru et al., 2025).

Numerous experiments confirm strong correlations between SB and field measurements of disease resistance after artificial inoculation. In wheat, responses to leaf rust measured under SB showed high concordance with field results (Riaz et al., 2016). Similarly, close correlations

were found for *Fusarium* head blight and yellow spot (Dinglasan et al., 2016; Chhabra et al., 2024). Sensitive genotypes often display more pronounced symptoms under SB, which facilitates scoring (Chhabra et al., 2024). This is because inoculation success in the field is weather-dependent, whereas SB allows control of temperature and humidity, promoting pathogen development (Hickey et al., 2012). Mycotoxin accumulation in grain may also be more active under SB (Chhabra et al., 2024). A major advantage is that up to six consecutive resistance tests per year can be performed under SB, versus a single cycle in the field (Riaz et al., 2016).

Selection for complex, multi-pathogen resistance is also feasible, enabling identification of <5% resistant plants in segregating populations. This requires repeated inoculations with a pathogen complex throughout the growth period under accelerated development (Hickey et al., 2017). Inoculation must target the infection stage characteristic of the pathogen; using the wrong stage may yield spurious conclusions about resistance/susceptibility (Hickey et al., 2012). For greater accuracy, a panel of the most virulent isolates is recommended instead of a single strain (Hickey et al., 2017).

Artificial inoculation demands optimal environmental conditions. Several studies indicate that extended photoperiods and 22 °C day / 18 °C night do not inhibit pathogen growth; to improve infection rates, moderate temperature reduction and raising relative humidity to 100% are recommended. Inadequate settings can produce misleading signals (Hickey et al., 2012, 2017).

After SB selection of segregating populations under artificial disease pressure, lines also show comparable resistance in the field. The method's accuracy often exceeds that of MAS alone, because not all resistance genes are known. When robust markers exist, the ideal is parallel molecular and phenotypic selection (with artificial infection) (Hickey et al., 2012, 2017).

For reliability, prior calibration is necessary: test known resistant standard cultivars and establish SB–field correlations. Each segregating population's assessment should include control cultivars to avoid erroneous conclusions stemming from flawed growth/inoculation conditions (Hickey et al., 2011, 2012, 2017).

Because environmental parameters in SB differ markedly from field conditions, most purely phenotypic selections cannot be performed exactly as in conventional breeding. For example, data showed no correlation between awn length and the number of glumes per spike

under field versus SB in wheat (Cha et al., 2023). Conversely, several traits that still express under SB correlate closely with field performance and can therefore be selected efficiently in the accelerated system. A further advantage is that conditions are constant between SB generations, so trait expression is not contingent on meteorological fluctuations (Watson et al., 2018).

To determine whether a trait can be selected under SB, preliminary experiments are carried out with collections that express the target trait to different degrees. These studies compare SB phenotypic performance with multi-year field observations (Hickey et al., 2009; Watson et al., 2018).

3.7.6.3. Gene introgression

SB is widely used to introgress genes rapidly into existing cultivars and hybrid parent lines. Near-isogenic lines (NILs) can be produced by serial backcrossing (Cha et al., 2024). Gene pyramids can be assembled by crossing NIL lines that each carry different, targeted loci in the same cultivar background (Baloch et al., 2024). Because SB combines excellently with marker-assisted selection, individuals lacking the desired allele can be culled quickly (Watson et al., 2018; Rana et al., 2019; Song et al., 2021; Cha et al., 2024; Taku et al., 2025). For many traits, SB correlates well with field conditions, allowing phenotypic and marker-based selection to proceed in parallel (Hickey et al., 2009, 2017; Alahmad et al., 2018). SB enables not only the introgression of single alleles (Cha et al., 2024), but also of haplotypes (Song et al., 2021), the construction of gene pyramids (Alahmad et al., 2018; Baloch et al., 2024), and allele replacement (Taku et al., 2025).

Beyond marker-assisted checks, introgression can be verified by resequencing the backcrossed individuals or by assessing similarity to the recurrent parent using KASP or SSR markers (Rana et al., 2019; Song et al., 2021; Cha et al., 2024; Taku et al., 2025; Wang et al., 2025). Selecting plants with the highest genome proportion ($\geq 90\%$) matching the recurrent parent minimizes background effects on key agronomic traits, allowing the target trait to be examined more cleanly while preserving the original cultivar's performance (Rana et al., 2019; Cha et al., 2024). Marker-based tracking of recurrent genome proportion reduces the number of required backcrosses: selection can stop once the desired level is restored (Taku et al., 2025).

Examples illustrating SB's efficiency for introgression include: in wheat, incorporation of *Glu-B1* allele variants to improve gluten quality (Aydin et al., 2024; Cha et al., 2024); in rice, introgression of *hst1* to create salt-tolerant lines (Rana et al., 2019); in canola, incorporation of

the *BnaA9.CYP78A9a* haplotype and loci *CRA3.7*, *CRA08.1*, *CRA3.2* for high yield and clubroot resistance (Song et al., 2021; Baloch et al., 2024); in cotton, introgression of *iaaM* to directly improve fibre fineness and yield (Wang et al., 2025); and in green soybean, replacement of *Lox2* with *lox2* to eliminate lipoxygenase-2 synthesis responsible for the “beany” flavour (Taku et al., 2025).

3.7.6.4. Genetic research

SB enables the rapid, laboratory-based screening of gene-bank and mutant collections for the many traits detailed above (Hickey et al., 2009, 2012; Watson et al., 2018; Cha et al., 2023), including crop duration and plant height (Watson et al., 2018; Cha et al., 2023), morphological characters (Watson et al., 2018), pathogen resistance (Hickey et al., 2012, 2017), and product quality (Hickey et al., 2009). To confirm trait expression, evaluations can be conducted across multiple successive cycles. Rapid scanning under SB facilitates the selection of donors for economically important traits and the identification of new allelic variants for breeding programs (Li et al., 2018).

SB also supports the development of recombinant inbred lines (RILs) for gene mapping and marker identification (Christopher et al., 2015; Mobini and Warkentin, 2016; Sandhu et al., 2024). These lines can be mapped directly under SB conditions (Hickey et al., 2011). In addition, SB rapidly fixes traits with simple (monogenic) inheritance into homozygous state (Somody et al., 2024).

Rapid introgression of target alleles via SB combined with marker-assisted selection facilitates the creation of near-isogenic lines for gene-effect studies. By tracking the recurrent-parent genome proportion, true NILs can be obtained quickly, minimizing donor-genome remnants that could confound the effect of the introgressed allele (Song et al., 2021; Cha et al., 2024; Taku et al., 2025).

Targeted manipulation of lighting and growth conditions under SB materially influences vegetative growth rate and trait expression. Such conditions are conducive to GWAS for uncovering QTLs controlling flowering time and crop duration, and for identifying candidate genes (Choi et al., 2023; Rossi et al., 2024).

A core topic in cytogenetics is the behavior of chromosomes during meiosis, which requires buds containing young, immature pollen (Alexandrov et al., 2022). SB rapidly provides sufficient bud material and is therefore effective for generating cytogenetic material.

Although few cytogenetic studies have used SB to date, investigations in wheat and in wheat–rye hybrids contrasting at the Ph1 locus showed no differences in chromosome pairing and recombination in meiotic metaphase I between material grown under SB versus conventional conditions. Both wheat and wheat–rye hybrids proved cytologically stable under SB (Watson et al., 2018).

SB also facilitates distant hybridizations; in later segregating generations, the size and frequency of incorporated segments can be tracked by FISH analysis. Karyotyping can be conveniently performed from selected root tips of tray-grown plants (Li et al., 2024).

3.7.6.5. Biotechnological and plant physiological research

SB functions as an experimental platform with which species-specific photoperiod thresholds, spectral effects, and temperature optima can be charted (Blinkov et al., 2025; Liu et al., 2022; Pipattanawong et al., 2009).

In many crops, the production of transgenic or gene-edited plants requires donor explants; in most cereals, the optimal starting material is the immature embryo (Ishida et al., 2007; Shimizu-Sato et al., 2020; Miroshnichenko et al., 2021). SB accelerates the production of donor embryos and is therefore a valuable tool in biotechnological research. Current results indicate that barley embryos developed under SB exhibit high morphogenetic potential and transformation efficiency comparable to that of conventionally grown plants (Watson et al., 2018).

A further advantage is the rapid advancement and seed production of the T_0 generation, enabling the earliest possible sowing and evaluation of segregating T_1 populations. Homozygous transgenic or edited plants can be phenotyped under SB while assessing their impact on key agronomic traits (Watson et al., 2018; Hatta et al., 2021).

SB also supports distant hybridization. Although such crosses may suffer post-zygotic incompatibility leading to embryo abortion, SB promotes the formation of viable embryos suitable for rescue, thereby broadening genetic diversity (Li et al., 2024).

The accelerated development in SB allows rapid investigation of growth responses to diverse factors. By targeted manipulation of light intensity (Liu et al., 2022), spectrum (Jähne et al., 2020), and photoperiod (Schilling et al., 2023), plant photobiology can be studied. In agrochemical experiments, macro- and micronutrient requirements of cultivars and their effects on final yield can be measured efficiently (Sandhu et al., 2024). Under customized conditions,

certain physiological studies—such as the biosynthesis of pigments during fruit ripening—can also be accelerated (Ma et al., 2024).

3.7.7. Prospects and limitations of speed breeding

The strategic promise of speed breeding (SB) lies in accelerating genetic gain by increasing the number of annual cycles—and thus tightening selection intervals—especially when integrated with genomic selection (GS), marker-assisted selection (MAS), and targeted crossing. In such “time-optimized” pipelines, shorter generation turnover and high-throughput genotyping reinforce one another, as demonstrated in cereals and legumes. Nevertheless, SB does not replace field evaluation: yield and abiotic stress tolerance still require multi-location, multi-year validation, because photothermal chamber/greenhouse environments only partially model G×E interactions (Watson et al., 2018; Li et al., 2018; Hickey et al., 2019).

Infrastructure and energy are the largest SB cost components: precise control of lighting and cooling—providing the required photoperiod, spectrum, and temperature profile—typically accounts for more than half of expenditures. This “bottleneck” is eased by low-cost, LED-only modular systems (the “Speed Breeding III” concept), which still deliver 4–5 generations per year, and by photothermal greenhouse systems developed for rice that, combined with dense tray culture and minimalist nutrient programs, enable stable, low-cost operation (O’Connor et al., 2013; Collard et al., 2017; Watson et al., 2018).

In lighting, near-term innovation will center on fine spectral programming (R:FR ratio, blue/green fractions) and photoperiod architecture: in triticale, enhancing the far-red component shortened generation time; in pepper, tailored light environments reduced time to ripening; and in short-day species, LED-controlled SD/LD staging is pivotal. While these approaches accelerate development, they can carry agronomic trade-offs (stem elongation, lodging risk, poor seed set), necessitating cultivar- and goal-specific calibration (Blinkov et al., 2025; Liu et al., 2022; Jähne et al., 2020).

CO₂ enrichment generally increases photosynthetic capacity and vegetative biomass and, in several species—e.g., soybean—can raise generational tempo toward ~5 per year. However, effects on flowering time are genotype/species dependent, and unfavorable interactions can arise under extreme light or heat profiles. Accordingly, CO₂ should be optimized together with, not instead of, light and temperature settings (Nagatoshi and Fujita, 2019; Kabade et al., 2024).

Crops with vernalization requirements (winter cereals, biennials) pose one of SB’s most persistent constraints. Speed vernalization (germinating seeds at ~10 °C under long days) can

reduce chilling to ~28 days and works in several winter cereals, but genotypic variance is large: some winter wheats still fail to flower on time. In biennial root crops and sugar beet, partial genetic/physiological “threshold relaxations” and novel vernalization phenotypes are promising, yet broad applicability remains uncertain (Cha et al., 2022; Schoen et al., 2023; Kuroda et al., 2024).

Heat peaks are a general risk for the reproductive phase: sustained temperatures ≥ 33 °C can reduce pollen viability, increase male sterility, and impair seed set in crops such as soybean and rice. Classic and recent studies therefore support keeping temperature profiles within a narrow band, programming gentle light/temperature transitions, and protecting the flowering–pollination–fertilization window—key to SB quality assurance (Dupuis and Dumas, 1990; Watson et al., 2018).

Further acceleration comes from early seed harvest and embryo-rescue modules. In soybean, early harvesting and germination shortened cycles; in cereals and oat systems, early panicle/spike harvest added days; post-hybridization embryo rescue is routine in several crops—including maize and vegetables. Efficacy hinges on adhering to precise DAP windows and stringent hygiene/conditioning protocols (Mescouto et al., 2024; Rogo et al., 2023).

Accelerated workflows also open new genetic toolkits. A standardized whole-genome “speed introgression” platform is documented for *Aegilops tauschii* → wheat transfers; SB+MAS frameworks have been developed for backcross (MABC) introgression (e.g., targeted incorporation of the wheat *Glu-B1i* allele). “Clean-up” of gene-edited transformants (helper-construct removal, background homogenization) is noticeably faster under SB (Li et al., 2024; Cha et al., 2024; Ishida et al., 2007).

For selection and early phenotyping, SB’s controlled background reduces environmental variance, improving signal-to-noise. Large-sample root-architecture phenotyping and rapid assessment of adult leaf-rust resistance in wheat shifted allele frequencies already in early generations; GS modeling—including stochastic simulations for FHB resistance—indicates that SB-coupled GS yields cycle-time savings and faster genetic gain (Richard et al., 2015; Riaz et al., 2016; Nannuru et al., 2025).

The inclusion of short-day and/or hard-to-flower crops is a bellwether for SB’s future reach. With LED-controlled short days and avoidance of night breaks, reliable floral induction is achievable in multiple short-day species; in hemp, silver-based sex-reversal enables selfing and controlled hybridization. In perennials with long juvenile phases, graft-based floral

induction has yielded promising reductions (cassava) (Jähne et al., 2020; Schilling et al., 2023; Ceballos et al., 2017).

Standardization and knowledge transfer will likely accelerate adoption: in rice, a detailed SpeedFlower protocol exists (indica/japonica); in oat, “Single-Seed-SpeedBulks” integrates cost-effective SSD with SB; and “SpeedyPaddy” off-season rotation cheaply scales generation advancement. By unifying light/heat/nutrient parameters and workflows, these recipes lower entry barriers and facilitate inter-institutional protocol transfer (Kabade et al., 2024; Kigoni et al., 2023; Sandhu et al., 2024).

Industrial embedding is no longer merely prospective: in peanut breeding, SB is now part of commercial pipelines, with practical experience indicating that >50% of costs stem from climate control—further arguing for LED-based modular systems. Programs must, however, account for room adaptation and photoperiod-specific selection bias; thus SB-selected materials require indispensable, multi-site outdoor post-validation (O’Connor et al., 2013; Watson et al., 2018).

Protocol fine-tuning remains timely, especially to identify factors that further shorten vegetative duration. At present, one SB generation ranges from a few months (crop-dependent) up to a year (D’Angelo and Goldman, 2019; Kuroda et al., 2024). Drought stress is a potentially underexploited physiological lever that can hasten development (Anjum et al., 2017). The key is to craft conditions that accelerate while preserving optimal physiological status, sustaining high seed yield and quality across cycles. Additional priorities include reducing genotype dependence and overcoming technical bottlenecks—for example, providing alternatives to embryo-culture-dependent protocols.

Developing further accelerated procedures can reduce reliance on model organisms and refocus on economically important crops. While *Arabidopsis* benefits from an extremely short life cycle, SB can cut wheat’s vegetative phase to roughly two months—already comparable to *Arabidopsis* (Watson et al., 2018).

Even so, SB cannot replace field breeding and variety trials, since controlled conditions differ markedly from target field environments. Nonetheless, several positive correlations have been documented—for disease resistance (Hickey et al., 2012, 2017), plant height (Watson et al., 2018; Cha et al., 2023), and morphological traits (Watson et al., 2018).

In sum, SB cannot substitute for field phenotyping of certain traits (Somody and Molnár, 2025). Given its relatively short history, it is currently used mainly for the rapid production of

pure lines and RILs (Batista et al., 2024; Mitache et al., 2024b; Somody and Molnár, 2025) and for gene introgression (Song et al., 2021; Cha et al., 2024; Taku et al., 2025). Its role is expected to expand in other applied and basic research arenas. SB is also an excellent platform for student training—hybridization, line development, evaluation and selection, creation of mapping populations—since modern BSc/MSc/specialist/PhD programs of 2–4 years are often too short to generate and study pure lines using conventional methods (Bhatta et al., 2021; Wanga et al., 2021).

Another potential use is accelerated pre-evaluation of developed cultivars and hybrids to speed registration and support faster replacement pipelines. Currently, DUS testing (distinctness, uniformity, stability, and novelty) takes roughly three years. In principle, uniformity and stability could be estimated under SB by recording morphological descriptors—e.g., presence/absence of awns, growth rate, plant height—across two consecutive generations; only non-segregating candidates would then proceed to field testing. This could materially streamline registration (Jamali et al., 2020).

The long-term outlook for SB is strong but differentiated. In short-season, long-day selfers and several legumes the technology is mature; in short-day, warmth-loving vegetables and biennials it can be extended gradually via control/physiological modules (LED programming, vernalization, hormonal interventions, CO₂ enrichment). Major constraints—energy/equipment demand, genotype-dependent compatibility, reproductive sensitivity, and the G×E gap—can be mitigated by protocol standardization and by integrating MAS/GS and genome-editing-based introgression (Cha et al., 2022; Li et al., 2024; Jähne et al., 2020).

3.7.8. Speed breeding of hemp

Alongside hop, hemp was among the first plants in which photoperiodic control of flowering was demonstrated (Kobayashi and Weigel, 2007). Substantial variation exists in flowering time among *C. sativa* cultivars, including day-length–neutral or “autoflowering” types that are photoperiod-independent and capable of flowering under continuous light. These cultivars mature more rapidly and are generally shorter, enabling cultivation even in northern countries (Stack et al., 2021).

Speed breeding (SB) of hemp (*Cannabis sativa* L.) has, in recent years, become one of the most effective tools for drastically shortening generation time and accelerating genetic gain through deliberate manipulation of photoperiod sensitivity and controlled environmental conditions. Its importance is heightened by the multi-purpose value chains of industrial hemp

(fiber, grain/oil, specialized metabolites) and by the European regulatory environment—particularly the uniformly applied 0.3% THC threshold since 1 January 2023—which demands precise, rapid, and reliable selection systems. SB is therefore not an end in itself, but the engine of modern, genomically informed cultivar development and regulatory compliance (Schilling et al., 2023; European Commission, 2023).

A hemp-adapted, fully documented SB protocol reports that plants flower, are pollinated, and set seed after ~2 weeks of continuous light followed by a short-day phase (~4 weeks), with seed maturation again under constant light and mild water stress; in this way a ≤ 9 -week seed-to-seed cycle and up to five generations per year are attainable. The 22 h light / 2 h dark photoperiod, widely adopted in long-day/day-neutral crops, likewise accelerates floral induction and the overall cycle when coupled with temperature, light-intensity, and nutrient management. The protocol operates routinely in greenhouses or growth chambers with programmable LED lighting (Schilling et al., 2023).

Hemp flowering is classically under short-day control, yet the response to photoperiod shows marked genotype-dependent variability (critical daylength/nightlength thresholds; quantitative SD behavior). Experimental data indicate that some cultivars do not flower even at 13–14 h days, whereas in others flowering can be halted above 18 h; recent transcriptomic work points to CO/FT module regulation gated by the critical daylength (CDL), a key factor for SB timing (Haiden et al., 2025).

Photoperiod-insensitive (“autoflowering,” day-neutral) hemp is pivotal for rapid-cycle breeding: with such backgrounds, the waiting time between generations can be further reduced. Recent results report an association of a *C. sativa* *FLOWERING LOCUS T* (FT) ortholog with photoperiod insensitivity, and identify an alternative-splicing variant of *PRR37* as a day-neutrality candidate; routine MAS deployment of these markers is among the most efficient levers for cycle shortening (Dowling et al., 2024).

Hemp is a dioecious species with an XY sex-determination system; early detection of Y-specific sequences (e.g., *MADC2*) is critical for rapid population cleanup. High-throughput qPCR panels can identify male plants already at the seedling stage, yielding considerable resource savings in SB schemes (Torres et al., 2022).

The rapid expansion of genomic resources—new chromosome-level references and pangenome assemblies—substantially supports SB. Copy-number variation of cannabinoid synthase genes and diversity in regions linked to pathogen resistance have been characterized;

comparative genomics now guides QTL mapping and parameterization of genome-wide selection (Ryu et al., 2024; Stack et al., 2025).

Breakthroughs in haploid/doubled-haploid (DH) systems aimed at rapid production of homozygous lines appear imminent. Although the species is recalcitrant to androgenesis, new results suggest microspore-derived de novo organogenesis and DH formation; once routine, SB cycles could be shortened further (Ahsan et al., 2025).

Genetic engineering and editing tools (Agrobacterium-mediated transformation, CRISPR/Cas) have been demonstrated in hemp, although regeneration remains challenging. Reports of successful targeted mutagenesis indicate that short-term functional validation cycles can be incorporated, and—over the medium term—edited alleles can be rapidly fixed (DH + SB) (Zhang et al., 2021).

In controlled-environment phenotyping, fine-tuning light quality and intensity serves both rapid cycling and targeted trait selection. Spectral components (blue, red, far-red) substantially modulate morphology and metabolite allocation; a 22-h photoperiod with a minimal dark phase accelerates development, though energy and light-use optima are cultivar-specific (Collado et al., 2024).

Direct industrial deployment on the fiber track involves rapidly combining stem strength with fiber yield and quality, and aligning maturity with agronomic windows (e.g., early sowing/harvest); rising demand for bio-based composites and building materials further incentivizes this direction (Schilling et al., 2023).

A pressing case in pathogen resistance is Hop latent viroid (HLVd), which causes major yield and quality losses. Recent syntheses on infection biology and spread, and successful sanitation via meristem culture plus thermotherapy, argue for prioritizing resistance and sanitation strategies (Torres et al., 2025).

In seed supply, feminized seed production is a key technique: male flowers induced on female plants with silver thiosulfate (STS) provide genetically female pollen to secure all-female stands. Optimizing STS concentrations and treatment schedules within the SB timetable increases the efficiency of crossing schemes (Schilling et al., 2023).

High-throughput phenotyping (HTP) and digital quality assessment—for example, hyperspectral imaging to monitor quality changes during drying—shorten the feedback loop between selection and processing technology; supplemental greenhouse lighting can improve water-use efficiency and vegetative performance (Yoon et al., 2024; Collado et al., 2024).

Genomic selection and machine learning have entered hemp for multi-trait prediction (e.g., cannabinoid-profile optimization). Combined with rapid generation turnover, these approaches can drastically accelerate genetic gain; EGS frameworks that elucidate genotype \times environment relationships support the definition of target populations of environments (Stack et al., 2025).

Application domains (fiber composites, construction materials, functional oils, phytomedicinal inputs, phytoremediation) serve industrial and environmental sustainability goals simultaneously. Methodological standardization and open SB protocols—especially the 22/2 photoperiod, critical temperature/PPFD ranges, and early seed harvest—are already available in hemp-adapted form; scaling programs depends on integrated, data-driven decision support and a clean, viroid-free propagation chain (Schilling et al., 2023; European Commission, 2023).

The role of the accelerated approach in conventional plant breeding should not be underestimated. Schilling et al. (2023) published an SB protocol highlighting that viable hemp seed can be produced, although seed set proved limited. Even prior to that publication, we conducted SB-based selection in hemp for both early- and late-maturing lines, with particular emphasis on stabilizing the yellow stem color (Somody et al., 2024; Somody and Molnár, 2025).

4. MATERIALS AND METHODS

4.1. Characterization of the hemp genotypes used in the studies

To generate my own breeding germplasm, I systematically surveyed the cultivars available. Given the paucity of published literature on these cultivars, I established both field and greenhouse trials to characterize their traits. Table 2. contains the list of the tested varieties.

Table 2. The varieties involved in the breeding process.

No.	Variety	Type	Country of origin	Intended use
1	Adzelvieši	Dioecious	Latvia	seed
2	Balaton	Dioecious	Hungary	seed
3	Bialobrzeskie	Monoecious	Poland	seed/dual-purpose
4	Carmagnola	Dioecious	Italy	fiber
5	Chamaeleon	Dioecious	Netherlands	fiber
6	CS (Carmagnola Selezionata)	Dioecious	Italy	fiber
7	Dioica 88	Dioecious	France	fiber
8	Earlina 8 FC	Monoecious	France	seed
9	Eletta Campana	Dioecious	Italy	fiber
10	Fasamo	Monoecious	Germany	fiber
11	Fedora 17	Monoecious	France	seed/dual-purpose
12	Felina 32	Monoecious	France	dual-purpose
13	Férimon 12	Monoecious	France	seed
14	Fibrimon 56	Monoecious	France	fiber
15	Fibrol	Monoecious	Hungary	seed/dual-purpose
16	Fibror 79	Monoecious	France	fiber
17	Finola	Dioecious	Finland	seed (oil)
18	Futura	Monoecious	France	dual-purpose
19	Futura 75	Monoecious	France	dual-purpose
20	Helena	Dioecious	Serbia	fiber
21	Juso 11 (USO-11)	Monoecious	Ukraine	dual-purpose
22	Juso 14 (YUSO-14)	Monoecious	Ukraine	dual-purpose
23	KC Dora	Monoecious	Hungary	seed
24	KC Zuzana	Monoecious	Hungary	seed
25	Kompolti	Dioecious	Hungary	fiber/dual-purpose
26	Marina	Dioecious	Serbia	fiber
27	Markant	Monoecious	Netherlands	fiber
28	Monoica	Monoecious	Hungary	dual-purpose
29	Pūriņi	Dioecious	Latvia	seed
30	Santhica 27	Monoecious	France	fiber/CBG
31	Santhica 70	Monoecious	France	fiber/CBG
32	Secuieni Jubileu	Monoecious	Romania	seed
33	Tiborszallasi	Dioecious	Hungary	fiber
34	USO-31	Monoecious	Ukraine	dual-purpose
35	Zenit	Monoecious	Romania	seed (oil)

My principal target was the dioecious sexual type; accordingly, the following sections describe the cultivars selected for inclusion in the subsequent accelerated breeding program.

Balaton is an open-pollinated cultivar characterized by rapid early vigor, moderately short stature, and early flowering and maturity. It exhibits excellent year-to-year stability, with a dry stem yield of 6–8 t ha⁻¹. Fiber content ranges from 20% to 23% (moderate). THC content is reliably low; CBD content in inflorescences typically ranges from 2.0% to 2.5%. Technical maturity for fiber is reached approximately 60–70 days after sowing, while seed ripens in 90–100 days. Female and male plants occur in roughly equal proportions (50:50). Under wide spacing, plants have a compact, “A-shaped” habit. Stems are dark green and moderately ridged. On each petiole, upper leaves typically bear 3–5 leaflets and lower leaves 5–7. Under dense stands and favorable conditions, plant height is about 1.5 m; at wider spacing, 1.6–1.9 m can be exceeded. The perianth segments of male flowers are white, though anthocyanic inflorescences also occur. Seeds have a grey, marbled, moderately reticulated coat; seed size is medium. TKW: 14–15 g.

Carmagnola is a dioecious cultivar. Plants may attain 2.5–6.5 m in height. The vegetative cycle is 160–180 days.

Chamaeleon is a dioecious, yellow-stemmed cultivar with high fiber content, produced by crossing Kompolti Yellow-Stemmed × Ferimon.

CS (Carmagnola Selezionata) is a dioecious cultivar reaching 4.5–5.5 m in height. Sowing from April through late May is recommended. The vegetative cycle is 170–190 days, with flowering typically in late August. An industrial fiber hemp displaying high CBD content.

Dioica 88. is a dioecious cultivar grown for industrial fiber and CBD. It is late-flowering. Technical maturity is reached at 120–125 days; the total growing period is about 140 days. Selected in France for high fiber yield and late flowering. It blooms in August and grows to 3.0–3.5 m.

Eletta Campana is a dioecious cultivar with high CBD content. The vegetative cycle is 170–190 days, and plants can reach up to 5 m in height.

Finola is a low-growing, early-maturing, seed-type cultivar from northern latitudes that flowers independently of photoperiod (dioecious). At approximately 50° N, emergence occurs 5–7 days after sowing; first true leaves appear by days 7–10; flowering begins on days 15–25; peak flowering occurs on days 30–35; male plants senesce around day 100; and with mid-May to early-June sowing, seed can be harvested at 100–120 days. TSW is 12–14 g. The optimal stand density is about 100 plants m⁻², requiring 25–30 kg ha⁻¹ of seed. Basal fertilization of 295–330 kg ha⁻¹ of a 23–3–6 NPK formulation is recommended, followed by additional top-

dressed nitrogen. With 150 kg ha⁻¹ of nitrogen, plant height may exceed 2 m. Under wet conditions and/or following poor preceding crops, *Sclerotinia sclerotiorum* and *Botrytis cinerea* can be problematic.

Kompolti is a dioecious fiber hemp cultivar developed by selection from the southern-type F-hemp (Fleischmann). It is the oldest open-pollinated dioecious cultivar on European variety lists. Derived from F-hemp (Fleischmann), it was officially registered in Hungary in 1954. For decades it ranked among the world leaders for fiber content and still remains among the best at 30–32%. Its stem-yielding capacity is high, reaching 11–12 t ha⁻¹ under optimal conditions. Beyond being one of the premier fiber cultivars, Kompolti also ranks highly among CBD cultivars. Seed productivity is moderate, as expected for a dioecious type. Owing to its high fiber content, it is well suited for pulp and paper applications. For fiber, harvest at technical maturity, achieved at 115–120 days after sowing; seed ripens at 145–155 days. THC content is generally 0.10–0.15%, while recent interest has focused on its relatively high CBD content (2.0–2.5%). TSW is 20–21 g. Leaves are medium green with numerous leaflets per petiole; the stem is dark green, moderately ridged, and profusely branched. Seeds have a grey-brown coat with moderate reticulation. Kompolti is, after Kompolti Hybrid TC, the second latest Hungarian cultivar in terms of phenology; early sowing is therefore recommended. For seed production, sow from early April and complete by 20 April at the latest; for fiber, sowing can begin in the third ten-day period of March. Recommended target densities are 20,000–40,000 viable plants ha⁻¹ for seed and 3–4 million viable seeds ha⁻¹ for fiber. Yield can be increased with nitrogen fertilization, although excessive N reduces quality.

Tiborszállási is a mid-season, dioecious fiber hemp cultivar. It was selected from Italian-origin hemp cultivated in the Tiborszállás region. Its fiber content is approximately 25%. The fiber quality is among the best globally—fine and strong—which is of particular significance for the textile industry. Stem yield is typically 9–11 t ha⁻¹. Under appropriate agronomic management, above-ground biomass can reach 13–15 t ha⁻¹. Leaves are dark green; the stem is a slightly lighter green and longitudinally ridged. Each petiole bears about nine leaflets. The proportion of male plants in stands is 51–52%. In Central Europe, the growing period is 105–110 days for fiber production and 135–140 days for seed production. Plant height depends on production goal and sowing density: 2.5–3.0 m under dense stands, and up to 4–5 m at wide spacing. Thousand seed weight (TSW) is 18–22 g, varying with seasonal weather conditions. It can be grown on a wide range of soils, though higher-quality soils support greater yields; cultivation on low-lying, waterlogged ground is not advisable. Excess precipitation after

emergence may significantly reduce yield. With appropriate stand density and nutrient supply, high yields and excellent fiber quality can be achieved, although performance is latitude-dependent and varies by region.

4.2. Characterization of the greenhouse and protected-cultivation conditions

Compared with fully indoor cultivation under entirely artificial light, greenhouse production offers markedly lower operating costs. In Gothic-arch structures, incident light is maximized and snow sheds more readily. Sufficient gutter height is essential to maintain airflow above the canopy and to allow the installation of an energy screen.

Island-style bench layouts are preferable to long continuous rows, as they facilitate varietal separation. Heating is typically the most expensive operating parameter. Where soil/substrate heating is provided, a more uniform root-zone temperature is achieved, permitting a lower (and thus cheaper) air-temperature setpoint. The use of energy screens can reduce heating costs by $\approx 50\%$; in summer these screens also provide shading, thereby reducing the duration and intensity of ventilation needs.

Cooling is achieved with fans and venting. During summer, an airflow of $\sim 12 \text{ m}^3 \text{ h}^{-1}$ is required. Natural ventilation is provided via side and ridge vents. Supplemental lighting with high-pressure sodium (HPS) and/or LED fixtures is most efficient; a supplemental photosynthetic photon flux density (PPFD) of $\sim 500\text{--}600 \mu\text{mol m}^{-2} \text{ s}^{-1}$ is generally adequate. Hemp requires higher relative humidity (RH) during the vegetative phase than during flowering. Photoperiodic darkening is necessary to induce flowering; $\sim 12 \text{ h}$ of complete darkness is required for floral induction. The process scheme is shown in Figure 1.

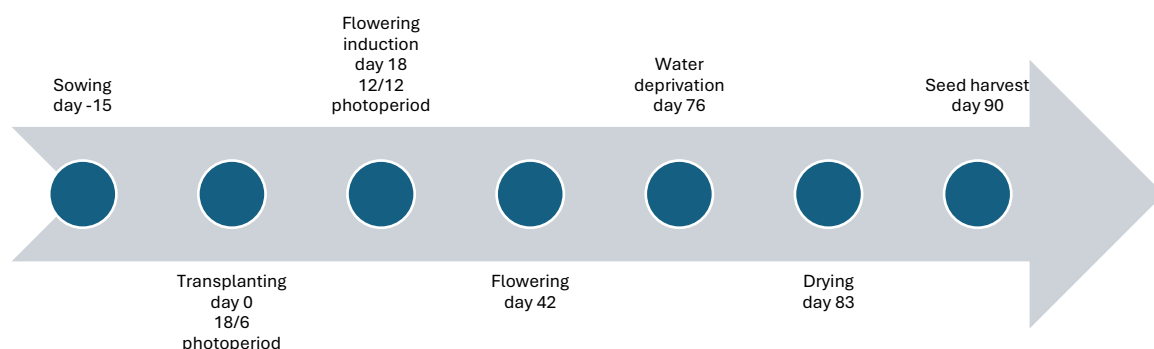


Figure 1. The scheme for accelerated hemp cultivation

For the present research, a 200 m² greenhouse was installed (Figure 2.), enabling multiple crop cycles within a calendar year. The double-bay plastic house has a ridge (gutter) height of 4 m. Ventilation is provided by two circulation fans and an automated continuous ridge vent.



Figure 2. Picture of the installed greenhouse

Heating is supplied by three unit heaters (“thermoventilators”) with a combined capacity of ~42 kW. Lighting is provided by thirty 250 W full-spectrum LED fixtures (Parfactworks

Seedlings were raised in propagation trays filled with 170 cm³ Pindstrup Plus Blue substrate (pH 6.0, 10 mm fraction) at 18–22 °C under a 16-h photoperiod. Trays were sub-irrigated (bottom watering). At ~13 cm plant height, following a 3-day acclimation, seedlings were transplanted into 20-L containers filled with Pindstrup Mix + Clay (pH 6.0, 10–30 mm fraction). Drip irrigation was supplemented with water-soluble horticultural fertilizers. Fertilizer program is shown in Table 3.

Table 3. Greenhouse fertilization program

In 1000 liters of water	YaraTera Calcinit (15.5% N + 26.3% CaO)	YaraTera Kristalon Yellow (NPK13-40-13 + B, Cu, Fe, Mn, Mo and Zn)	YaraTera Kristalon White LB (NPK15-5-30 + Mg, S, B, Mo, Cu, Fe, Mn and Zn)	YaraTera Kristalon Brown (NPK3-11-38 + Mg, S, B, Cu, Fe, Mn, Mo and Zn)
week 1.-2.	240 g	240 g	120 g	-
week 3.	320 g	320 g	160 g	-
from flowering	90 g	180 g	90 g	540 g
7 days before harvest	water deprivation			

Harvesting was done by hand, and a Wintersteiger LD350 laboratory threshing machine was used to thresh the seed.

In case of preliminari trials silver-thiosulfate (STS) treatments were conducted according to Lubell and Brand (2018) as foliar spraying with 3 mM STS.

4.2.1. Morphological parameters recorded in the greenhouse

One of our primary objectives was varietal development. This requires morphological distinctness from already registered cultivars. Within the European Union, the Community Plant Variety Office (CPVO) has issued a harmonized list of characteristics, effective as of 1 January 2023, which I have summarized in the Table 4.

Under the current CPVO methodology, hemp cultivars are distinguished as low-THC (<0.3%) or high-THC. By contrast, Hungarian regulation continues to define non-criminalized “industrial hemp” as having a THC content below 0.2%. Candidate varieties are further subclassified by mode of propagation: seed (A), vegetative propagating material (B), and feminized seed (E). Categories C and D encompass high-THC hemp, allocated—respectively—to clones and feminized seed propagating material.

Table 4. List of main characteristics according to CPVO methodology

CPVO N°	Characteristic
1	Leaf: variegation
2	Only varieties with leaf variegation: Leaf: intensity of green colour
3	Leaf: length of petiole
4	Leaf: anthocyanin coloration of petiole
5	Leaf: number of leaflets
6	Central leaflet: length
7	Central leaflet: width
8	Only varieties of type A: Time of male flowering
9	Only varieties of types B, C, D and E: Time of female flowering
10	Only varieties of types A: Inflorescence: anthocyanin coloration of male flowers
11	Only varieties of types B, C, D and E: Inflorescence: anthocyanin coloration of female flowers
12	Plant: proportion of hermaphrodite plants
13	Plant: proportion of female plants
14	Plant: proportion of male plants
15	Only varieties of types C and D: Flower: length of stigmas
16	Only varieties of types C and D: Flower: thickness of stigmas
17	Only varieties of types C and D: Flower: contortion of stigmas
18	Only varieties of types A, B and E: Plant: natural height
19	Only varieties of types C and D: Plant: height
20	Main stem: colour
21	Only varieties of types A, B and E: Main stem: length of internode
22	Only varieties of types C and D: Main stem: length of internode
23	Only varieties of types A, B and E: Main stem: thickness
24	Only varieties of types C and D: Main stem: thickness
25	Main stem: depth of grooves
26	Only varieties of types A, B and E: Inflorescence: THC content
27	Only varieties of types C and D: Inflorescence: THC content
28	Inflorescence: CBD content
29	Main stem: pith in cross-section
30	Seed: 1,000 seed weight
31	Seed: colour of testa
32	Seed: marbling

Although we conducted preliminary exploratory trials on the production of clones and feminized seed, we elected to propagate the breeding materials via open-field seed production; accordingly, I describe the characteristics pertaining to CPVO Category A (Table 5.).

Table 5. The main characteristics and examples according to CPVO

Characteristics		Examples	Note	Characteristics		Examples	Note	Characteristics		Examples	Note	
Leaf: of green colour	Leaf: Absent	Futura 75	1	Central leaflet: width	very narrow		1	Main stem: colour	yellow	Fibror 79	1	
	Leaf: intensity of green colour	Light	Fibror 79		1	very narrow to narrow	Celeste (type MGC 1013)		2	medium green	Felina 32	2
	Leaf: length of pedicel	Medium	Fedora 17		2	narrow to medium			3	dark green	Dioica 88	3
		Dark	Finola		3	medium to medium to broad	Fibrol Hulkberry		4	purple	Fibranova	4
Short		Fibrol	1		broad to very broad	USO 31	5	very short	Finola	1		
Leaf: anthocyanin coloration of petiole	Absent or Weak	Fibrol	1		very early to early		6	very short to short		2		
	Medium	Dioica 88	3		early to medium	USO 31	7	short to medium		3		
	Strong	M-1337 (type)	4		medium to late		8	medium	Uso 31	4		
	Very strong	Finola	5		late to very late		9	medium to long		5		
Leaf: number of leaflets	Very few	Bedrolite (type)	1	Time of male flowering	very early to early		1	long	Futura 75	6		
	Few	Finola	2		early to medium		2	long to very long		7		
	Medium	USO 31	3		medium to late	Fibrol	3	very long		8		
	Many	Fibror 79	4		late to very late		4	thin	Finola	9		
	Very many		5		very late		5	medium	Futura 75	1		
Central leaflet: length	Very short	Damato Red	1		Inflorescence: anthocyanin coloration of male flowers	absent or very weak	Santhica 27	1	thick	Dioica 88	2	
	Very short	MGC 1013	2			weak to weak to medium		2	shallow	Finola	3	
	Short	Divina (type C)	3			medium to strong	USO 31	3	medium	Futura 75	2	
	Short to Medium		4			medium to strong to very strong		4	deep	Dioica 88	3	
	Medium	Aida (type C)	5	very strong			5	absent or very low	Santhica 27	1		
	Medium to Long		6	very short		Felina 32	6	very low to low	Fedora 17	2		
	Long	Felina 32	7	short to short to medium			7	low	Futura 75	3		
	Long to very Long		8	medium to medium to long			8	absent or very low	Santhica 27	1		
	Long	Carmagnola	9	strong		Adzelveisi	9	very low to low	Fedora 17	2		
Central leaflet: length	Very short	Damato Red	1	Plant natural height	very short to short	Finola	1	low	Futura 75	3		
	Very short	MGC 1013	2		short to medium		2	low to medium	Chuy (type C)	4		
	Short	Divina (type C)	3		short to medium to long		3	medium	Bediol (type C),	5		
	Short to Medium		4		long	USO 31	4	medium to high	Sibari (type C)	6		
	Medium	Aida (type C)	5		long to very long		5	high	Goya (type C)	7		
	Medium to Long		6		very long		6	high to very high	A1 Philadelphia	8		
	Long	Felina 32	7		very long		7	very high		9		
	Long to very Long		8				8	absent or thin	Santhica 27	1		
	Very long	Carmagnola	9				9	medium	Fedora 17	2		
							thick	Finola	3			

The characteristics of the seed are included in Table 6.

Table 6. The characteristics of hemp seed based on CPVO methodology.

Seed: 1000 seed weight	very low	Finola	1
	low	Chamaeleon	2
	medium	Felina 32	3
	high	Santhica 27	4
	very high	Fibror 79	5
Seed: colour of testa	light grey	Finola	1
	medium grey	USO 31	2
	grey brown	Fedora 17	3
	yellowish brown	Fibror 79	4
	brown	Dioica 88	5
Seed: marbling	weak	Finola	1
	medium	Felina 32	2
	strong	Dioica 88	3

To conduct the selection, achieve homogeneity, and prepare the subsequent varietal description, an Andoid based digital framework was developed for high-throughput data acquisition.

Because greenhouse cultivation of hemp requires rigorous record-keeping, every individual plant was barcoded (Figure 4), thereby ensuring end-to-end traceability and accurate data entry.



Figure 4. Barcoded plant for accurate data entry

In each selection cycle, the process began with evaluation of the sown plants. Specifically, we recorded germination percentage and measured the width and length of the shorter and the longer cotyledon.

In the greenhouse the recorded dataframe is in Table 7.

Table 7. The dataframe used in the breeding process

Parameter	Notes
Inflorescence detected	Presence/absence flag
Sex	Male / female / hermaphrodite
Date of male flower emergence	Date (if applicable)
Maturity photograph (record)	Photograph taken at maturity
Date of female flowering	Date (if applicable)
Stem colour	Yellow/Light green/Green/Dark green
Petiole colour	Anthocyaninity
Plant height	Full height in cm
GV (node)	In which node GV point was detected
Leaflet length	At GV
Leaflet width	At GV
Stem diameter	At second internode
Other (notes)	Free-text
Harvest date	Date
Pathology (disease notes)	Mite, fungal necrosis or disease
Harvestable	Yes/no
Seed mass	Seed mass after threshing
Number of seeds	Estimated or counted number of seeds
Thousand seed weight (TKW)	Calculated TKW
Seed coat colour	Light grey/medium grey/grey brown/yellowish brown/brown
Marbling (testa pattern)	Weak/medium/strong
Green fraction (%)	Proportion classified as green, immature, useless seed
White fraction (%)	Proportion classified as white, useless seed
Dehisced (%)	Split-opened, useless seed proportion
Threshing waste sample	Threshing waste for cannabinoid analysis – more, better biomass yield
CBD	TLC measurement/result field
THC	TLC measurement/result field

4.2.2. Meteorological characteristics of the greenhouse cultivation

In what follows, I present only the meteorological characteristics of the final selection cycles, as the more stable, homogeneous generations permit more reliable evaluation and afford more meaningful comparison with open-field observations. The principal greenhouse meteorological parameters for the early (B) selection material are shown in Table 8.

Table 8. Main meteorological parameters during the last greenhouse cycles in case of early selection.

Period	Period length	Maximum (°C)	Minimum (°C)	Average (°C)	No. of days > 30°C	No. of days > 35°C
Jul.-Oct. 2022.	92	46.2	12.2	26.34	58	34
May.-Aug. 2023	88	43	15	27.39	70	56

The principal greenhouse meteorological parameters measured for the mid-season selection material (E) are likewise presented in Table 9.

Table 9. Main meteorological parameters during the last greenhouse cycles in case of medium selection.

Period	Period length	Maximum (°C)	Minimum (°C)	Average (°C)	No. of days > 30°C	No. of days > 35°C
Aug.-Nov. 2022.	89	45.6	12.2	25.07	46	21
Feb.-May. 2023	81	34	8	25.43	58	0
Aug.-Nov.2023.	94	44	12	25.49	51	31

4.3. Field trials

Open-field trials were conducted in 2022 and 2023 on the outskirts of Hédervár, Hungary. Sowing was performed with a Wintersteiger plot drill. Net plot area was 12 m², with a seeding depth of 3 cm. Harvesting was carried out manually; the cut plants were stacked in conical field shocks for post-harvest field curing. Threshing was done with a laboratory-scale thresher.

Aerial imagery was acquired on 21 June 2023 using a DJI Phantom 4 equipped with a DJI FC6310 camera, flown at 24 m above ground level.

The Visible Atmospherically Resistant Index (VARI) emphasizes vegetation in the visible domain while mitigating illumination and atmospheric effects. It is suitable for RGB imagery and uses all three channels:

$$\text{VARI} = (\text{Green} - \text{Red}) / (\text{Green} + \text{Red} - \text{Blue}),$$

where

Green, Red, and Blue are the pixel values in the respective channels.

The limitations of VARI—and vegetation indices more generally—are well known (Vélez et al., 2023); here, indices were used in a representational manner to quantify visually discernible differences. Numerous studies apply vegetation indices to assess leaf color (Jang et al., 2023; Koji et al., 2023; Park et al., 2024).

Raster and vector analyses were performed in QGIS 3.32.2 “Lima.” Digital elevation models (DEMs) and 3D model files were generated with OpenDroneMap/WebODM. SPAD measurements were taken with a Konica Minolta SPAD-502 Plus.

4.3.1. Meteorological characteristics of the field trials

Using monthly observations for April–September in 2022 and 2023, the record indicates modest interannual shifts in both thermal and hydrological regimes. Mean air temperature declined slightly from 18.25 °C in 2022 to 17.88 °C in 2023 (−0.37 °C, ≈2%). The seasonal structure, however, changed appreciably: April–June averaged 14.53 °C in 2023 compared with 16.33 °C in 2022, evidencing a cooler spring, whereas July–September warmed from 20.17 °C (2022) to 21.23 °C (2023). Monthly contrasts show 2023 was cooler in April (−0.3 °C), May (−2.8 °C), and June (−2.3 °C), broadly similar in July (+0.2 °C) and August (−0.9 °C), and markedly warmer in September (+3.9 °C), suggesting warmth was shifted toward late summer and early autumn.

Total precipitation increased from 346.40 mm in 2022 to 369.49 mm in 2023 (+23.09 mm; +6.7%), but its intra-seasonal distribution was reconfigured. Accumulations in April–June rose from 189.50 mm to 229.74 mm (+40.24 mm), driven by large surpluses in April (+53.23 mm) and May (+44.38 mm). This early-season excess was followed by a June deficit (−57.37 mm) and a generally drier late season: July–September decreased from 156.90 mm to 139.75 mm (−17.15 mm), with small month-to-month anomalies thereafter (July −4.13 mm, August +7.78 mm, September −20.80 mm).

Relative to 2022, the 2023 season featured a cooler, wetter spring, a pronounced rainfall shortfall in June, and a warmer late season extending into September.. Figure 5. summarizes the main meteorological observations during the two-year experimental period.

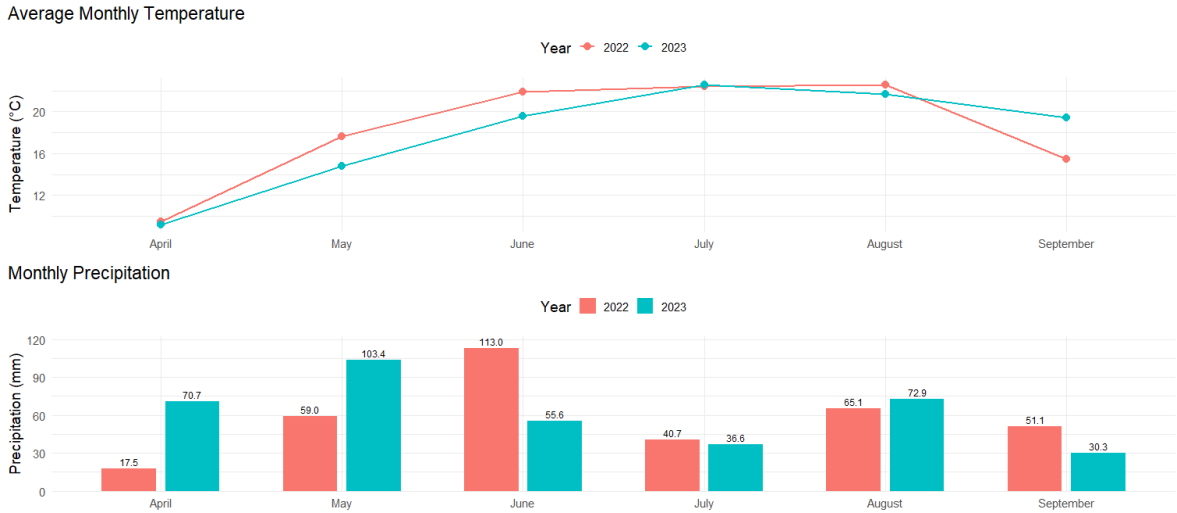


Figure 5. The average monthly temperature and precipitation during the trial periods

In case of thermal sum, 2022 (covering 28 April–15 September) accumulated 2950.65 GDD, whereas 2023 (covering 21 April–21 September) accumulated 3046.70 GDD. On this basis, 2023 exceeded 2022 by 96.05 GDD, a +3.26% increase relative to 2022.

Up to 15 September, 2022 = 2950.65 GDD and 2023 = 2921.45 GDD, so 2023 trailed by 29.20 GDD (−0.99%) at that point. The higher full-season total in 2023 therefore results entirely from additional accumulation during 16–21 September 2023, pushing 2023 above 2022.

Seedling/emergence appears slightly earlier in 2023 than in 2022, implying an earlier start to heat accumulation. Flowering begins a few days earlier in 2023 (mid-June, slightly before the solstice) and ends earlier as well (late June/very early July), suggesting that reproductive onset was advanced relative to the light maximum—likely a function of early establishment and accumulated GDD rather than photoperiod cues alone. By contrast, harvest benchmarks occur later in 2023 than in 2022, extending the tail of accumulation and explaining the higher end-of-season GDD in 2023.

Through mid-September, 2023 accrued slightly less heat than 2022; only with additional late-season warmth did 2023 surpass 2022 in total GDD. Practically, this pattern implies a comparable or modestly slower development rate through mid-season in 2023, followed by

favorable late-season conditions that prolonged maturation and increased cumulative heat exposure. Combined graph is visible in Figure 6.

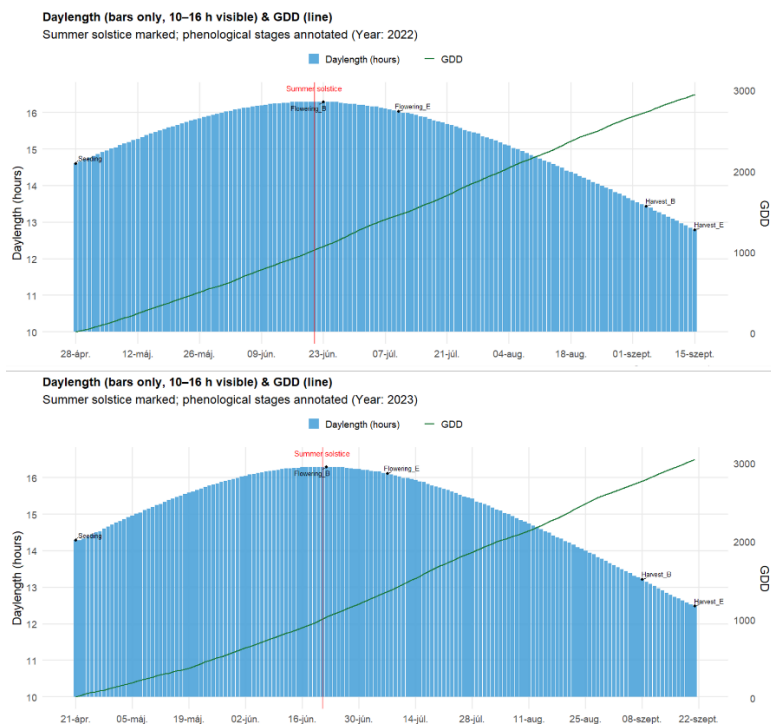


Figure 6. Daylength, GDD and phenological observations in case of the open-field trials

4.4. Cannabinoid analysis

Preliminary cannabinoid analysis conducted by Albert Kázmér Faculty of Széchenyi István University according to the following method:

Pre-dried hemp inflorescences (moisture content 8–13%) were comminuted to ~1 mm particles. From the dried, homogenized material, 500 mg was extracted with 5 mL of methanol:chloroform (9:1, v/v) as follows: 10 s vortex mixing, followed by 15 min ultrasonication, with additional vortex mixing at 5, 10, and 15 min. The extract was then centrifuged. This constituted the primary sample-preparation step.

Decarboxylation was subsequently performed. An aliquot of 200 μ L of the extract was transferred to a derivatization vial and evaporated to dryness under nitrogen. The sample was decarboxylated for 15 min at 210 $^{\circ}$ C, and the residue was reconstituted in 200 μ L of methanol:chloroform (9:1, v/v). The resulting solution was further diluted with methanol in two steps. The final solution was filtered through a 0.22 μ m hydrophilic syringe filter into a 0.8 mL HPLC vial.

Analyses were carried out by reversed-phase high-performance liquid chromatography (RP-HPLC) using an acetonitrile:water mobile phase. The column was maintained at 30 °C, and detection was achieved with a diode-array detector. Qualitative identification and quantitative determination of the analytes were performed using calibration with standard solutions of known concentration.

Total percent of THC and CBD calculated with following equations:

$$\%THC_{total} = \%THC + \%THCA \times 0.877$$

$$\%CBD_{total} = \%CBD + \%CBDA \times 0.877$$

Exploratory cannabinoid screening employed thin-layer chromatography (Alpha-Cat TLC, Canabe SRO, Figure 7). Total CBD and THC calculation was not necessary, because chromatograms were analysed after heat treatment.

Final, official determinations were performed by the NÉBiH laboratory using AOAC 2018.11. Sampling followed the European Union recommended procedure (Official Journal of the European Communities, 28 December 2000, L 332/63; Commission Regulation (EC) No 2860/2000, Annex VI, Annex XIII, Article 7b(1)).



Figure 7. TLC plates used for quick and cheap cannabinoid analysis

4.5. Characterization of the applied breeding workflow

In 2021 we launched a hemp-breeding program to develop proprietary germplasm with distinctive morphological traits and high uniformity. Primary selection targets were high fiber yield and the low tetrahydrocannabinol (THC) content expected of dioecious industrial stands; secondarily, we aimed to maximize cannabidiol (CBD).

Based on the literature, registered cultivars were sourced and grown under greenhouse conditions. After pilot crosses and progeny tests, we focused on two parents: the Italian cultivar Eletta Campana (marketed by Canapuglia; Barbieri and Tedeschi, 1968) and the Dutch yellow-stemmed Chamaeleon (Wageningen University). Crossing logistics were complicated by markedly different flowering times: Chamaeleon is early (~70 days to flowering), whereas Eletta Campana is late (~130 days).

To bridge this gap, we implemented a speed breeding (SB) workflow that shortened generation time while enabling detailed morphological assessment and ideotype discovery. With short cycles, controlled crosses became feasible—albeit with trait expression that can differ in emphasis from open-field observations. Open-field hybridization was impractical because of asynchronous flowering; in the greenhouse, however—since both cultivars are photoperiod-sensitive—direct control of daylength enabled synchronized crossing.

Seeds were germinated in trays in a nursery room; vigorous seedlings were transplanted to the greenhouse. Using growing-degree-day (GDD) calculations, once plants exhibited cultivar-typical traits and sufficient vegetative biomass, we imposed short-day conditions (12 h continuous darkness with blackout screens). Sex expression became evident within ~1 week; primary sexing traits were visible and flowering initiated by ~day 10. Manual pollination was performed on day 14 to secure seed set. For Chamaeleon we retained both male and female plants; for Eletta Campana only females were maintained. During summer, to avoid ingress of external pollen, hand pollination was delayed until stigmas had developed unpollinated for ~7 days (Figure 8).



Figure 8. Well developed stigmas due to shifted, directed pollination

A 12-h photoperiod was maintained throughout the generative phase. Upon appearance of seeds with the desired color and mottling, we applied moderate water stress to hasten ripening. Plants were harvested manually; after threshing, residual plant material was screened for cannabinoids. Seed lots from low-THC / high-CBD plants were advanced. This cycle was repeated ten times over two years (Somody et al., 2024; Somody and Molnár, 2025). Figure 9 shows the rapid growth of biomass.

Transplanting



7 days after transplanting



14 days after transplanting



21 days after transplanting



28 days after transplanting



Figure 9. Illustration of rapid biomass growth

4.6. Statistical analysis

Statistical analyses were conducted in ARM 9.1.0 (Gylling Data Management) and R 4.4.2. ANOVA, post-hoc tests, and graphics were produced in R using the packages multcompView, ggplot2, car, tidyr, and dplyr. Where homoscedasticity was violated, Welch's ANOVA was applied, followed by Games–Howell post-hoc testing via rstatix. For correlation analysis and visualization Hmisc and corrplot were used.

5. RESULTS

5.1. Preliminary assessments

5.1.1. Cannabinoid analysis for high-throughput measurements

I needed to select a rapid, low-cost method suitable for high-throughput measurements, because accelerated breeding leaves no off-season window for evaluation; moreover, analysis of fresh samples provides a more accurate representation of the population. Unfortunately, validated laboratory HPLC methods were unsuitable—both in terms of cost and throughput—for determining cannabinoid content between cycles. Therefore, I implemented an in-house TLC assay.

Five hemp samples were analyzed for CBD and THC by two independent laboratories and by a thin-layer chromatography (TLC) procedure (Table 10). Inter-laboratory agreement for HPLC was evaluated in terms of overall association and dispersion, and the TLC readouts were compared with the HPLC means to judge whether TLC was sufficiently discriminative for ranking.

Table 10. Cannabinoid analyses performed to assess the reliability of TLC method

Sample	CBD %			THC%		
	Laboratory 1	Laboratory 2	TLC	Laboratory 1	Laboratory 2	TLC
K21B103F1 1/4	0.4018176	0.346965316	1.6	0.0185812	0.017077436	<0.2
K21B103F 1/3	0.4062224	0.384698152	1.6	0.0255079	0.027301606	<0.2
K21T102F 1/2	0.4420645	0.392489836	1.2	0.0182689	0.063068146	<0.2
K21B102F1 3	0.6215523	0.37682315	1.1	0.0264908	0.043204931	<0.2
K21T104F1 1/2	1.3311402	1.443027022	3.7	0.0601029	0.083152365	<0.2

For CBD, the two HPLC laboratories showed strong linear agreement, but with non-trivial spread between labs. Most samples differed by a meaningful margin and one showed particularly large divergence, indicating that while HPLC quantitation is broadly consistent, single measurements still carry appreciable uncertainty. For THC, the agreement between laboratories was only moderate.

The TLC behaved as a semi-quantitative screen. For CBD it tracked overall magnitude—correctly highlighting K21T104F1 1/2 as the most CBD-rich—but it failed to preserve the ordering among the mid- to low-CBD samples; for example, K21B102F1 3 appears lowest by TLC yet is second-highest by HPLC. For THC, the TLC outputs were essentially at or below a

practical detection threshold (<0.2) which makes them unsuitable for discriminating among these samples.

In conclusion, the TLC results were sufficient to rank the samples and choose the individuals with outstanding CBD content. The exact active ingredient content can then be determined using HPLC on a limited sample size. TLC can flag an obviously high-CBD sample, but it misorders the remainder and offers no useful resolution for THC in case of low content, although may be suitable for the selection of intermediate or extremely THC dominant individuals.

5.1.2. Selection of parental cultivars for breeding

Our primary objective was to develop a founder germplasm with a distinctive phenotype, a CBD content significantly higher than that of the starting material, and an extremely low THC content. The line had to be amenable to greenhouse cultivation and to produce sufficient seed for small-plot field trials and for multiplication, including within three-month cycles.

Monoecious and dioecious cultivars procured for the study were established in a greenhouse experiment with three replicates. At that time, no accelerated breeding protocol for hemp was available in the international literature. Under the predefined cultivation conditions, all monoecious and dioecious cultivars produced viable seed that could be harvested within the intended 90-day interval.

This requirement constrained our selection: the northern, extremely early, short-stature cultivars (Pürini, Finola) cannot have flowering controlled solely by manipulation of the dark period. Other environmental stressors—heat, water deficit, and nutrient limitation—likewise induce undesirably early flowering in these cultivars, but at the expense of seed yield. Although directed crossing is technically feasible, because the flowering of late-maturing cultivars can be advanced, we chose not to pursue this approach. In view of the cultivar-registration regulations governing hemp, we wished to retain the option of fiber-oriented utilization.

Because no data were available in the literature, it was necessary to determine the CBD and THC contents under greenhouse (forced) cultivation. The CBD content of the monoecious cultivars at flowering is presented in Figure 10.

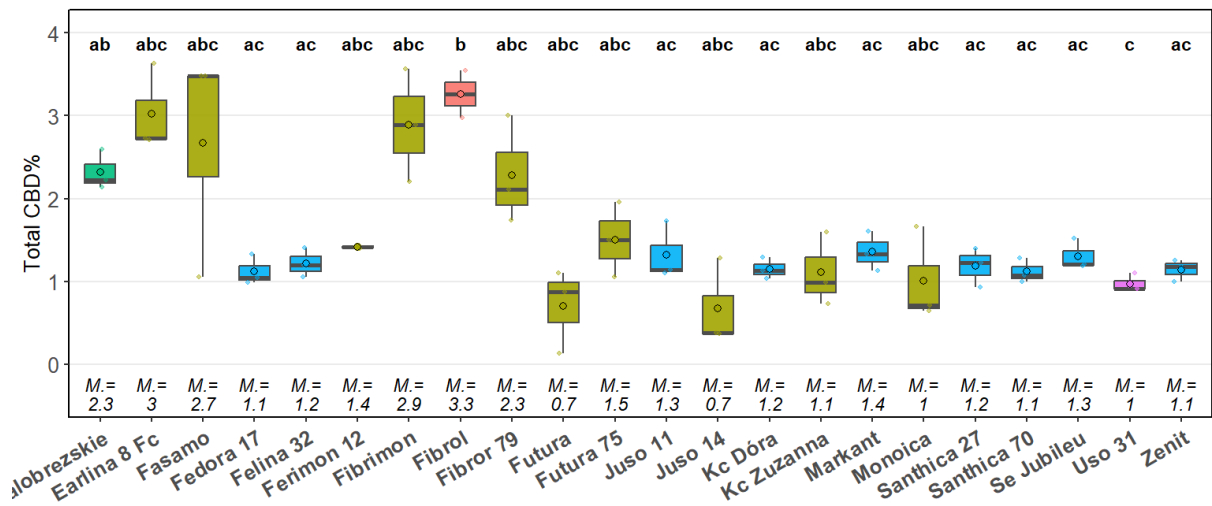


Figure 10. The total CBD m/m% of the monoecious varieties in case of the first greenhouse trial

The dataset comprises results from four plants across three replicates. Despite this limited sample size, substantial within-group variability is evident, and it is apparent that total CBD contents exceeding 3% can be achieved under accelerated cultivation.

The measurements for the dioecious cultivars are shown in Figure 11.

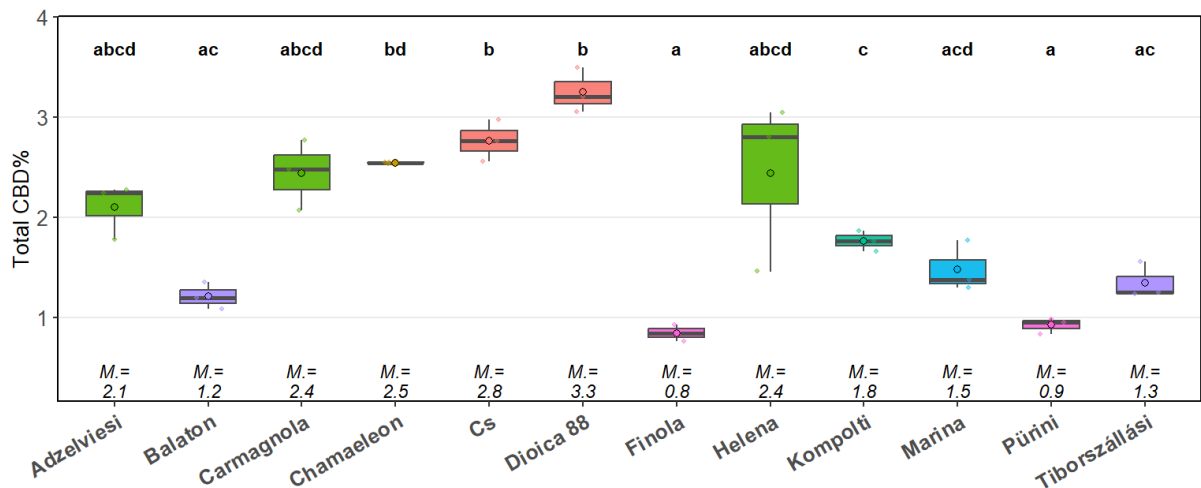


Figure 11. The total CBD m/m% of the dioecious varieties in case of the first greenhouse trial

A similar distributional pattern is observed for the dioecious cultivars, and the results are consistent with cultivar recommendations regarding CBD utilization. Notably, Dioica 88 exhibited outstanding values here and later performed exceptionally well in the open-field cultivar series as well.

The more decisive parameter was the THC content. Figure 12. presents the corresponding measurements for the monoecious cultivars.

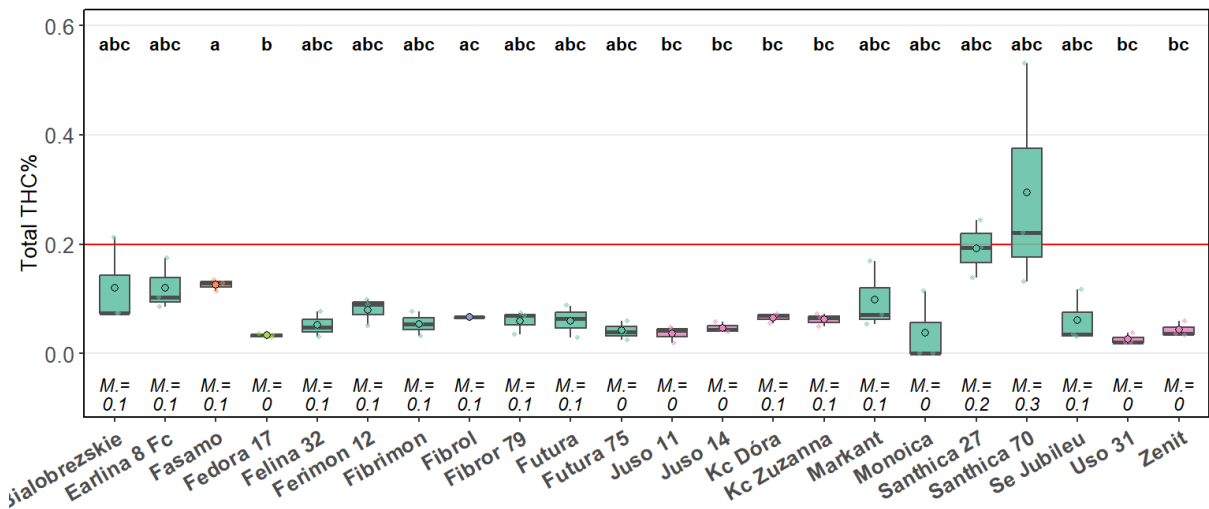


Figure 12. The total THC m/m% of the monoecious varieties in case of the first greenhouse trial

With the exception of three cultivars, the THC content of the monoecious lines did not exceed Hungary's statutory 0.2% limit (red line). In case of the dioecious varieties THC data is shown on Figure 13.

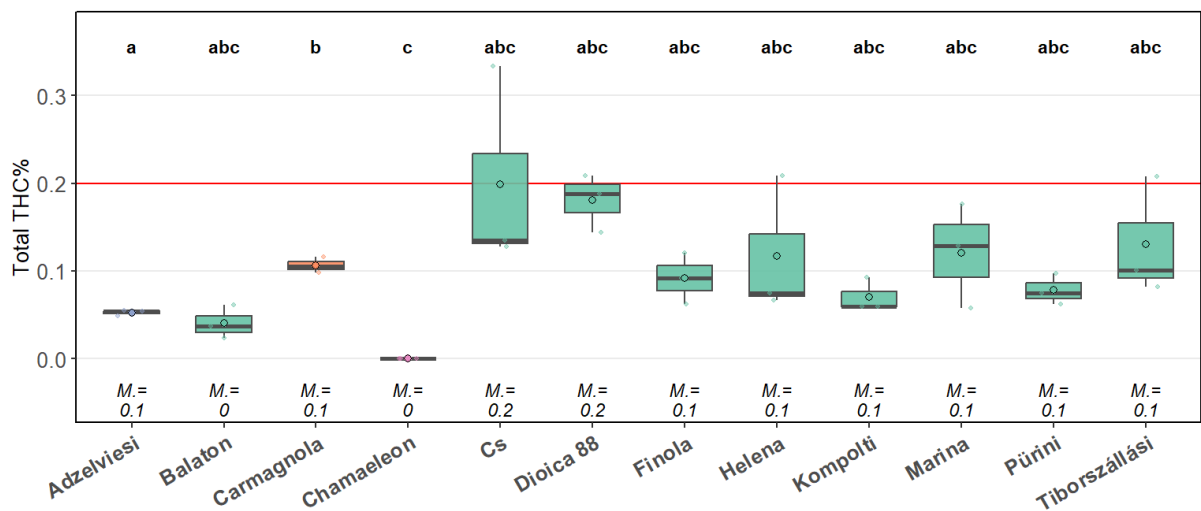


Figure 13. The total THC m/m% of the dioecious varieties in case of the first greenhouse trial

The dioecious cultivars exhibited a more erratic profile, which substantially influenced—and ultimately narrowed—the pool of cultivars selected for subsequent use as parental lines.

Table 11. contains the data summary of CBDA, CBD, THCA and THC analysis.

Table 11. Preliminary examination of varietal CBD and THC content

Rating Type		CBDA %	CBD %	TOTAL CBD %	THCA %	THC %	TOTAL THC %	Rating Type		CBDA %	CBD %	TOTAL CBD %	THCA %	THC %	TOTAL THC %
No.	Variety	1	2	3	4	5	6	No.	Variety	1	2	3	4	5	6
1	Adzelveisi	1,75	0,56	2,10	0,06	0,00	0,05	18	Futura 75	1,30	0,36	1,50	0,03	0,01	0,04
2	Balaton	1,16	0,20	1,21	0,04	0,01	0,04	19	Helena	2,42	0,09	2,43	0,13	0,00	0,12
3	Bialobrezskie	1,69	0,84	2,32	0,06	0,07	0,12	20	Juso 11	1,28	0,21	1,32	0,02	0,02	0,04
4	Carmagnola	1,65	0,99	2,44	0,11	0,01	0,11	21	Juso 14	0,56	0,18	0,67	0,03	0,02	0,05
5	Chamaeleon	1,71	0,95	2,54	0,00	0,00	0,00	22	Kc Dóra	1,19	0,11	1,15	0,03	0,04	0,07
6	Cs	1,74	1,23	2,76	0,08	0,13	0,20	23	Kc Zuzanna	1,10	0,14	1,11	0,05	0,02	0,06
7	Dioica 88	1,72	1,74	3,25	0,15	0,05	0,18	24	Kompolti	1,19	0,13	1,17	0,07	0,01	0,07
8	Earlina 8 Fc	1,11	2,05	3,02	0,07	0,06	0,12	25	Marina	1,47	0,19	1,48	0,13	0,01	0,12
9	Fasamo	1,27	1,56	2,67	0,08	0,06	0,13	26	Markant	1,34	0,18	1,36	0,07	0,04	0,10
10	Fedora 17	1,18	0,09	1,12	0,02	0,01	0,03	27	Monoica	0,93	0,14	1,00	0,04	0,00	0,04
11	Felina 32	1,31	0,07	1,22	0,03	0,02	0,05	28	Pürini	0,86	0,17	0,92	0,06	0,02	0,08
12	Ferimon 12	1,41	0,18	1,42	0,08	0,01	0,08	29	Santhica 27	1,07	0,24	1,18	0,19	0,02	0,19
13	Fibrimon	2,76	0,14	2,88	0,06	0,00	0,06	33	Santhica 70	0,97	0,27	1,12	0,29	0,04	0,29
14	Fibrol	3,18	0,08	3,26	0,08	0,00	0,07	31	Se Jubileu	1,19	0,26	1,31	0,04	0,03	0,06
15	Fibror 79	2,29	0,08	2,28	0,06	0,00	0,06	32	Tiborszálási	1,37	0,14	1,35	0,15	0,00	0,13
16	Finola	0,88	0,06	0,84	0,06	0,04	0,09	33	Uso 31	0,86	0,22	0,97	0,02	0,01	0,03
17	Futura	0,69	0,09	0,70	0,03	0,03	0,06	34	Zenit	1,05	0,22	1,14	0,03	0,02	0,04

We subsequently focused on the dioecious form. This choice substantially complicates selection, as analytical profiling of cannabinoid content in male plants was not feasible. Producing only clones or individuals derived from self-fertilized, feminized seed appeared risky for open-field multiplication and cultivar development. Moreover, deploying clones of promising males validated by progeny testing would have exhausted the available time frame.

By contrast, incorporation of yellow stem colour—presumed to be a monogenic recessive trait—was adopted as a breeding objective, and crosses were continued accordingly. We omitted assays of active constituents at flowering, because removal of the main shoot precludes seed harvest. Figure 14. presents the CBD content, at physiological maturity, of the first cross progeny, measured from threshing waste. The famous Eletta campana was involved in the process at this point, because extremely homogeneous propagation material with high biological value was obtained.

CAN 20 comes from a seed bank. It has a very unique leaf morphology. Individuals with fused leaves were very common. Only female plants were cultivated. Experimentally feminized seeds with silver thiosulfate treatment were produced.

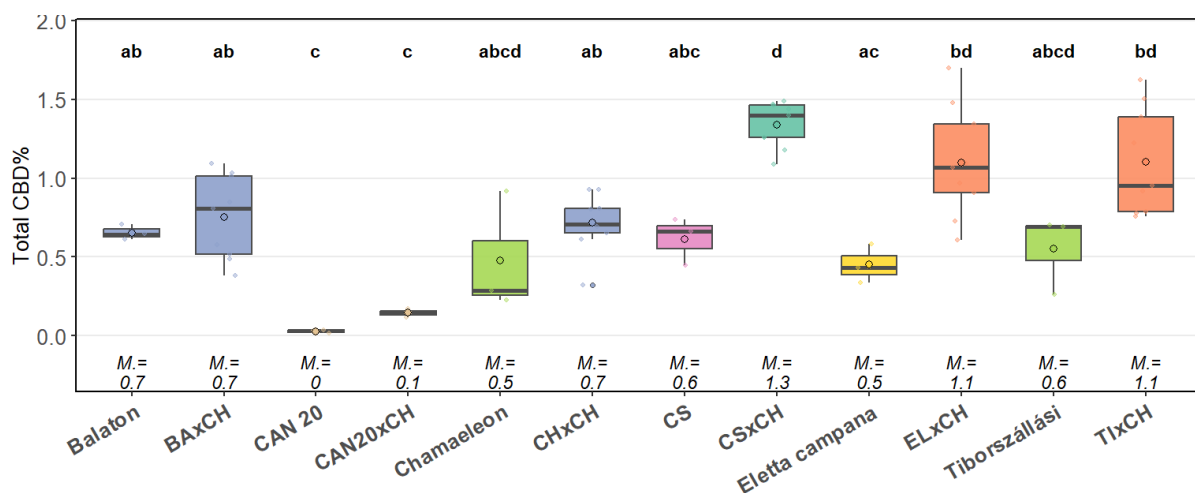


Figure 14. The total CBD m/m% of the progenies from the first controlled crosses and standard varieties

It appeared that the increase of CBD content could be achieved through individual selection alone, as the CBD content measured in the progeny exceeded that observed in clones of the parents. This trend subsequently slowed, and later confirmation was hindered by our inability to supply sufficient numbers of clonal plant material for every cycle to enable robust comparisons.

The THC content values depicted in Figure 15. entirely determined which lines were advanced.

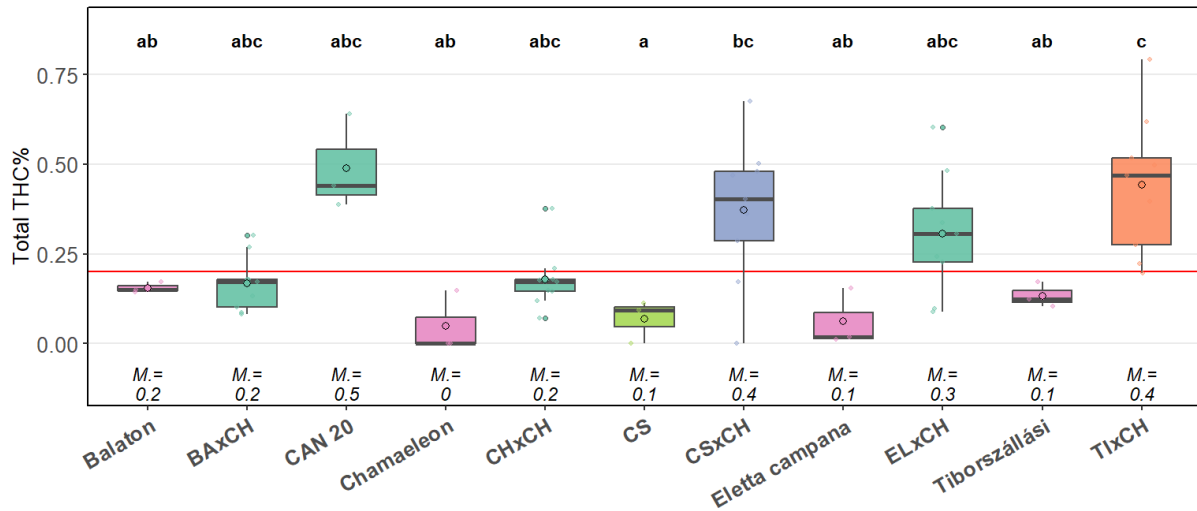


Figure 15. The total THC m/m% of the progenies from the first controlled crosses and standard varieties

Given the limited timeframe, it was not feasible to maintain plants with inconsistent low THC levels or progenies that were excessively heterogeneous. Among the originally intermediate-chemotype CAN20 progeny, a procedural error resulted in the retention of only THC-dominant individuals (with more than 3 m/m% THC) consequently, this material was not continued into subsequent cycles. From this juncture, the breeding program bifurcated into two streams: crosses with Balaton aimed at earliness, and crosses with Eletta campana targeting mid-late to late maturity. Although the CS material appeared highly promising, its erratic THC content rendered it too risky. Work with the historic Hungarian variety Tiborszallási could not be pursued, owing not only to THC content but also to the pronounced morphological heterogeneity of the available stock.

Across the mid-late/late progenies, issues related to THC content arose in each case. However, in the Eletta campana crosses there was clear segregation between maternal-type plants—very tall with large leaves—and paternal-type plants—of medium height with low seed yield. Figure 16. shows leaf morphological differences. Accordingly, we advanced this material into further progeny lines with the explicit objectives of incorporating yellow stem colour, reducing THC content, and improving homogeneity.



Figure 16. Leaf morphological differences in case of Chamaeleon (left) and Eletta campana (right)

5.1.3. Phytopathological assessments

Under greenhouse conditions, damage by mites was the principal arthropod threat; such injury can be mitigated by adjusting environmental parameters. Among phytopathogenic fungi, gray mold (*Botrytis cinerea* Pers., Figure 17) was most frequently observed and reduced harvestability. Guided by observations in the literature, we therefore conducted an assay (Somody and Aranyi, 2022).



Figure 17. The increasing severity of Botrytis bud rot observed in our breeding material. As shown in Figure 18., the dense inflorescence architecture—advantageous for CBD yield—concomitantly increases the risk of gray mold (*Botrytis cinerea*) infection.

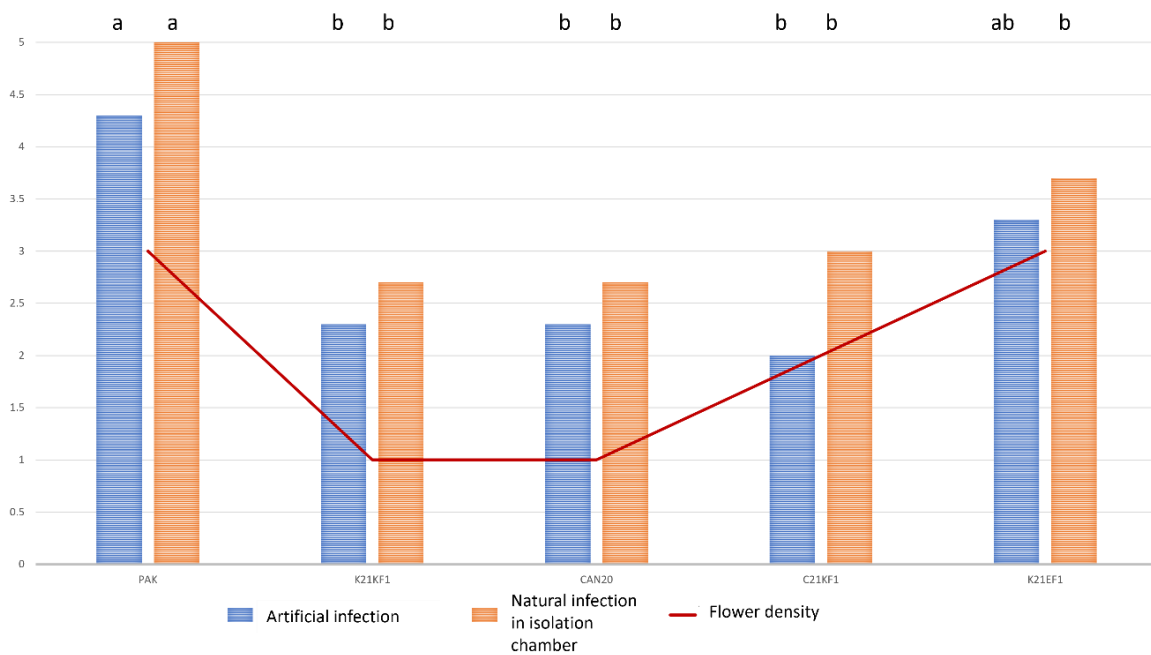


Figure 18. Relationship between flower density and grey mold severity scores (Punja and Ni, 2021). Marked with same letter do not significantly differ (P=.05, SNK)

5.2. Results for the early-maturing selection material

In the first filial generation (F1, second cycle) we evaluated progenies from the crosses ‘Balaton’ × ‘Chamaeleon’ (BA×CH) and ‘Chamaeleon’ × ‘Chamaeleon’ (CH×CH). From each combination, five seed parents were chosen and—following the procedures described above—100 seedlings per parent were transplanted. Evaluation followed the CPVO protocol for distinctness, uniformity, and stability (DUS). In this study the main-stem color was recorded in four categories: yellow (1), medium green (2), dark green (3), and purple (4). At baseline, ‘Balaton’ exhibits a dark-green stem (3), whereas ‘Chamaeleon’ is yellow-stemmed (1).

During flowering and subsequent ripening, no yellow-stemmed plants were found in the BA×CH progeny, while all plants in CH×CH expressed yellow stem color. We therefore inferred a monogenic, recessive inheritance for the trait and, to accelerate and broaden progress, backcrossed the BA×CH progeny to the ‘Chamaeleon’ male line. The CH×CH results confirmed the absence of unwanted pollen contamination.

In the second generation (third cycle) we transplanted a total of 400 seedlings derived exclusively from four BA×CH backcross seed parents. At flowering, we counted 179 yellow-stemmed and 187 green-stemmed plants; 34 individuals had been removed earlier due to failure to emerge or poor development. Pollination (Figure 19.) was carried out using a bulk pollen mix collected from yellow-stemmed males selected within the BA×CH backcross progeny. Prior to harvest, 192 female plants remained in the greenhouse; among these, 91 were yellow (1) and 101 were green-stemmed. Four elite plants were selected for the 4th cycle.



Figure 19. Pollination with mixed pollen from selected male plants

In the fourth cycle, 500 seedlings were transplanted to the greenhouse. Pollination again used a bulked pollen mix from yellow-stemmed males, after which the male plants were removed. In total, 246 female plants were harvested. At harvest, 155 cannabis plants displayed yellow stem color, with the remainder green. By the fifth growing cycle the yellow stem color was fully stabilized. At this stage, 295 elite female plants derived from five mothers were harvested, all exhibiting yellow stems.

The yellow stem trait was thus introgressed into the base material; in subsequent generations we stabilized additional attributes (harmonized flowering time, leaf-morphological features) and targeted increases in seed yield and CBD content. The timing of the cycles and stem-color observations are summarized in Table 12.

Table 12. Stem color observations in case of the early strain

No. of cycle	Period	Origin of plants	Breeding method	No. of harvested females	Yellow stemmed phenotype %
1.	May-Aug. 2021.	Balaton females – commercial seed	Cross with Chamaeleon males	300	Balaton: 0% Chamaeleon: 100%
2.	Aug.-Nov. 2021.	5 half-siblings of BAxCH Cycle 1	Backcross Chamaeleon males	100	BAxCH: 0% Chamaeleon: 100%
3.	Jan.-Mar. 2022.	4 half-siblings of (BAxCH)xCH Cycle 2	Family selection	192	47.4%
4.	Apr.-May. 2022.	4 half-siblings Cycle 3	Family selection	246	63%
5.	Aug.-Oct. 2022.	5 half-siblings Cycle 4	Family selection	295	100%
6.	May.-Jul. 2023.	16 half-siblings Cycle 5	Family selection	465	100%

Given the pattern above—particularly the irregularities observed in Cycles 3 and 4—I repeated the stem-color assessments using reserve seed lots. This cross involves highly contrasting parents (dark-green vs. yellow). Guided by field RGB imaging, we distinguished, in addition to yellow and green, a light-green stem color recorded at flowering and in the pre-maturity stage (Table 13).

Table 13. Results of the repeated stem color observation

No. of cycle	Period	Origin of plants	Breeding method	No. of harvested females	Yellow stemmed phenotype %	Light green stemmed phenotype %	Green stemmed phenotype %
3.	Repeated in 2024.	4 half-siblings of (BAxCH)xCH Cycle 2	Family selection	248	34.3%	41.1%	24.6%
4.	Repeated in 2024.	4 half-siblings Cycle 3	Family selection	250	60%	40%	0%

In brief, these proportions are most consistent with a single major locus for stem colour with incomplete dominance (or additive action): the two homozygotes express green and yellow, while the heterozygote appears light-green. Cycles 1 and 4 show near-fixation of opposite alleles (100% green vs. 100% yellow). Graph of the segregation is shown in Figure 20.

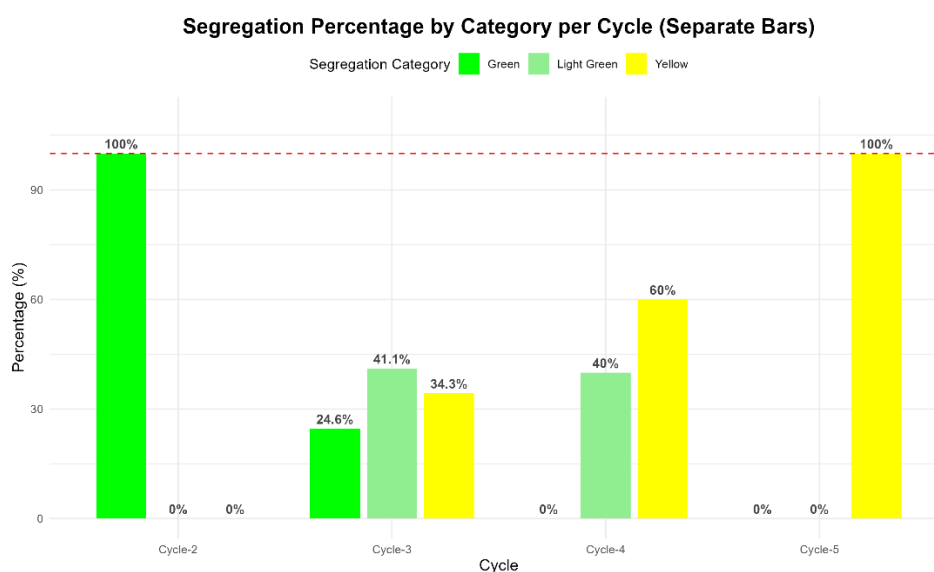


Figure 20. Segregation of stem color in case of early (B) selections

Cycle 2 approximates the 1:2:1 expectation for an F₂ from heterozygous parents, though the heterozygote is under-represented. Chi-square test was performed to check the expectation (Table 14).

Table 14. Chi-square test for segregation

=== Chi-square GOF test: 1:2:1 ===				
1	2	3		
85	102	61		
N = 248				
Chi-square = 12.452, df = 2, p = 0.00198				
class	observed	expected	resid	contrib
1	85	62	2.921	8.53226
2	102	124	-1.976	3.90323
3	61	62	-0.127	0.01613
=== Chi-square GOF test: (1+3) vs 2, expected 0.5 : 0.5 ===				
extremes_1+3	hetero_2	hetero 2		
146	102			
Chi-square = 7.806, df = 1, p = 0.00521				

The overall pattern shows a significant deficit of the intermediate class (2) and excess of class 1, inconsistent with ideal Mendelian 1:2:1 segregation. Possible causes include viability/selection against heterozygotes, stage-dependent or environment-dependent expressivity, scoring thresholds, or segregation distortion.

However, the principal component analysis, presented in the next chapter, did notify the effect of a single parent. If we exclude this from the analysis, the proportion will be shaded. 49% of the population were yellow-, 33% light-green- and 18% green-stemmed.

5.2.1. Morphological evaluation of selection

The interpretation of the data is difficult, so principal component analyses (PCA) were performed to check the lineages and for group formation. The data is displayed, and the extreme values to be selected or removed can be clearly represented. Figure 21. shows the main observed parameters on a PCA biplot in case of the 4th cycle.

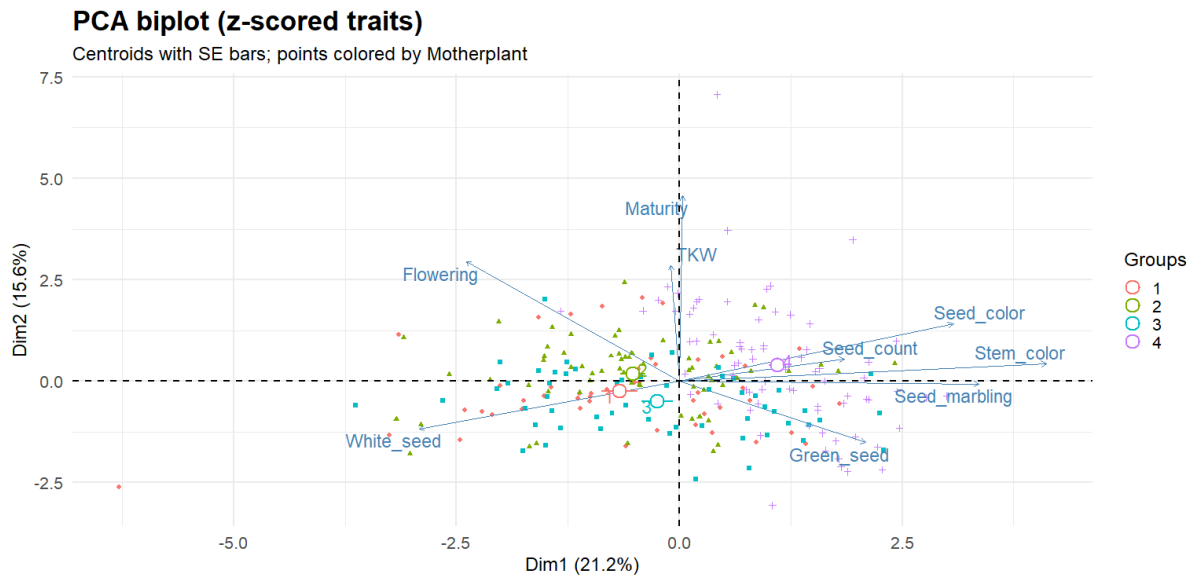


Figure 21. PCA biplot of the harvested plants from Cycle-4.

The figure explains only a relatively small proportion of the variance; nevertheless, it draws attention to the markedly divergent characteristics of individuals derived from Motherplant 4. Accordingly, the set of parameters was restricted in Figure 22. to improve visualization.

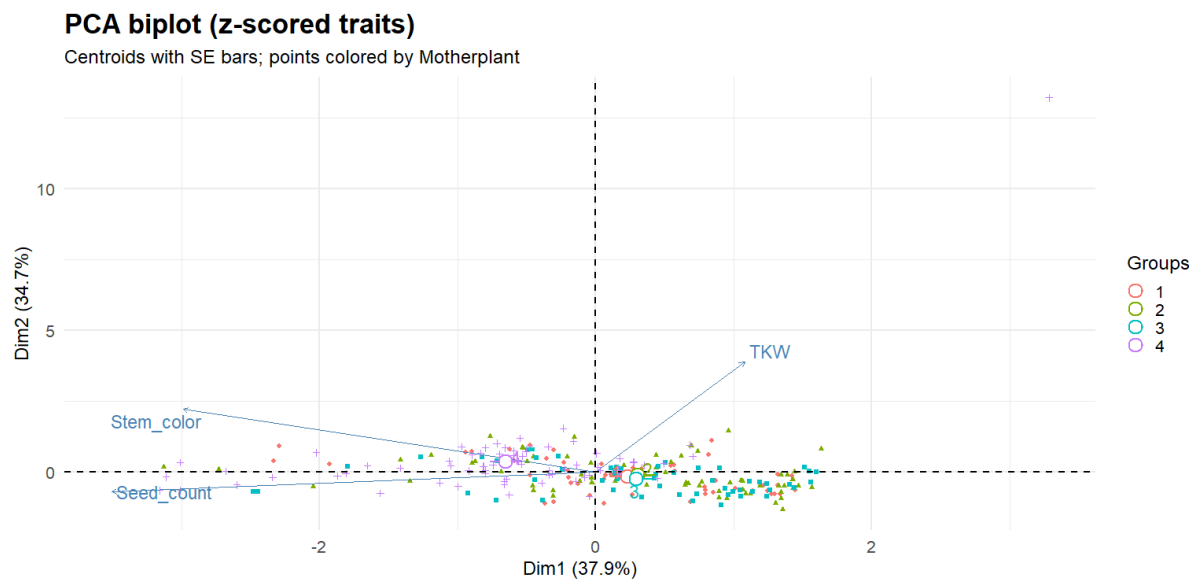


Figure 22. PCA biplot with reduced parameters from Cycle-4.

Groups differ overall, but the effect size is modest only 8% of variance explained by Motherplant (Global PERMANOVA: $R^2 = 0.083$, $F = 7.34$, $p < 1e-4$).

The choice of Motherplant 4 proved suboptimal: we obtained only a single true-yellow individual. This outcome also highlighted another difficulty of the selection program, namely that Group 4 exhibits a significantly higher seed yield. In the early phases, segregation for stem colour was accompanied by a reduction in seed yield.

Accordingly, the set of parameters was restricted in Figure 23. to improve visualization for Cycle-5 observations.

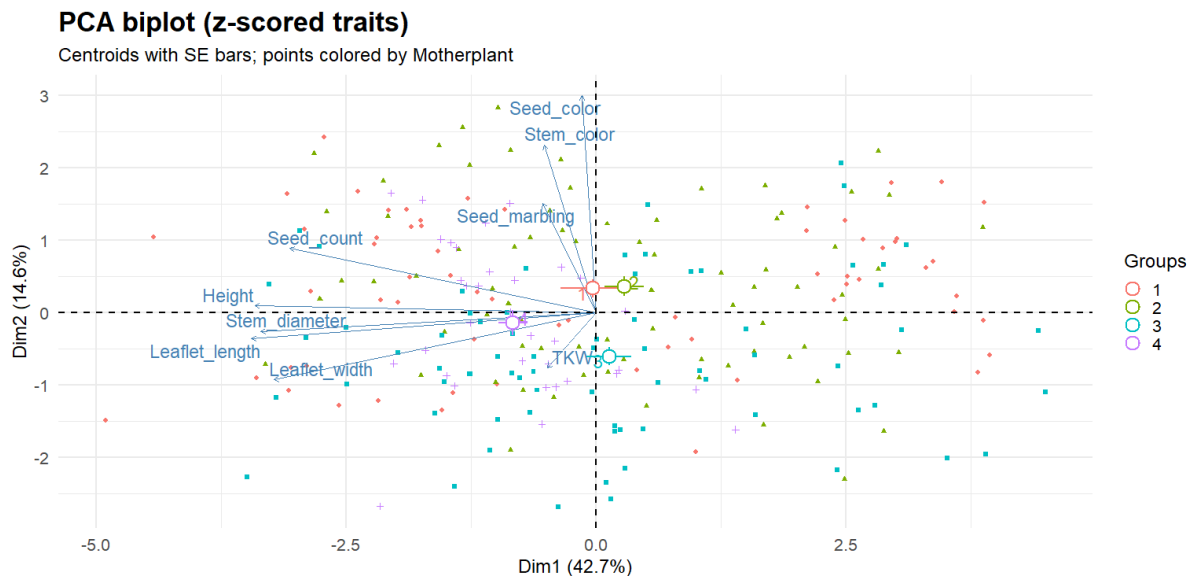


Figure 23. PCA biplot with reduced parameters from Cycle-5.

The biplot summarizes 57.3% of total variance in two axes (PC1 = 42.7%, PC2 = 14.6%). PC1 separates a seed-appearance/pigmentation complex (positive loadings for Seed_color, Stem_color, Seed_marbling) from a vigour/fecundity complex (negative loadings for Leaflet_length/width, Stem_diameter, and Seed_count). PC2 opposes pigmentation (positive for Seed_color/Stem_color) to seed weight (TKW negative), with smaller contributions from the other traits. Group centroids lie near the origin and SE bars overlap, indicating that between-group shifts are present but modest relative to within-group scatter.

Multivariate differences among Motherplant groups are real but weak ($R^2 = 0.063$, $p < 10^{-4}$). The dominant biological axis contrasts seed/stem pigmentation (and seed marbling) with vegetative size/seed number, while seed weight (TKW) varies largely orthogonally. Because Group 1 is much more dispersed and Group 4 is tightly clustered.

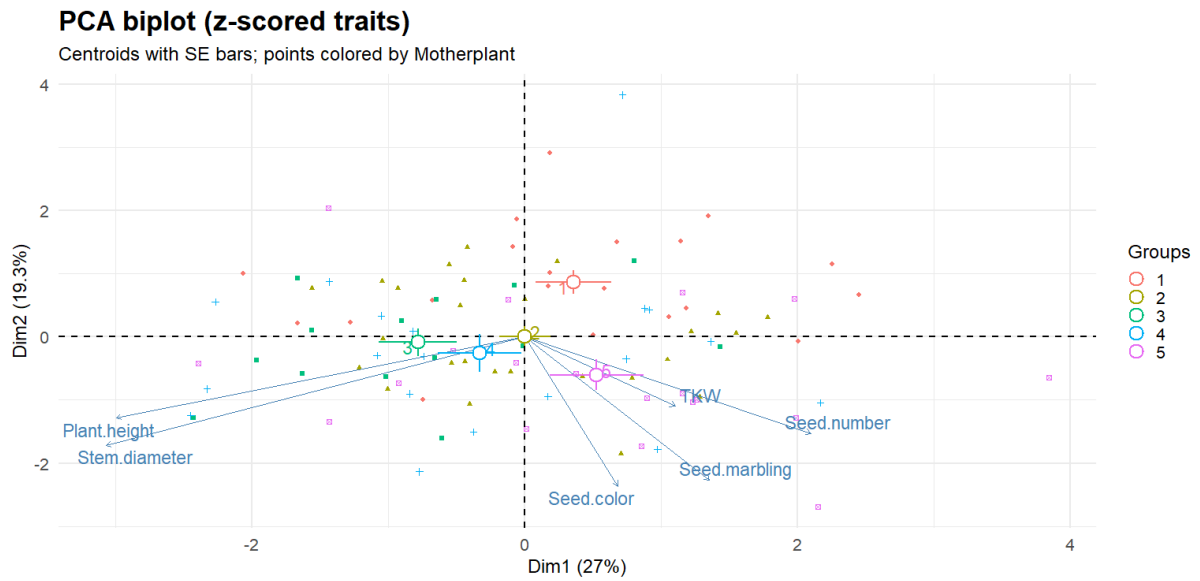


Figure 24. Multivariate structure across motherplants (PCA biplot) in case of Cycle-6

On Figure 24. using six traits strengthens the biological signal ($R^2 \approx 0.10$) relative to larger, noisier panels, and clarifies a seed-investment vs stature axis. Group 1 is seed-biased; Group 5 emphasizes seed size/pigmentation; Groups 3–4 are more stature-biased. However, within-group heterogeneity and overlap keep classification accuracy modest.

On Figure 25. the result of the morphological selection is clearly visible. With smaller, compact plants higher yields were possible.

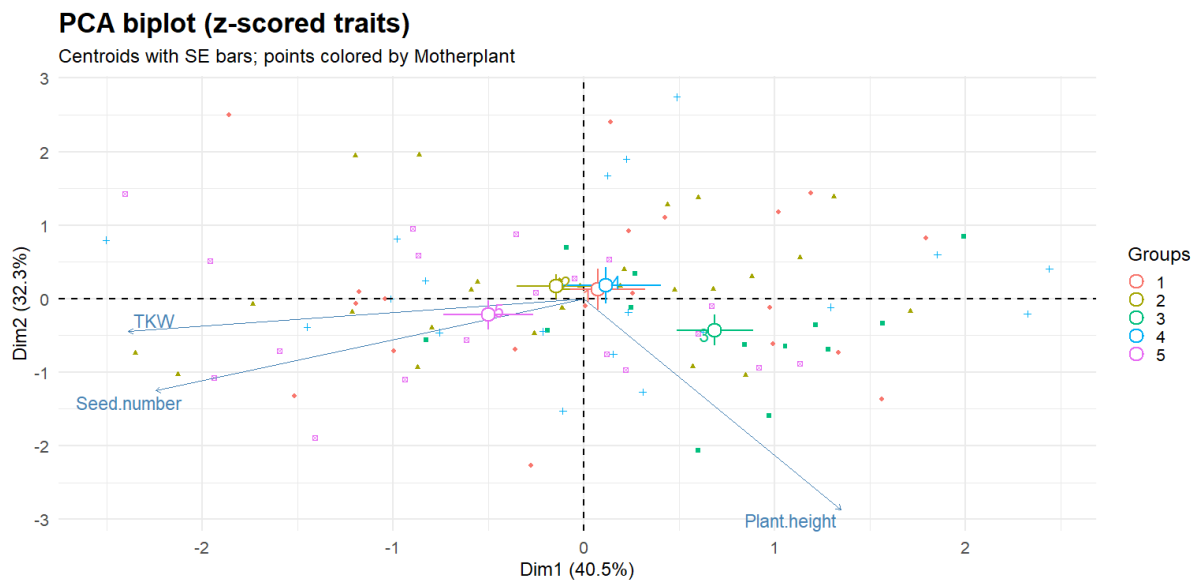


Figure 25. Cycle-6 PCA of morphological and seed traits

The first two components explain 72.8% of variance. PC1 captures a clear stature–reproduction trade-off: Plant height loads strongly positive, whereas Seed number and TKW

load negative. PC2 is largely a secondary gradient with height projecting downward. Group centroids cluster near the origin with only Group 3 shifted to the right/down (taller plants, fewer/smaller seeds), and Group 5 slightly left (smaller plants, more/larger seeds). Overlap among groups is substantial.

Global effect is not significant ($R^2 = 0.061$, $p = 0.114$). Only two BH-adjusted pairwise contrasts reach significance—2 vs 3 ($R^2 \approx 0.10$, $p_{\text{adj}} = 0.026$) and 3 vs 5 ($R^2 \approx 0.13$, $p_{\text{adj}} = 0.026$). With only Plant height, Seed number and TKW, a biologically sensible axis was created, but group separation is weak and mostly driven by Group 3.

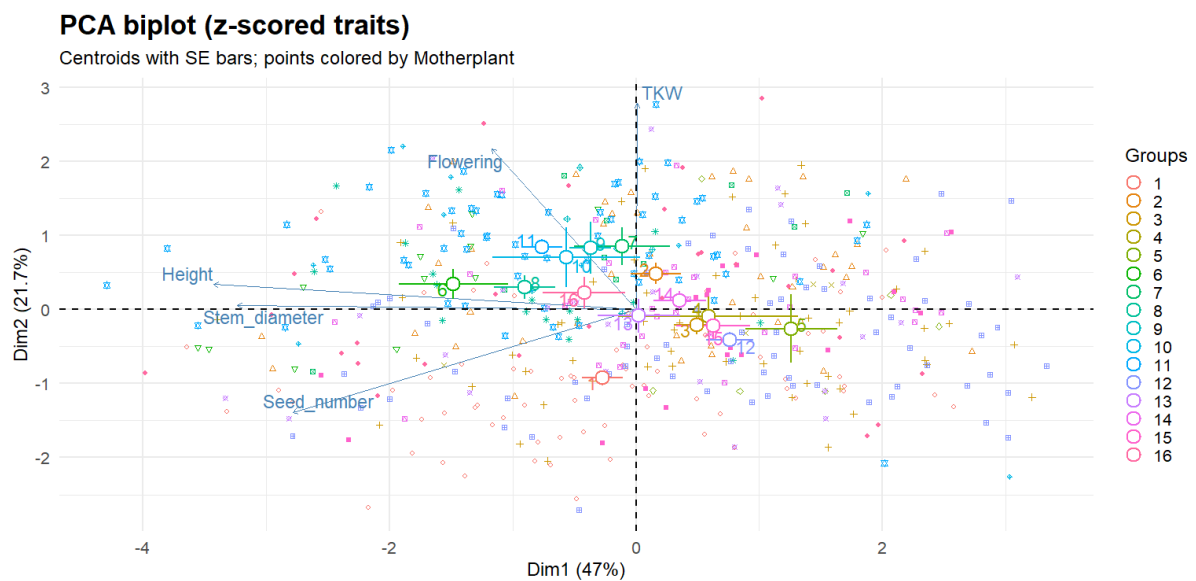


Figure 26. Cycle-7 observations on PCA biplot

Using five standardized traits on Figure 26. (Flowering, Height, Stem diameter, Seed number, TKW), the first two PCs capture 68.7% of total variance. PC1 loads positively on seed traits (TKW, Seed number) and negatively on vegetative size (Height, Stem diameter), indicating a seed–vegetative trade-off axis. PC2 is driven mainly by Flowering (earlier–later), with a weaker contribution of Height.

A global PERMANOVA shows a statistically detectable but moderate motherplant effect ($R^2 = 0.195$; $F = 7.38$; $p < 10^{-4}$; $N = 472$). Pairwise tests identify several contrasts with relatively large effect sizes, notably 1 vs 11 ($R^2 \approx 0.22$), 1 vs 7/8, and 1 vs 2/3, indicating that offspring from motherplant 1 are compositionally different from multiple others along the seed–vegetative and flowering axes.

Groups with positive PC1 scores tend to have heavier and more numerous seeds and relatively smaller stems/shorter plants; negative PC1 scores indicate the opposite. Movement

along PC2 corresponds chiefly to flowering time. The scattered cloud and overlapping SE bars show that most motherplants sample broadly from the trait space, with a few (e.g., 11) shifting the centroid toward the high-TKW/seed-rich quadrant.

Motherplant identity explains about one-fifth of multivariate trait variation. However, unequal dispersion across groups and modest classification accuracy indicate considerable overlap among progenies.

Across cycles 4–8 PCA was used to visualise lineage structure and to guide the removal of outliers. In Cycle-4, the biplot captured only a small share of variance, yet it clearly highlighted the unusual spread of progeny from Motherplant 4. Reducing the trait set improved readability but did not change the inference: groups differed, though only modestly (PERMANOVA $R^2 \approx 0.083$). Motherplant 4 proved a poor choice for the yellow-stem objective—only one true-yellow plant was recovered—and, importantly, this group also produced higher seed yield, revealing an early trade-off: segregation for stem colour initially coincided with reduced yield.

In Cycle-5, two axes explained $\approx 57\%$ of variance. PC1 contrasted a pigmentation complex (seed/stem colour, marbling) with a vigour–fecundity complex (leaflet size, stem diameter, seed number); PC2 opposed pigmentation to seed weight (TKW). Groups were distinct but largely overlapping ($R^2 \approx 0.063$), with Group 1 more dispersed and Group 4 tighter.

Using a smaller, biologically targeted panel in Cycle-6 strengthened signal ($R^2 \approx 0.10$) and clarified a seed-investment vs stature gradient. The concomitant morphological selection—toward compact plants—was associated with higher yields. When restricted to height, seed number and TKW, the first two PCs explained $\approx 73\%$ of variance and revealed a clear stature–reproduction trade-off; global group differences were weak ($R^2 \approx 0.061$), driven mainly by contrasts involving Group 3.

Finally, in Cycle-7 (five traits), PC1 again represented a seed vs vegetative size axis and PC2 captured flowering time. Group differences were statistically clear but moderate ($R^2 \approx 0.195$), with notable shifts for offspring of Motherplant 1 relative to several others. Nevertheless, unequal dispersion and broad within-group scatter kept classification accuracy modest.

Overall, motherplant identity explains small-to-moderate portions of multivariate variation, dominated by axes contrasting seed investment (number/weight, pigmentation) with vegetative stature and phenology. At this point selection toward smaller, compact plants appears to have improved yield, but substantial within-group heterogeneity persists across cycles.

Nevertheless true ideotype population was selected with excellent seed yield and the desired TKW. A sample is shown in Figure 27.



Figure 27. Motherplant of the early (B) selection

5.3. Results of the medium strain

In the first progeny generation (F1, cycle 2), we evaluated the progeny of *Eletta Campana* × *Chamaeleon* (EL×CH) and *Chamaeleon* × *Chamaeleon* (CH×CH). For each cross, five maternal plants were selected and 100 seedlings were transplanted as described above. Assessments followed the CPVO protocol for distinctness, uniformity, and stability (DUS). Main-stem color was classified into four categories: yellow (1), medium green (2), dark green (3), and purple (4). Whereas *Eletta Campana* exhibits a medium-green stem, *Chamaeleon* shows a yellow stem. No yellow-stemmed plants occurred among the EL×CH progeny, while all individuals in the CH×CH group displayed yellow stems, consistent with a recessive, monogenic inheritance of the trait.

To expedite progress, EL×CH progeny were backcrossed to the *Chamaeleon* male. The CH×CH progeny served as a control, confirming the absence of foreign pollen contamination. In the second progeny generation (cycle 3), a total of 400 seedlings were raised from four EL×CH backcross maternal plants. At flowering, 183 plants exhibited yellow stems and 186 green stems; 31 individuals were excluded due to poor emergence or underdevelopment. Controlled pollination was performed using pollen from yellow-stemmed males; at harvest, 90 yellow-stemmed and 95 green-stemmed female plants were retained.

In cycle 4, two elite individuals were selected and 354 seedlings were transplanted. After pollination with a mixed pollen lot from yellow-stemmed males and removal of the males, 153 female plants were harvested, 19 of which expressed green stems. By the fifth cultivation cycle, all 150 elite plants derived from the five selected female parents were yellow-stemmed (Figure 28.)



Figure 28. The entirely yellow-stemmed medium strain

Subsequent cycles focused on stabilizing additional attributes—harmonizing flowering time, refining leaf morphology, improving seed set, and increasing CBD content. The yellow-stem trait was successfully incorporated into the base germplasm; cycle dates and stem-color observations are summarized in Table 15.

Table 15. Stem color observations in case of the medium strain

No. of Cycle	Period	Origin of Plants	Breeding Method	No. of Harvested Females	Yellow Stemmed %
1.	May–Aug. 2021.	Eletta Campana females—commercial seed	Cross with Chamaeleon males	300	Eletta Campana: 0% Chamaeleon: 100%
2.	Aug.–Nov. 2021	5 half-siblings of EL×CH Cycle 1	Backcross with Chamaeleon males	100	EL×CH: 0% Chamaeleon: 100%
3.	Jan.–Mar. 2022.	4 half-siblings of (EL×CH)×CH Cycle 2	Family selection	185	48.6%
4.	Apr.–May. 2022.	2 half-siblings Cycle 3	Family selection	153	87.6%
5.	Aug.–Oct. 2022.	5 half-siblings Cycle 4	Family selection	150	100%
6.	Feb.–May. 2023.	5 half-siblings Cycle 5	Family selection	649	100%
7.	Aug.–Nov. 2023.	2 half-siblings Cycle 6	Family selection	532	100%

5.3.1. Morphological evaluation of selection

The biplot on Figure 29. in case of the 3rd Cycle reveals one dominant trait gradient. Positive PC1 aligns with seed appearance and fecundity (Seed_color, Seed_marbling, Seed_count), whereas negative PC1 is driven by investment in seed mass (TKW) and, to a lesser extent, Branching. PC2 contrasts Branching (positive) against colour/TKW (negative). Group centroids (Motherplants 1–5) lie close to the origin and their SE bars overlap; groups 4–5 are slightly displaced toward the seed-appearance/seed-number quadrant, while group 1 trends toward higher TKW.

A global PERMANOVA detects small but significant among-group differences ($R^2 = 0.051$, $F = 2.07$, $p = 0.0044$). Pairwise tests (BH-adjusted) indicate that the clearest separations are 1 vs 3 ($R^2 \approx 0.057$, $p = 0.005$), 1 vs 5 ($R^2 \approx 0.047$, $p = 0.027$), and 2 vs 3 ($R^2 \approx 0.035$, $p =$

0.038); all other contrasts are nonsignificant. Crucially, multivariate dispersion is homogeneous (betadisper ANOVA $p \approx 0.24$; permutation $p \approx 0.24$), so the PERMANOVA signal reflects location (centroid) shifts rather than unequal within-group spread.

Motherplant identity explains only a minor fraction (~5%) of multivariate variation in these six traits. The principal biological axis contrasts many, more pigmented seeds with fewer but heavier seeds (lower TKW), with branching varying largely orthogonally. Groups 4–5 are slightly enriched for the former profile; group 1 is shifted toward higher TKW. However, broad within-group heterogeneity limits classification and indicates that population structure is weak for this trait set.

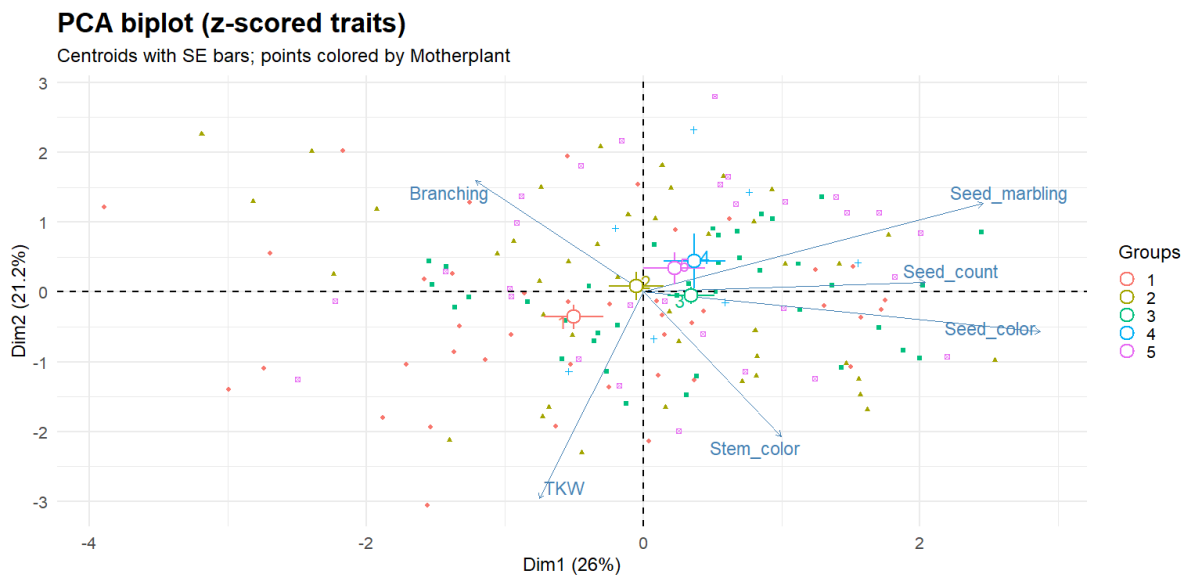


Figure 29. The distribution of observations based on motherplants on PCA biplot in case of Cycle-4

With just Stem color, Seed count, and TKW, the data reveal (Figure 30) a dominant biological axis contrasting seed mass/pigmentation with fecundity, and small but statistically credible lineage shifts along this axis—most notably Group 1 (heavier seeds, fewer in number) versus Groups 3–5 (more, lighter seeds). However, the effect size is modest (~7% of variance) and groups overlap broadly, limiting predictive classification.

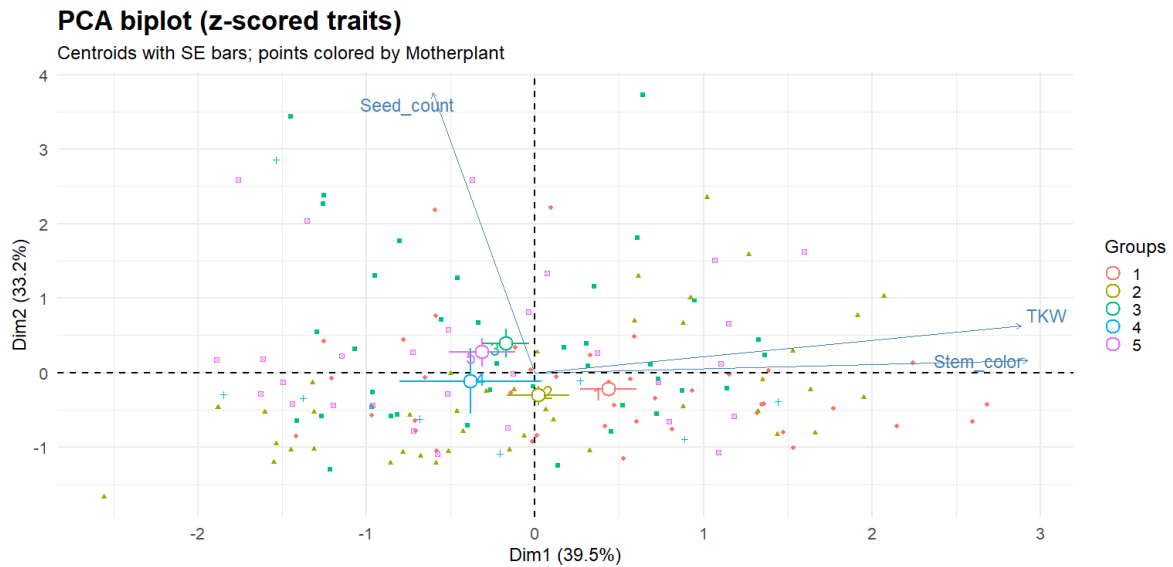


Figure 30. Cycle-4 PCA biplot focusing only on stem color and yield data

In case of Cycle-5 (Figure 31), only seeds from 2 motherplants were used. Global PERMANOVA shows a significant lineage effect with a small–moderate magnitude ($R^2 = 0.053$, $F = 5.82$, $p = 2 \times 10^{-4}$). Crucially, multivariate dispersions are equal (betadisper ANOVA $p = 0.94$; permutation $p = 0.94$), so the signal reflects centroid differences rather than unequal within-group spread. Motherplant 1 progeny are characterized by greater vegetative size and higher seed number, while Motherplant 2 progeny lean toward higher seed mass (TKW), reflecting a seed number–size trade-off modulated by stature.

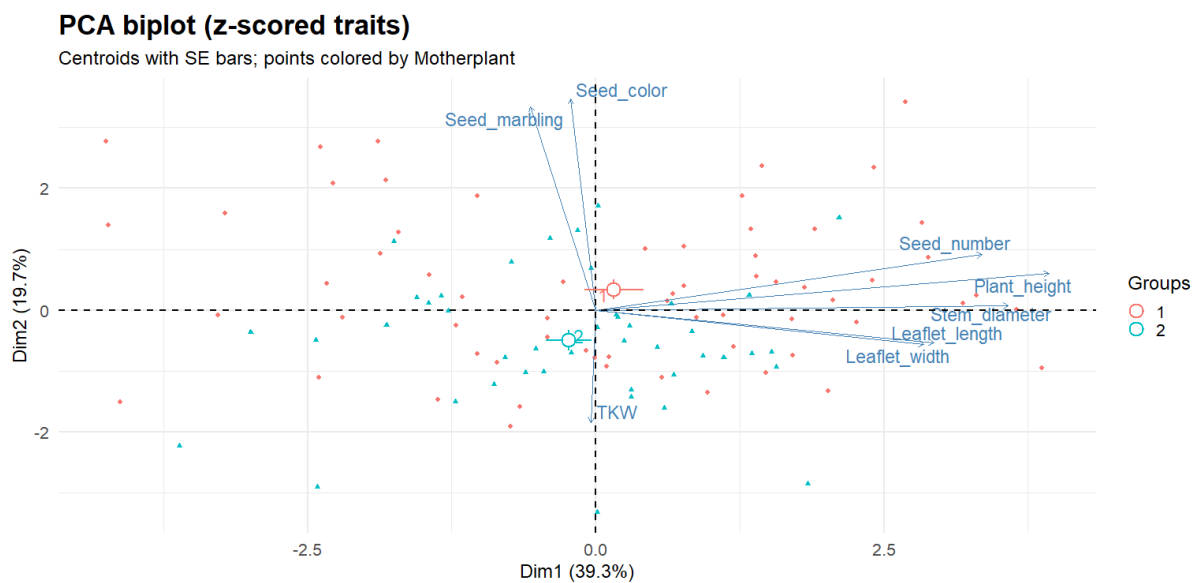


Figure 31. Cycle-5 PCA Biplot of standardized morphological and seed traits by motherplant

The first two PCs on Figure 32 capture 59.1% of the variance (PC1 = 41.6%, PC2 = 17.5%). PC1 is a clear seed-investment vs size/number axis. PC2 adds a secondary contrast in which TKW and seed pigmentation project upward, while leaflet width/length project slightly downward.

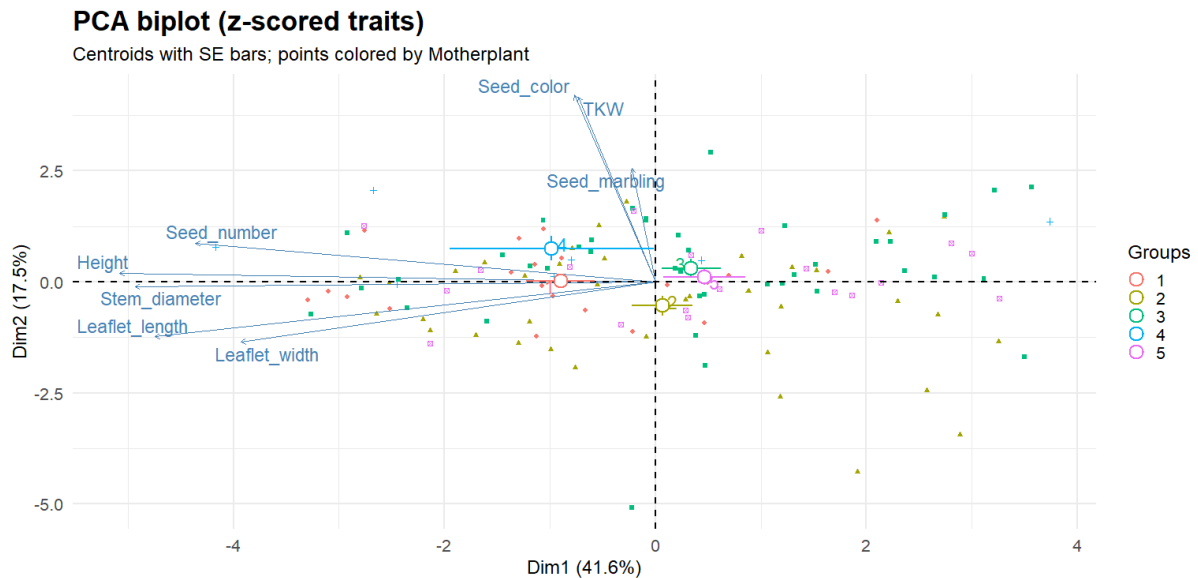


Figure 32. Ordination of progeny trait profiles (PCA; SE-centroids by motherplant)

Motherplant explains a modest but significant fraction of multivariate variation (PERMANOVA: $R^2 = 0.082$, $F = 2.71$, $p = 6 \times 10^{-4}$). Pairwise tests show the strongest and most consistent separations among 1 vs 2, 1 vs 3, 1 vs 5, 2 vs 3, and 3 vs 4 (BH-adjusted $p \leq 0.043$); 2 vs 4 is marginal (adj. $p = 0.057$). In the biplot, Group 3 sits slightly to the right/upper side (heavier, more pigmented seed tendency), Group 2 trends left/down (taller plants, broader leaves, higher seed number), while Groups 1, 4, 5 lie near the origin, indicating intermediate phenotypes.

Multivariate spread does not differ among groups (betadisper: $p \approx 0.31$), so the PERMANOVA result reflects centroid shifts rather than unequal within-group variability.

Across these eight traits, motherplant identity shapes progeny phenotypes detectably but modestly. The dominant biological gradient reflects a seed size/pigmentation–vs–plant size/seed number trade-off; Group 3 leans toward the former, Group 2 toward the latter, and the remaining groups are largely intermediate with comparable within-group dispersion.

On Figure 33. PC1 loads Height and Seed_number opposite to TKW. PC2 is driven mainly by Stem_diameter versus TKW. Height contributes little to PC2. Group centroids separate

along these axes, with broad but structured clouds—visually consistent with real (but not extreme) among-group differences. Motherplant explains ~14% of multivariate variance ($R^2 = 0.139$, $p < 1e-4$). All tested pairs are significant after BH correction ($p_{adj} = 1.25 \times 10^{-4}$), with the largest separations involving 2 vs 3 ($R^2 \approx 0.155$) and 1 vs 3 ($R^2 \approx 0.121$).

The dominant gradient opposes taller plants with more (but lighter) seeds and shorter plants with heavier seeds—a classic seed number–size trade-off modulated by stature; stem diameter adds an orthogonal component.

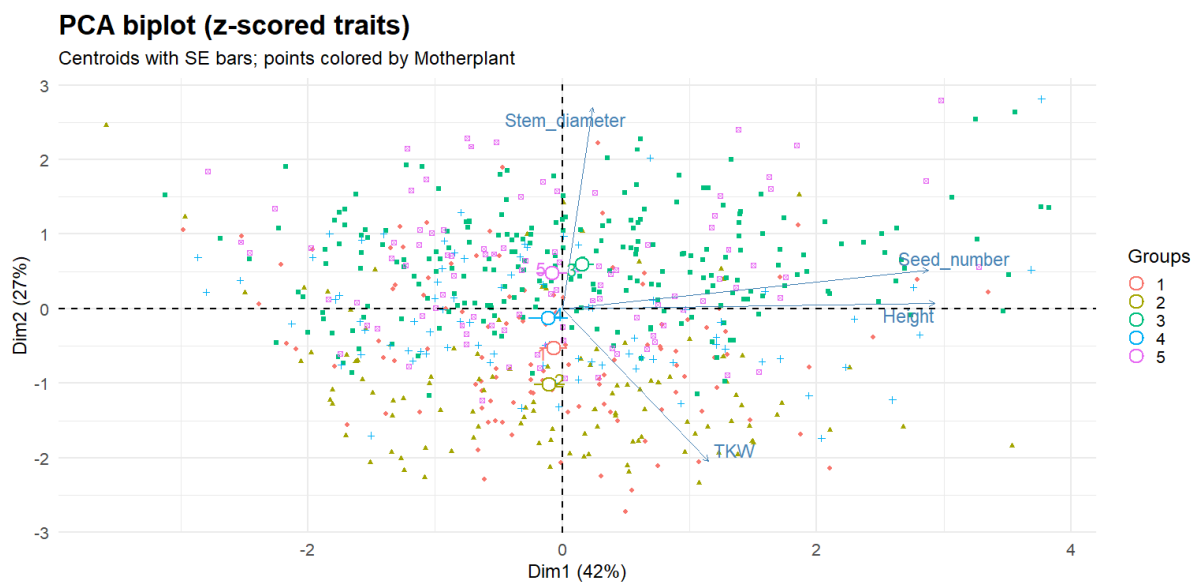


Figure 33. Cycle-7 observations visualized on PCA biplot

The dominant gradient of Figure 34. is a trade-off between vegetative size/seed number vs seed mass and pigmentation. Group differences are present but subtle relative to within-group variation; focusing selection on the PC2 axis (TKW ↔ pigmentation) should capture most of the between-group signal

Group centroids are close to the origin but offset: Group 1 sits slightly higher on PC2 (tending toward heavier seeds) and marginally to the right (slightly larger stature); Group 2 is slightly below the origin (more pigmentation signal; relatively lighter seeds). Point clouds overlap broadly, indicating substantial within-group heterogeneity.

Group differences. PERMANOVA shows a small but reliable motherplant effect ($R^2 = 0.031$, $F = 16.55$, $p < 10^{-4}$). Multivariate dispersions are not detectably different (betadisper $p \approx 0.084$), so the signal reflects centroid shifts rather than unequal spread.

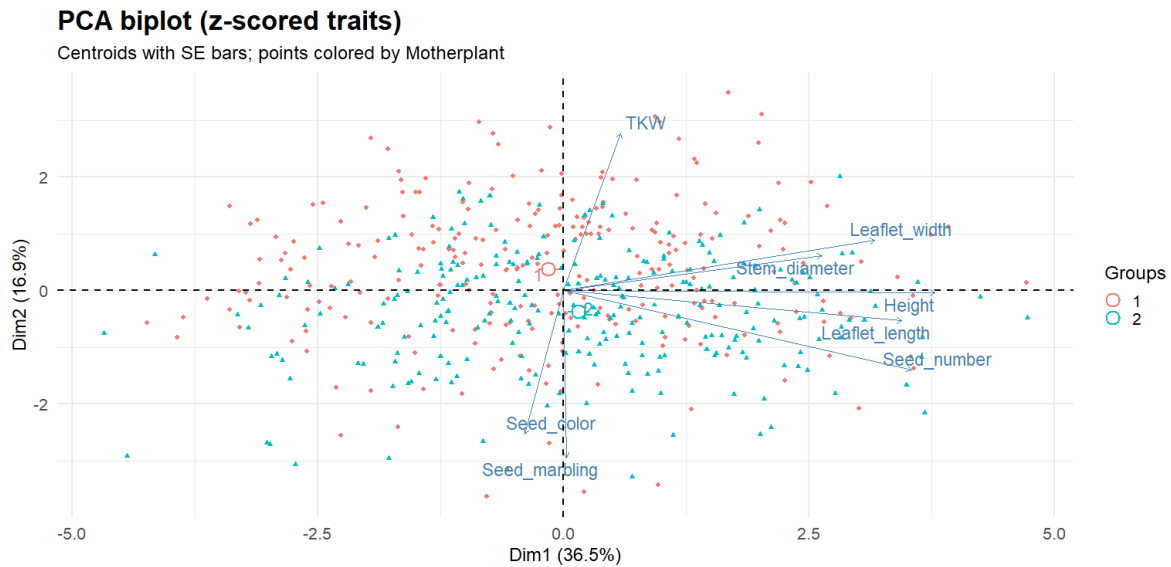


Figure 34. Cycle-8 lineage differentiation in breeding traits: PCA by motherplant

Across cycles, the PCA biplots reveal a consistent dominant gradient that contrasts a seed number/appearance syndrome against a seed mass (TKW) / pigmentation syndrome, with vegetative size traits (height, leaflet size, stem diameter) aligning most closely with the seed-number end of the axis.

Motherplant identity exerts a detectable but generally modest influence on multivariate phenotype—ranging from ~3–8% of explained variance in most cycles, rising to ~14% in Cycle 7. The principal biological axis is consistent: a seed size/pigmentation, plant size/seed number trade-off. Lineage shifts are real (centroid differences) but typically small relative to within-group heterogeneity, implying that classification power is limited and that selection gains will be greatest when targeting this dominant axis, particularly the TKW–pigmentation dimension.

In this case, we worked with a small number of mother plants, and the differences in thousand-seed weight could be spectacularly traced back to the characteristics of the starting plants.

5.4. Field Trials

To enable evaluation of families at larger sample size and to increase seed availability, we established field experiments. The objective was to obtain a comprehensive picture of the material with respect to flowering time, capacity for spontaneous pollination and seed set, realized plant height, and adaptation to ambient environmental conditions.

Seeds from 30 maternal plants of the propagated stock were sown. Ten plots each originated from the initial cross (F1, Cycle 1), from backcrossed seed (BC1, Cycle 2), and from the first family-selection harvest (Cycle 3). The trial was set on 12 April 2022 at Hédervár (North-West Hungary) and sown with a Wintersteiger plot seeder. Plots measured 12 m²; sowing depth was 3 cm, row spacing 50 cm, and the target plant density 45 plants m⁻². Five plots exhibited low stand density (<30 plants m⁻²) and were excluded from further evaluation.

To direct the use of the breeding material, all male plants were removed from plots sown with Cycle-1 seed, whereas in plots derived from Cycles 2 and 3 only yellow-stemmed male plants were retained. At harvest, seed was collected exclusively from yellow-stemmed female plants.

Within each plot, 100 plants were sampled at random for assessment. Field observations closely matched the previous year's greenhouse data. Among plants derived from the first family selection (Cycle-3 seed), 94.57% exhibited yellow stems. In Cycle-2 progeny, the proportion of yellow-stemmed individuals was 50%, while no yellow-stemmed plants were detected in plots from Cycle 1.

In 2023, stabilized families were resown in a small-plot trial analogous to the previous year to further increase seed quantities (Figure 35). Establishment parameters were identical to the earlier field experiment. In total, 45 plots were sown from various half-sibs of Cycles 6 and 7, as well as descendants of the initial field test. In this year, no green-stemmed individuals were observed; consequently, male removal was performed according to breeding criteria other than stem color.



Figure 35. Small plot trial in case of early strain for seed multiplication in 2023.

5.4.1. Evaluation of Stem Color Field Assessments

In 2023, seeds from all cycles were sown in a small-plot experiment to assess morphological differences and uniformity. The proportion of yellow-stemmed plants was determined at the time of seed set by visually scoring 100 randomly selected plants per plot. In addition, we piloted a UAV-based procedure by acquiring aerial imagery at seed set in the cultivar *Chamaeleon*.

Figure 36 presents VARI values (Visible Atmospherically Resistant Index) computed from post-flowering aerial images (Gitelson et al., 2002).

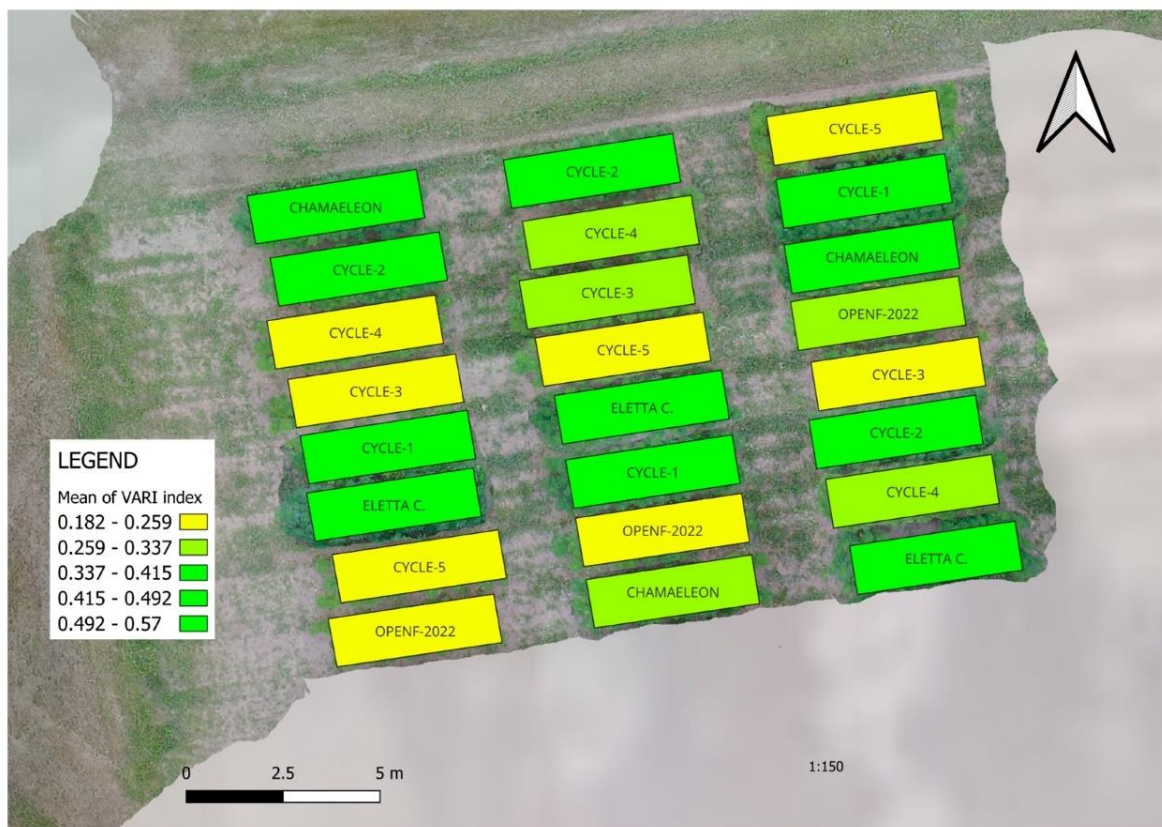


Figure 36. VARI index of the open-field trial in 2023

Based on the data analysis summarized in Table 16, the stem-color classes derived from VARI indices were concordant with manual observations. However, differences in plant numbers among plots affected the VARI values. We also noted that leaves of yellow-stemmed plants exhibited less intense green pigmentation and progressively yellowed over the course of the season. This pattern was likely strongly influenced by our selection regime: to avoid

unintended pollination, conspicuously greener individuals were removed prior to flowering, i.e., before the stem-color shift became unequivocally apparent.

Table 16. Comparison of VARI indices and manual observations

	Origin of Seeds	VARI Index	Sig. Group *	% of Green-Stemmed Plants	Sig. Group *
1	CYCLE-1	0.42	ab	100.0	a
2	CYCLE-2	0.36	abc	52.0	b
3	CYCLE-3	0.25	c	0	c
4	CYCLE-4	0.28	bc	0	c
5	CYCLE-5	0.24	c	0	c
6	OPENFIELD-2022	0.25	c	0	c
7	ELETTA CAMPANA	0.46	a	100.0	a
8	CHAMAELEON	0.34	abc	8.3	c
Tukey's HSD ($p = 0.05$)		0.166		9.44	
Standard Deviation		0.058		3.28	
CV		17.78		10.07	

5.5. Evaluation of Additional Distinctive Traits

In 2023, we established a cultivar comparison trial to assess the performance of newly developed lines under dense, row-sown stands. The intensity of leaf greenness is a cultivar-specific trait and should therefore be included in variety evaluation. Leaves of yellow-stemmed cultivars exhibit less intense green pigmentation irrespective of phenological stage; nevertheless, cultivar comparisons are best conducted prior to flowering. Figure 37 presents an aerial image of the cultivar trial.



Figure 37. Aerial image of the dense row cultivar test in 2023

At the plot level, the intensity of leaf greenness can be assessed visually (subjectively); in addition, we compared VARI-derived values with quantitative readings obtained using a SPAD (Leaf Soil–Plant Analysis Development) chlorophyll meter, as summarized in Table 17.

Table 17. Comparison of measured SPAD value and VARI index in case of leaf greenness

No.	Variety	SPAD Value		VARI Index	
		Mean	Sig. Group*	Mean	Sig. Group*
1	B	31.63	e	0.37	de
2	Balaton	40.53	a	0.50	a
3	Carmagnola	37.40	abc	0.47	a–d
4	Chamaeleon	32.70	de	0.38	cde
5	Dioica 88	39.77	ab	0.52	a
6	E	31.73	e	0.35	e
7	Eletta Campana	35.80	cd	0.43	a–e
8	Fedora 17	37.70	abc	0.52	a
9	Felina 32	35.60	cd	0.47	a–d
10	Fibrol	37.23	abc	0.52	a
11	Fibror 79	31.43	e	0.39	b–e
12	Finola	38.70	abc	0.38	b–e
13	Futura 75	36.63	bc	0.49	ab
14	Santhica 27	35.17	cde	0.45	a–e
15	Uso 31	36.97	abc	0.48	abc
Tukey's HSD ($p = 0.05$)		3.765		0.106	
Standard Deviation		1.243		0.035	
CV		3.46		7.79	

Correlation is strong between the measured and predicted values ($r=0.76$, Figure 38) and express the varietal characteristic.

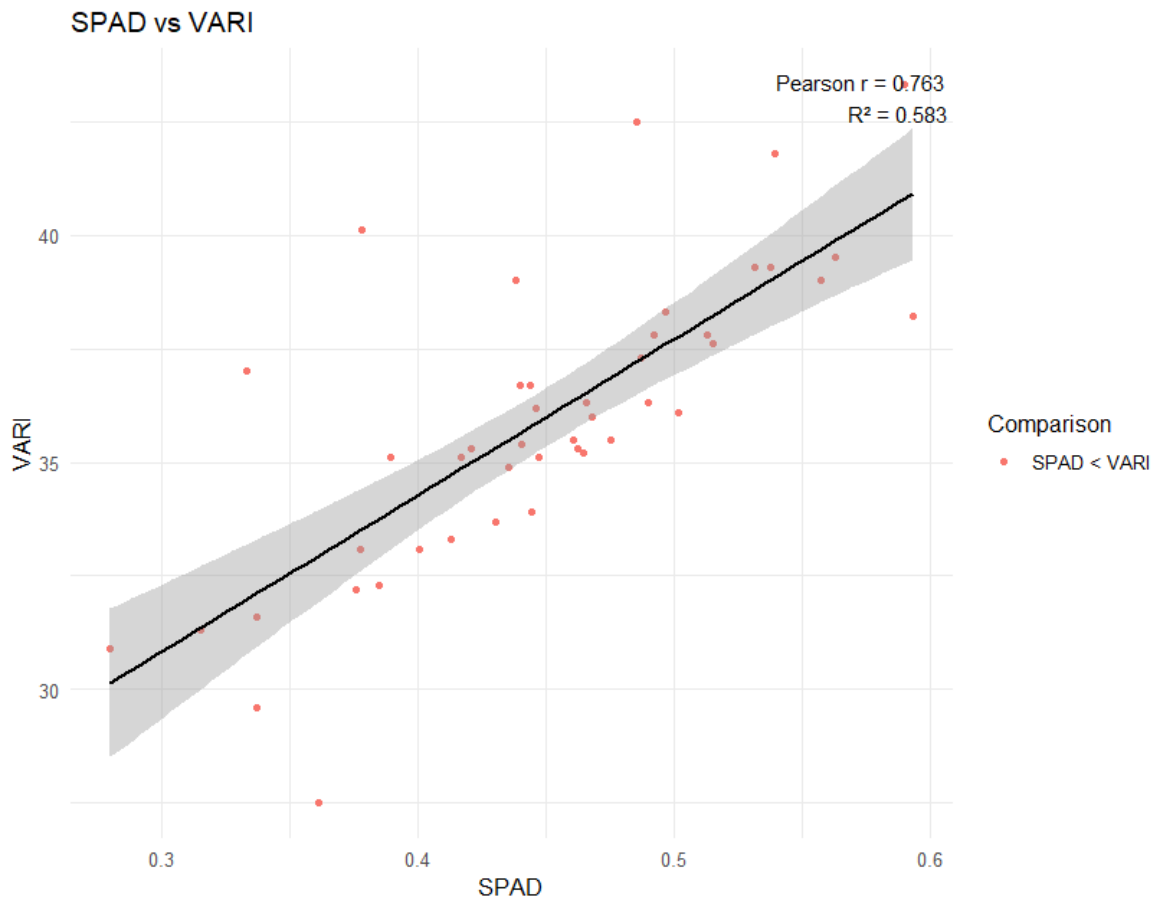


Figure 38. Correlation between VARI index and measured SPAD values

From the aerial imagery we generated a digital surface model (DSM), a digital terrain model (DTM), and a three-dimensional model (Figure 39).



Figure 39. The generated 3D model from the aerial images

In this densely sown experiment, we observed a strong correlation between predicted and directly measured plant heights ($r = 0.93$; Figure 40).

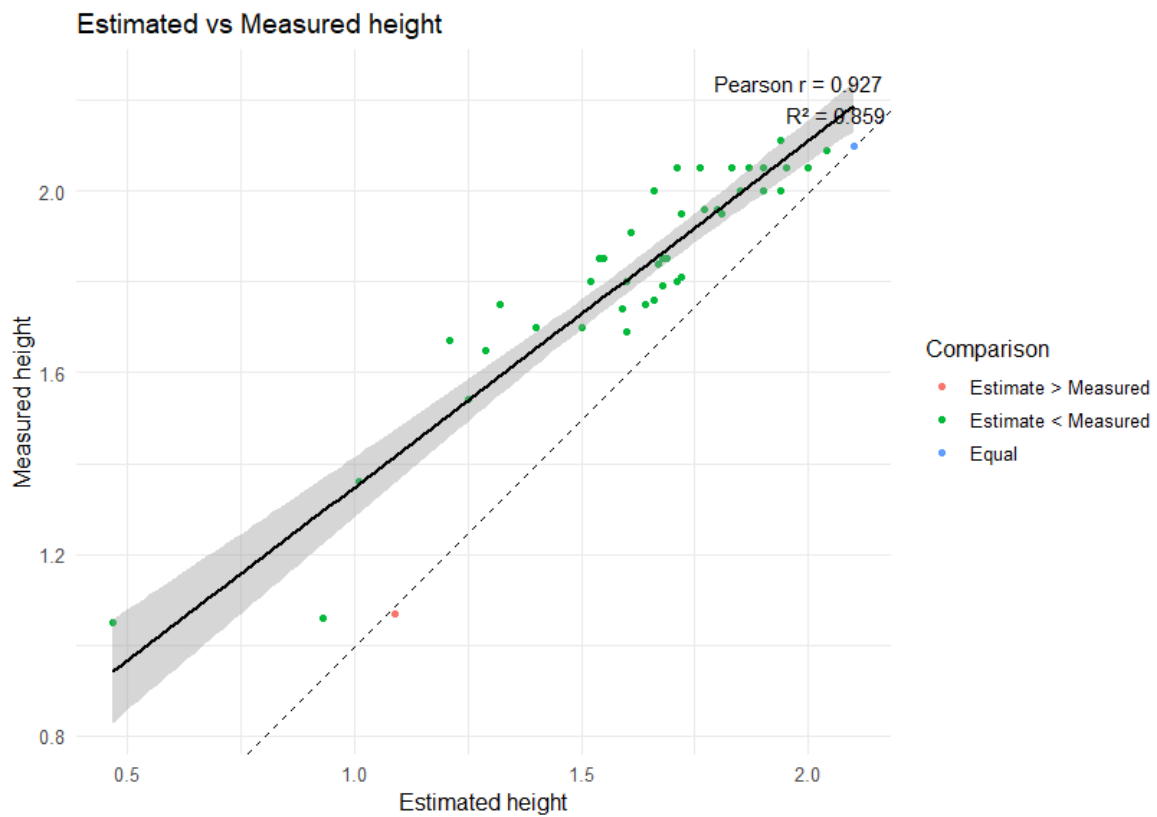


Figure 40. Correlation between predicted and measured plant heights

5.6. Evaluation of Maturity Time and Climatic Data

Our primary objective was to develop cultivars suited to open-field production; accordingly, we sought to relate our greenhouse observations to field performance in ways that could facilitate selection. As summarized in Table 18, in the Eletta Campana \times Chamaeleon (E) cross, the duration from sowing to harvest across greenhouse cycles 4–6 ranged from 78 to 93 days. The accumulated heat units (growing degree days, GDD)—calculated from unadjusted mean temperature data—varied between 2013 and 2397 GDD. In the Balaton \times Chamaeleon (B) selection, cycle length ranged from 83 to 91 days.

18. Table. Accumulated GDD and length of the main phases of Cycle-4, -5, and -6 of the speed breeding process

Date	Event	Days from Sowing		Accumulated Growing Degree		Modified Growing Degree	
Cycle-4-E (N = 126)							
17 August 2022	transplanting	13	±0	306	±0	199	±0
10 September 2022	change photoperiod to 12/12	37	±0	997	±0	556	±0
20–25 September 2022	full male flowering	49	±2	1298	±62	764.5	±45.5
28–31 October 2022	harvest	87	±2	2200.5	±31.5	1491.5	±9.5
Cycle-5-E (N = 633)							
10 March 2023	transplanting	14	±0	314	±0	214	±0
5 April 2023	change photoperiod to 12/12	40	±0	1007	±0	670	±0
13–17 April 2023	full male flowering	50	±2	1270.5	±49.5	852	±38
13–15 May 2023	harvest	79	±1	2036.5	±23.5	1389.5	±19.5
Cycle-6-E (N = 513)							
14 August 2023	transplanting	13	±0	298	±0	195	±0
7 September 2023	change photoperiod to 12/12	37	±0	1023	±0	518	±0
17–20 September 2023	full male flowering	48	±2	1337	±39	731.5	±25.5
1–2 November 2023	harvest	92	±1	2384.5	±12.5	1512.5	±9.5
Cycle-4-B (N = 98)							
4 August 2022	transplanting	13	±0	306	±0	257	±0
27 August 2022	change photoperiod to 12/12	36	±0	1015	±0	591	±0
5–12 September 2022	full male flowering	49	±3	1369	±95	782	±54
17–21 October 2022	harvest	89	±2	2374.5	±48.5	1516.5	±36.5
Cycle-5-B (N = 472)							
24 May 2023	transplanting	14	±0	307	±0	289	±0
18 June 2023	change photoperiod to 12/12	39	±0	1015	±0	639	±0
22–26 June 2023	full male flowering	45	±2	1203.5	±63.5	721	±28
1–5 August 2023	harvest	85	±2	2360	±51	1327.5	±35.5

5.6.1. Evaluation of phenological stages and thermal time

The differences observed among individual plants in their phenological stages are primarily attributable to the pronounced divergence in morphology and maturity time of the parental cultivars.

Ultra-early (day-neutral/autoflowering) and excessively late individuals were culled, as our principal objective was line stabilization and seed increase under open-field conditions.

The most critical time with temperature changes is the transfer from the nursery to the greenhouse environment. Continuous acclimatization is crucial at this point. In order to avoid stress-induced early flowering and misleading morphological parameters, only uniformly developed, healthy plants were transferred to the vegetative stage (Figure 41).



Figure 41. Homogenous, well developed vegetation after acclimatization

We set the switch to short-day (blackout) operation at the point when accumulated growing degree days (GDD) approached ~ 1000 °C·day. In our system, this threshold coincided with the attainment of sufficient vegetative biomass and the target final plant height.

Figure 42 depicts two complete early (B) cycles—one from late summer into autumn and the other from spring into mid-summer—each aligning daily air temperature, cumulative growing-degree days (GDD), phenological stage, and light exposure. GDD accumulates more rapidly in the spring–summer window than in the late-summer–autumn window, implying that the same cultivar should mature sooner.

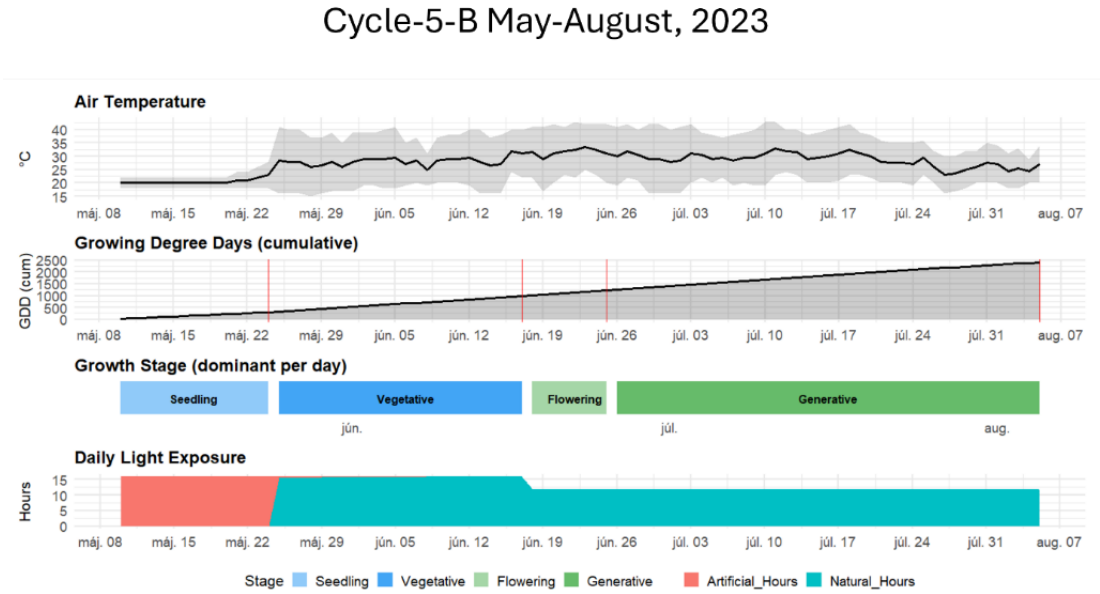
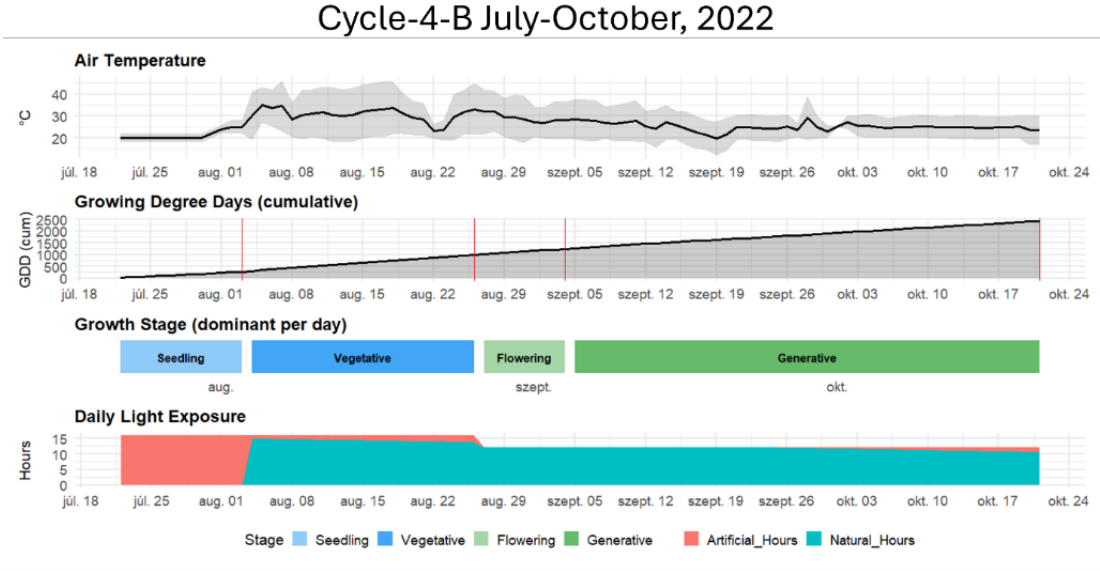


Figure 42. Air temperature, accumulated GDD, observed phenological stages and light control in case of early (B) strain

Photoperiod management follows a standard regime: a 16-hour long day during vegetative growth and an abrupt reduction to 12 hours to trigger flowering and sustain the generative

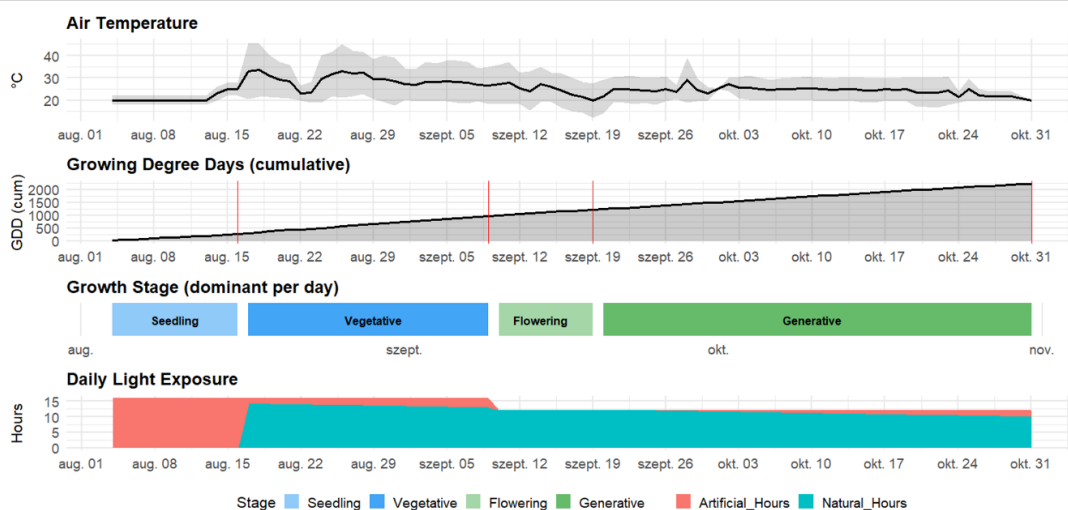
phase. In late summer, supplemental lighting is required through much of August to maintain long days, after which natural daylength suffices for the short-day reproductive period. By contrast, during early summer, natural days are too long, so blackout is used to enforce the short-day signal despite abundant daylight. The red markers on the GDD graphs coincide with these photoperiod switches, indicating that stage changes are governed by light cues in concert with minimum thermal-time thresholds.

Stage timing differs between seasons in ways that matter agronomically. In the late-summer–autumn cycle, seedling and vegetative phases occupy roughly the first month, a brief flowering transition occurs in late August, and the generative stage extends deep into October. Cooler nights during this period slow GDD accumulation, lengthening maturation even though calendar time advances. In the spring–summer cycle, a similar early trajectory is followed, but the reproductive period unfolds under warmer conditions, so thermal time accrues faster and the crop finishes earlier, although that means only 4 days advantage in favor of spring-summer cycle (Table 18).

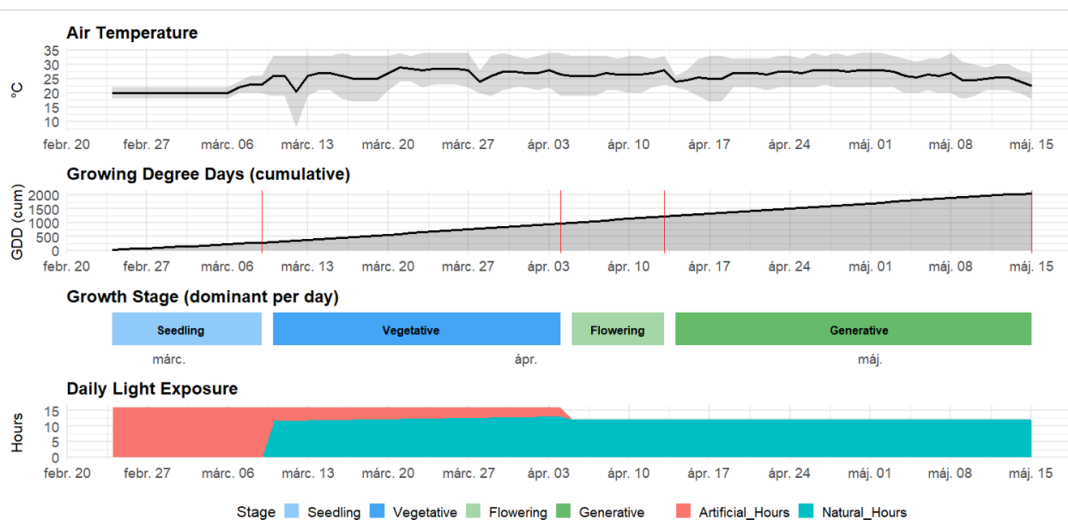
These dynamics have practical implications. Spring–summer production aligns the generative stage with higher temperatures, shortening the cycle and improving schedule reliability, provided blackout infrastructure is available. Late-season production reduces the need for blackout but risks prolonged finishing and potential yield or quality penalties if cool nights depress assimilate supply; selective night heating or cultivars with lower base temperatures can mitigate this. Brief heat spikes near induction appear in both cycles and may warrant shading or evaporative cooling for sensitive genotypes. From an energy standpoint, the autumn schedule expends electricity on supplemental lighting during August, whereas the spring schedule incurs operational costs for blackout without equivalent electrical draw; the preferred window thus depends on the trade-off between energy and climate control capacity.

Figure 43. shows the late-summer to late October (top), late winter to mid-May (middle), and late summer into early November (bottom) cycles in case of the medium (E) strain. In all cases, the phenology follows the standard pattern.

Cycle-4-E August-October, 2022



Cycle-5-E March-May, 2023



Cycle-6-E August-November, 2023

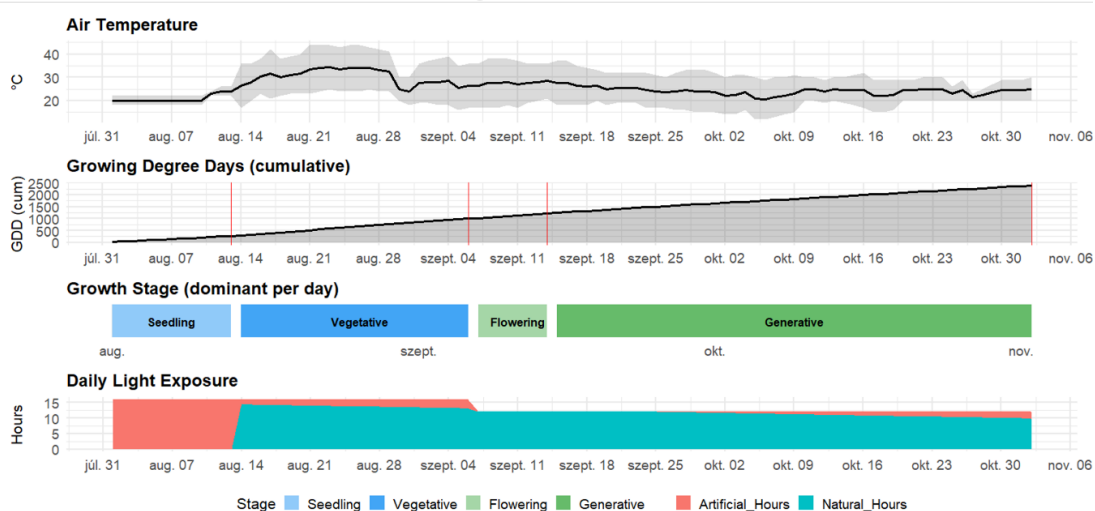


Figure 43. Air temperature, accumulated GDD, phenological observation and light control in case of the medium (E) selection

In the late-summer–autumn cycle (top panel), the GDD curve starts relatively steep and gradually flattens, indicating slower daily thermal accrual as nights cool. Vegetative growth is maintained with 16-h days using supplemental light in early–mid August; the schedule then shifts to 12h to induce flowering and carry the crop through a cool generative finish. The red ticks on the GDD axis coincide with the photoperiod switch, underlining that stage transitions are coordinated by light cues in tandem with minimum GDD thresholds. Agronomically, this window reduces the need for blackout after induction but risks an extended, cooler maturation that may require night-heat support to keep finish times predictable.

The late-winter–spring cycle (middle panel) shows a different constraint set. Initial temperatures are lower so the early GDD slope is shallow; it steepens into April as conditions warm, yet it never matches midsummer rates. Long days during the vegetative phase are achieved mainly with artificial light, reflecting short natural photoperiods in late February–March. Around early April the schedule is cut to 12h to trigger flowering; because natural daylength is increasing in this period, sustaining a short day likely requires blackout. The generative stage then proceeds under comparatively warm, stable conditions into May, giving a quicker and more reliable finish than the top panel despite the earlier cool start—provided the blackout operation is well controlled.

The third cycle (bottom panel) also starts in high summer but extends deeper into autumn, and its temperature trace declines more gently than in the first panel. The GDD line keeps a steadier slope into October and even early November, so thermal time continues to accumulate at useful rates late in the crop. After a brief, artificially extended vegetative period in August, the system switches to short days in early September and holds them through harvest.

Following Mediterranean phenology literature (Lisson et al., 2020; Amaducci et al., 2008; Cosentino et al., 2012) we also computed modified GDD values. For the Hungarian cultivar ‘Tiborszállási’, whose morphology and growth habit are comparable to our material, the base temperature and thermal sum were defined as:

$$C_d (GDD) = \sum_{i=1}^n \frac{(T_{\min,i} - T_b) + (T'_{\max,i})}{2},$$

where

- n : number of days to the end of the vegetative period;

- $T_{\min,i}$: daily minimum temperature on day i ;
- T_b : base temperature ($^{\circ}\text{C}$) below which development ceases; for ‘Tiborszállási’, $T_b = 1.9^{\circ}\text{C}$;
- $T'_{\max,i}$: the modified daily maximum temperature, defined piecewise as
 - if $T_{\max} \leq T_{\text{opt}}$, then $T'_{\max,i} = T_{\max}$;
 - if $T_{\max} > T_{\text{opt}}$, then $T'_{\max,i} = T_{\text{opt}} - (T_{\max} - T_{\text{opt}})$ (i.e., reflected about T_{opt});
- T_{opt} : the optimum developmental temperature; for ‘Tiborszállási’, $T_{\text{opt}} = 25^{\circ}\text{C}$.

Although the table reports GDD computed with these base and optimum temperatures, in our case the modified metric did not yield a clear advantage: especially in early spring it tended to overestimate progress relative to actual photosynthetic activity and visible biomass accumulation. By contrast, in July–August—when incident radiation can be better replicated with supplemental lighting—the modified calculation may provide more reliable results.

Compared with field data, total crop duration was 140 days (sowing to harvest) in 2022 and 153 days in 2023, placing the material in a medium-to-late maturity class. The earlier (B) selection was harvested 129 days after sowing in 2022 and 140 days in 2023. Relevant open-field observations are summarized in Table 19.

Table 19. Accumulated Growing Degree Day (GDD) values and key phenological observations from open-field trials in 2022 and 2023

Event	Days from Sowing				Accumulated Growing Degree Days		Modified Growing Degree Days	
					E.	B.	E.	B.
	2022 (n = 250)							
	E.		B.		E.	B.	E.	B.
emergence	5	±1	5	±1	82	82	0	0
male flowering	68	±3	51	±2	1363	960	1062	773
female flowering	73	±4	56	±3	1460	1072	1150	860
harvest	140	±3	129	±2	2951	2735	2277	2086
	2023 (n = 250)							
emergence	6	±1	6	±1	90	90	0	0
male flowering	73	±4	55	±2	1268	878	1042	727
female flowering	77	±5	62	±3	1358	1033	1113	845
harvest	153	±2	140	±2	3047	2772	2428	2208

5.7. Assessment of Harvestable Yield

In evaluating the method, a key criterion is the number of harvestable seeds, alongside trait-linked indicators of end-use suitability and quality. Under greenhouse cultivation, seed yield from maternal plants selected on morphological criteria—benchmarked to be comparable with their open-field phenotype—must be sufficient to establish field plots and, in light of genetic gain, to serve as potential pollen donors across the breeding nursery.

Within the speed breeding framework, we designated pollen from male-flowering individuals originating from progeny families whose maternal plants surpassed predefined thresholds (cannabinoid profile, seed yield, plant height) and expressed the target attributes: stem color and diameter, leaf morphology, estimated maturity, thousand-seed weight, and seed-coat color and marbling.

Seed counts collected from individual plants are illustrated in Figure 44.

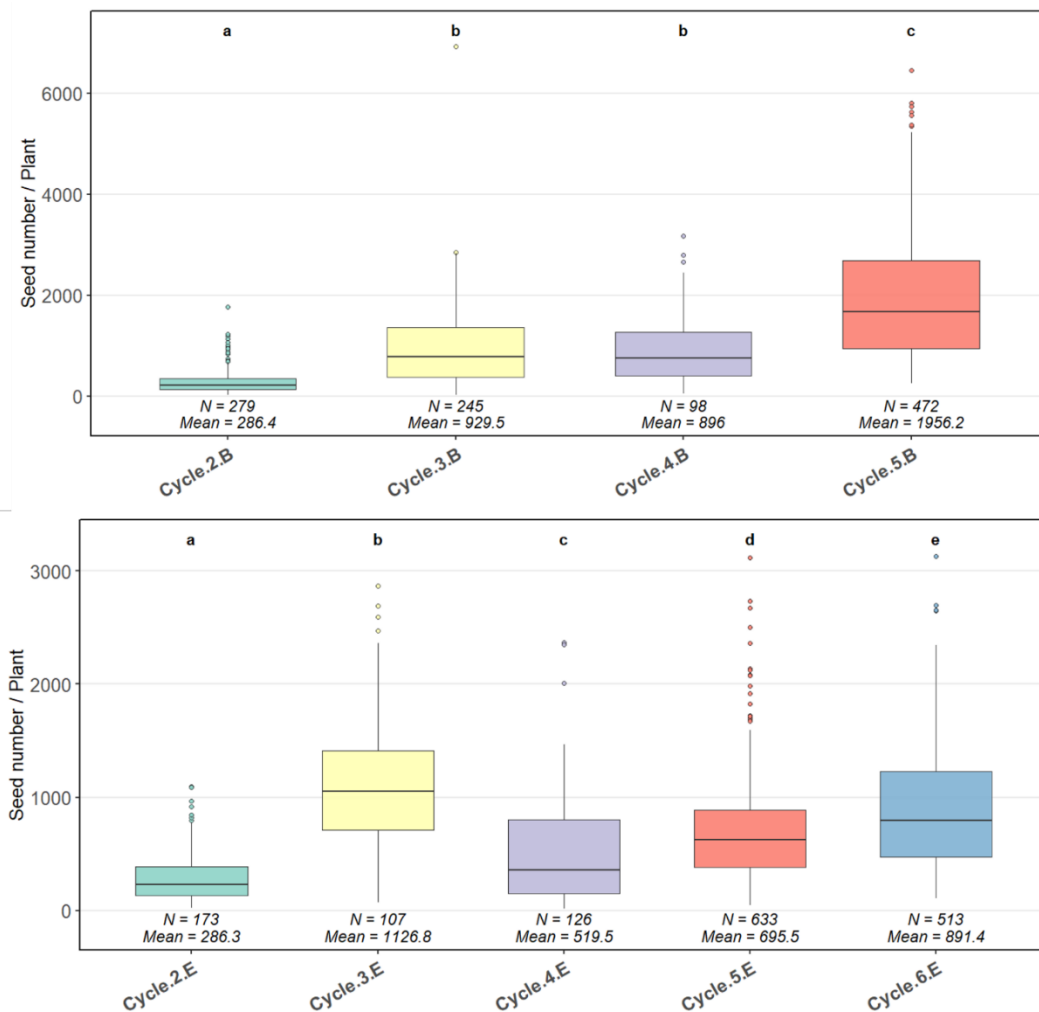


Figure 44. The number of seeds from individual plants in case of both selections

5.8. Evaluation of Thousand-Kernel Weight and Yield

Thousand-kernel weight (TKW) is a key varietal parameter and was therefore used as a selection criterion. Figure 45 depicts changes in TKW across accelerated generation cycles.

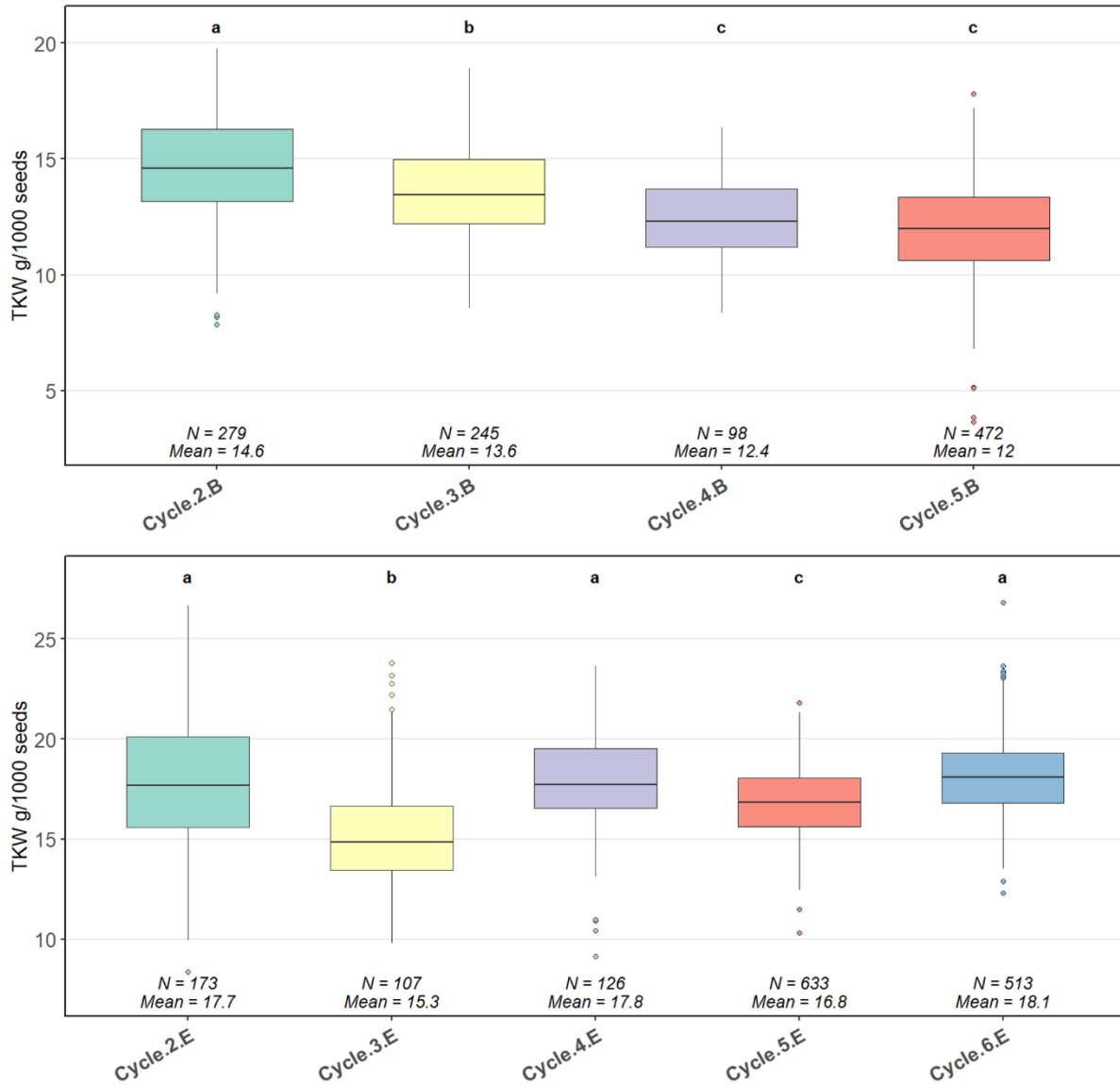


Figure 45. TKW changes across accelerated generation cycles

Seed yield and TKW from open-field plots were assessed in two growing seasons with markedly different environmental conditions (Figure 46).

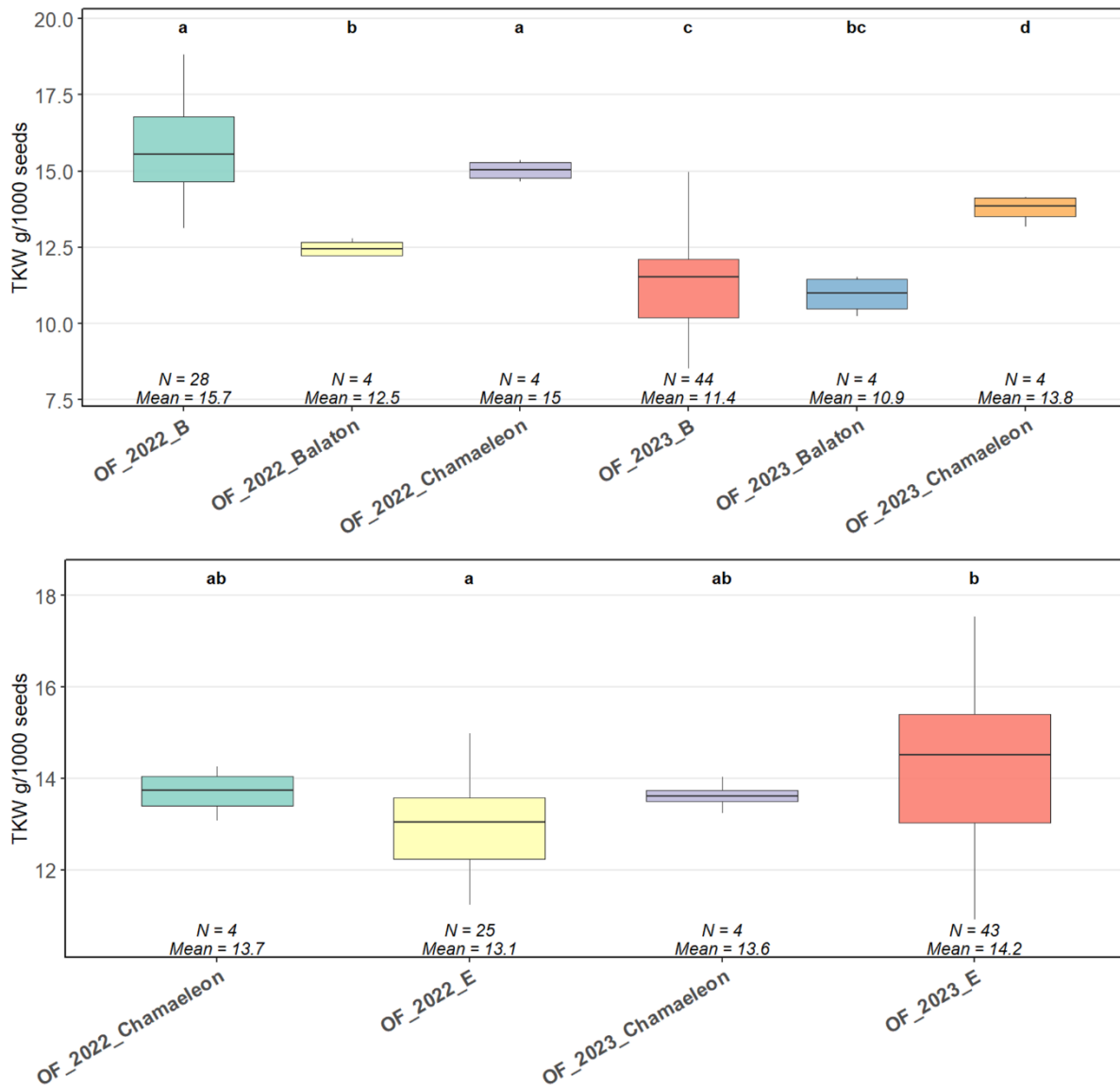


Figure 46. Open-field TKW observations in two growing season

Regarding the initial materials, the cultivar ‘Balaton’ used in the first cross had a TKW of 14.2 g, ‘Eletta Campana’ 20.3 g, and ‘Chamaeleon’ 16.2 g. For the mid-to-late maturing “E” selection, our primary objective was to maintain high TKW. In contrast, for the early “B” selection, seed yield took precedence; consequently, we retained and advanced more compact, “maternal-type” (Balaton-like) individuals.

Figure 47 presents seed yield and germination capacity for plots sown in the 2023 field trial. For comparison, plots originating from the 2022 field experiments (OF_2022_B and OF_2022_E) are also included. The OF_2023_E and OF_2023_B plots derive from lots produced in the preceding cycle of the speed-breeding scheme.

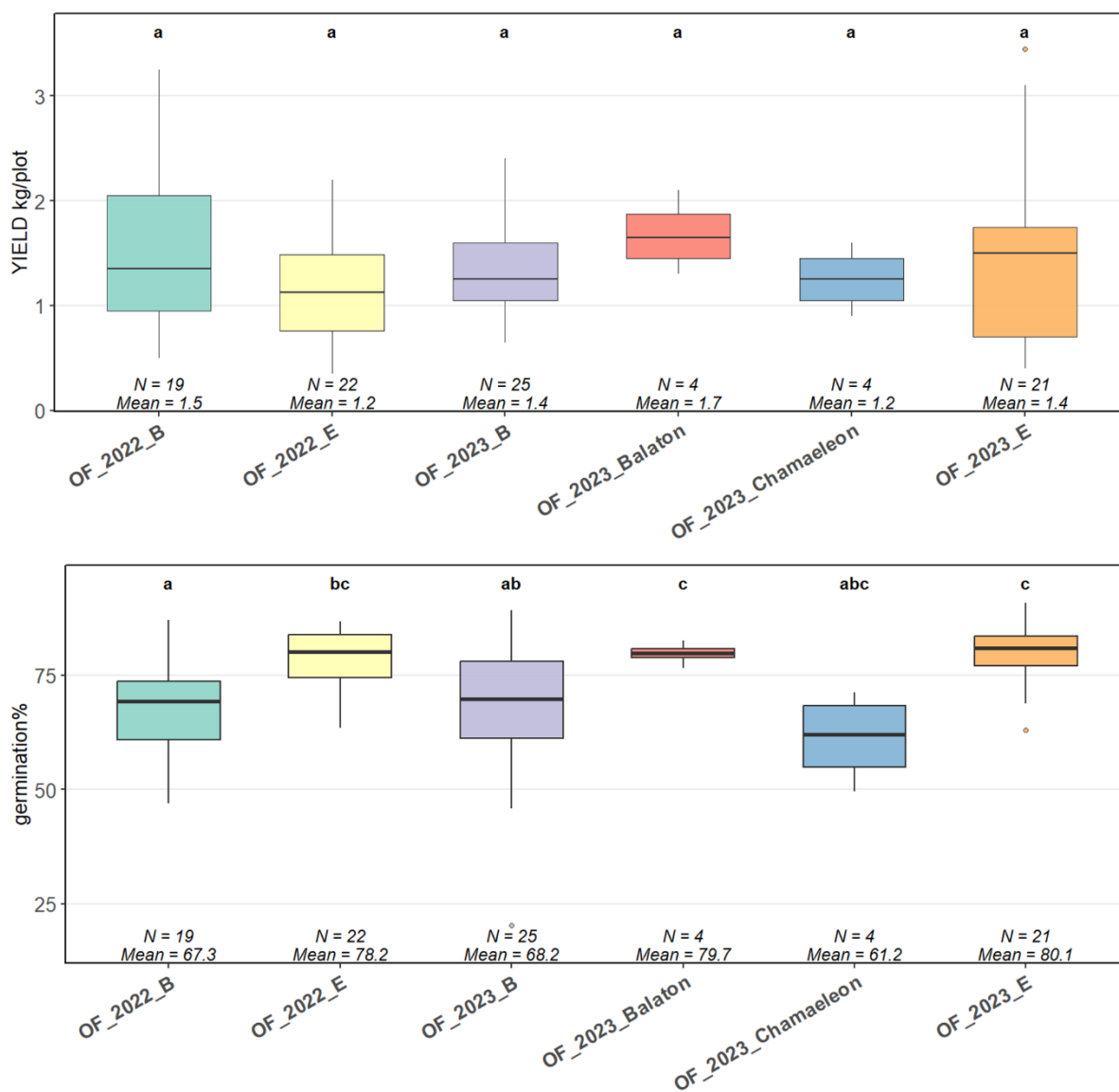


Figure 47. Seed yield and germination capacity

5.9. Comparative Evaluation of Cannabinoid Content

Throughout the entire breeding program, we continuously assessed the cannabinoid profiles of plants. Cultivation suitability in hemp is fundamentally constrained by the tetrahydrocannabinol (THC) level; in Hungary, the legal upper limit is 0.2%. For rapid, cost-effective prescreening of large numbers of individuals, we employed a thin-layer chromatography (TLC) procedure and advanced only the seed from plants exhibiting the lowest possible THC and the highest possible cannabidiol (CBD) contents. A ready-to-use commercial kit was utilized (Alpha-Cat TLC kit; Canabe s.r.o.).

Cannabinoid measurements were repeated in 2023. As shown in Table 20, the choice of initial crossing material is pivotal. Importantly, large number of plant-level selection based on chemical parameters was implemented only from Cycle 2 onward.

Table 20. Cannabinoid analysis results in case of the cycle comparison trial. Cannabinoid content is interpreted as m/m%

	$\Delta 9$ THC	THCA	TotalTHC	CBD	CBDA	TotalCBD	CBDV	CBDVA	CBG	CBGA	CBC	CBN	THCV
Cycle-1-B	0.179	0.075	0.245	2.091	1.846	3.729	0.007	0.004	0.010	0.015	0.143	0.018	0.002
Cycle-2-B	0.178	0.091	0.259	1.188	1.150	2.208	0.004	0.004	0.017	0.015	0.053	0.009	0.001
Cycle-3-B	0.029	0.010	0.038	1.343	0.988	2.220	0.007	0.005	0.010	0.006	0.039	0.003	0.000
Cycle-4-B	0.041	0.007	0.047	1.767	0.959	2.618	0.009	0.004	0.022	0.008	0.056	0.005	0.000
Cycle-5-B	0.045	0.012	0.055	1.790	1.195	2.850	0.008	0.006	0.030	0.014	0.055	0.005	0.000
Open-field-2022-B	0.032	0.010	0.041	1.653	0.908	2.458	0.007	0.005	0.013	0.009	0.044	0.003	0.000
Cycle-1-E	0.224	0.141	0.350	1.549	1.396	2.786	0.045	0.046	0.027	0.030	0.054	0.011	0.005
Cycle-2-E	0.058	0.019	0.075	1.661	0.783	2.356	0.005	0.005	0.011	0.009	0.058	0.003	0.001
Cycle-3-E	0.033	0.015	0.046	1.306	0.888	2.094	0.004	0.004	0.009	0.007	0.054	0.002	0.000
Cycle-4-E	0.037	0.012	0.048	1.373	1.080	2.331	0.004	0.003	0.011	0.007	0.063	0.003	0.000
Cycle-5-E	0.029	0.010	0.038	1.422	1.220	2.505	0.008	0.005	0.009	0.006	0.043	0.002	0.000
Cycle-6-E	0.037	0.016	0.051	1.416	1.387	2.646	0.005	0.005	0.013	0.012	0.051	0.002	0.000
Open-field-2022-E	0.069	0.017	0.084	1.930	1.337	3.115	0.005	0.005	0.037	0.019	0.057	0.006	0.000
Balaton	0.024	0.007	0.030	1.274	0.940	2.107	0.028	0.009	0.005	0.003	0.041	0.004	0.000
Carmagnola	0.230	0.133	0.348	4.574	3.405	7.595	0.013	0.009	0.115	0.084	0.077	0.009	0.001
Chamaeleon	0.039	0.008	0.046	1.619	1.329	2.798	0.004	0.004	0.015	0.010	0.045	0.002	0.000
Dioica 88	0.034	0.007	0.041	2.844	2.577	5.130	0.004	0.004	0.014	0.011	0.041	0.002	0.000
Eletta campana	0.053	0.005	0.058	4.686	2.646	7.032	0.048	0.024	0.024	0.011	0.057	0.002	0.001
Futura 75	0.025	0.010	0.034	2.602	3.039	5.298	0.007	0.009	0.008	0.008	0.038	0.002	0.000

Based on Table 20., a weakness of our selection strategy was that we neglected rare cannabinoids, even though they were detectable in the initial population—for example, cannabichromene (CBC; Cycle-1-B: 0.143%).

Figure 48 only illustrates the measured full CBD content from the 2023 field trial. Progress across cycles is modest and overshadowed by between-genotype differences. E line (green). Unlike B, Open-field-2022-E is conspicuously higher than both Cycle-3-E and Cycle-4 where it should “fit”, approaching the upper end of the E distribution. This point behaves as a positive deviation from the surrounding cycles.

These results indicate that genetic background is the primary driver of CBD %, with top cultivars reaching 2–3× the levels observed in most line cycles. Genetic effects dominate. The magnitude of differences among standard varieties far exceeds the incremental changes across B/E cycles.

The elevated value relative to Cycle-3-E and Cycle-4-E suggests environmental and/or measurement causes rather than abrupt genetic improvement between adjacent cycles.

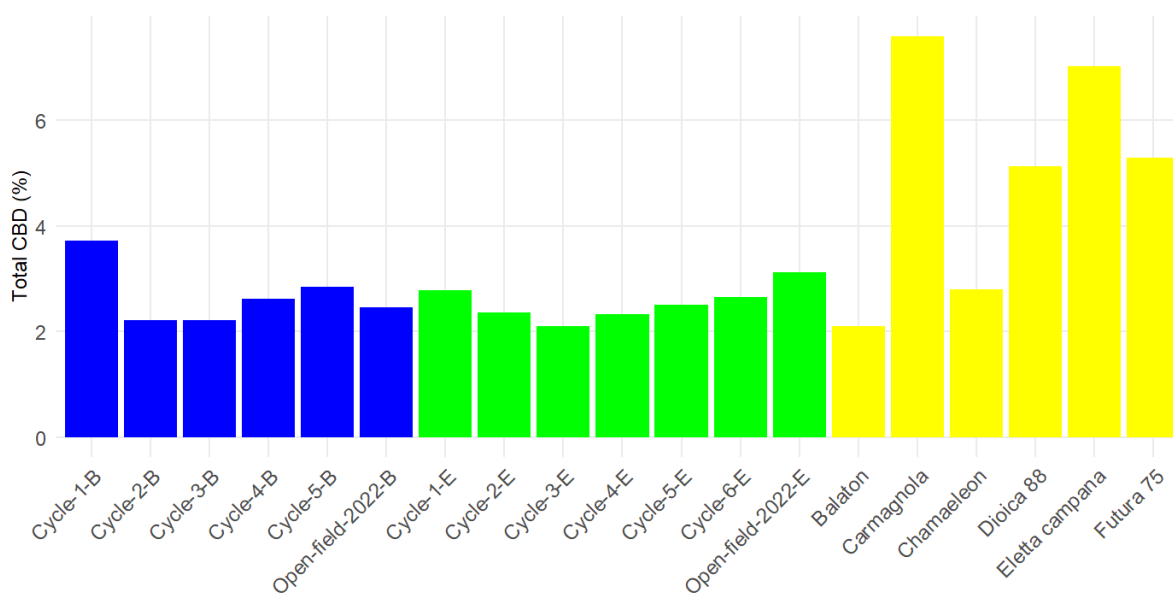


Figure 48. Total CBD content comparison from the 2023 open-field trial

The TLC-based overestimation of THC content unfortunately negatively affected and constrained the attainable CBD content, thereby slowing progress. The year effect (interannual variation) markedly confounds genetic inference; such high values have not previously been observed in standard cultivars. By contrast, in our own breeding material, progress is assessable, as illustrated by the linear trend observed in the mid-season E line shown in Figure 49.

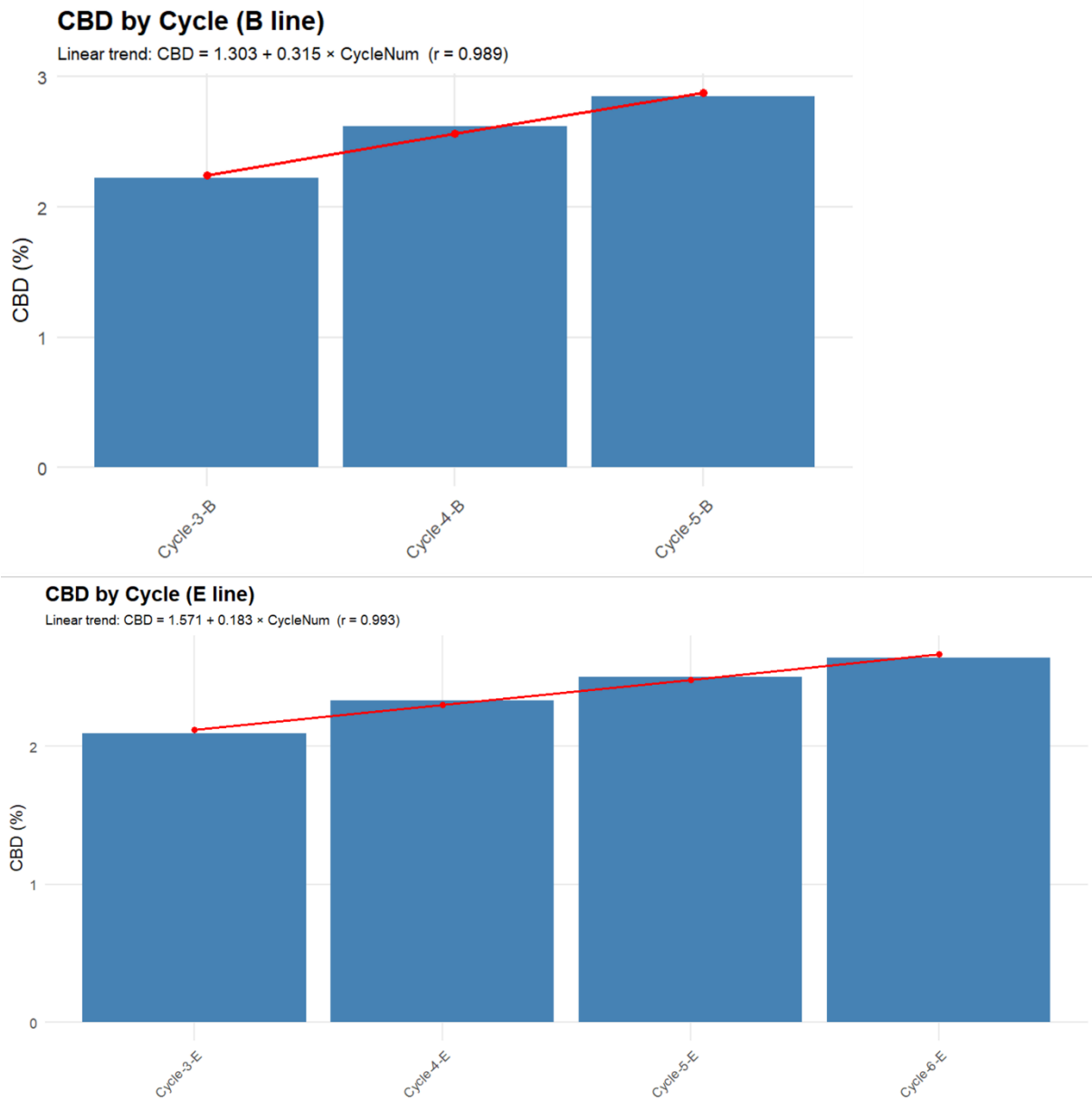


Figure 49. Open-field confirmation of the trend in case of Total CBD (m/m%) content

With respect to THC content, the pronounced overestimation associated with thin-layer chromatography (TLC) ultimately proved advantageous: leveraging large-sample screening, we removed individuals that could have constrained cultivar registration. Consequently, we established stable populations with consistently low THC content (Figure 50).

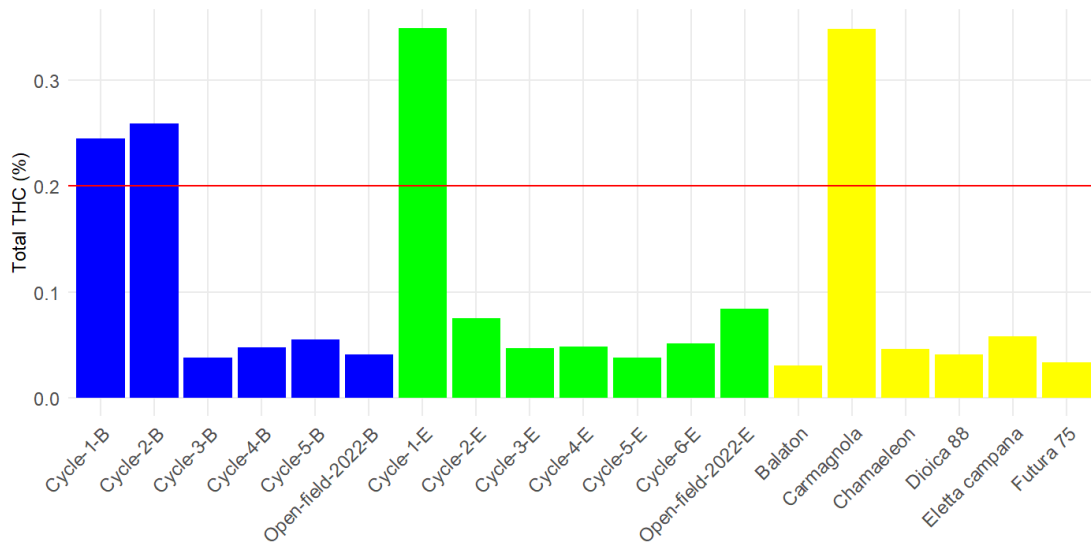


Figure 50. Total THC content comparison from the 2023 open field trial

Moreover, in the case of the early-maturing variety candidate (KB 101/A – resulted from B selection), the Hungarian authority detected non-compliant values during the evaluation of variety registration tests conducted at 5 locations in 2024. The famous Kompolti variety was also among the standards (Figure 51).

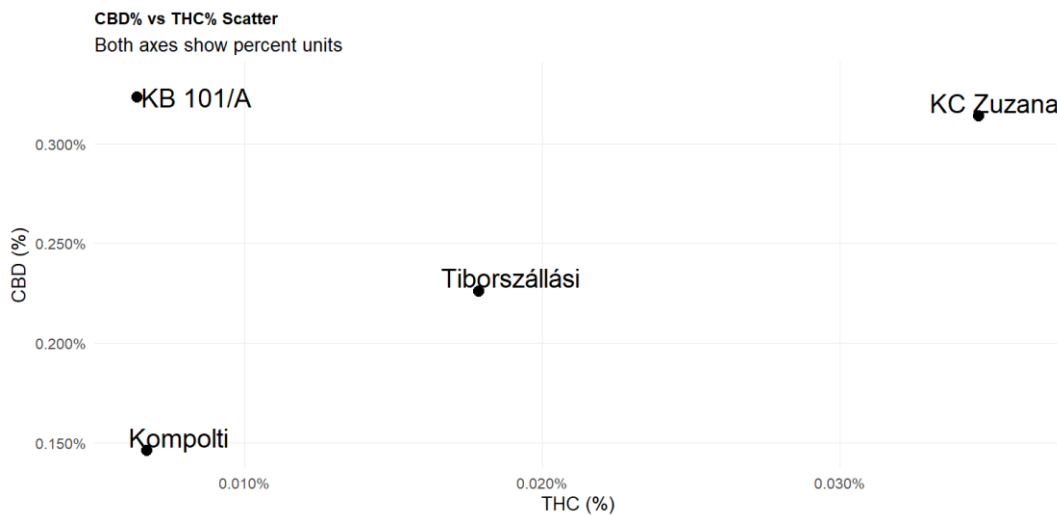


Figure 51. CBD and THC content during the variety registration process (Hungarian Food Safety Authority- NéBiH, 2024)

It can be stated that during accelerated breeding, with strict selection, completely unique CBD/THC ratio can be achieved, which can be confirmed under open field conditions conducted at several locations (Figure 52).

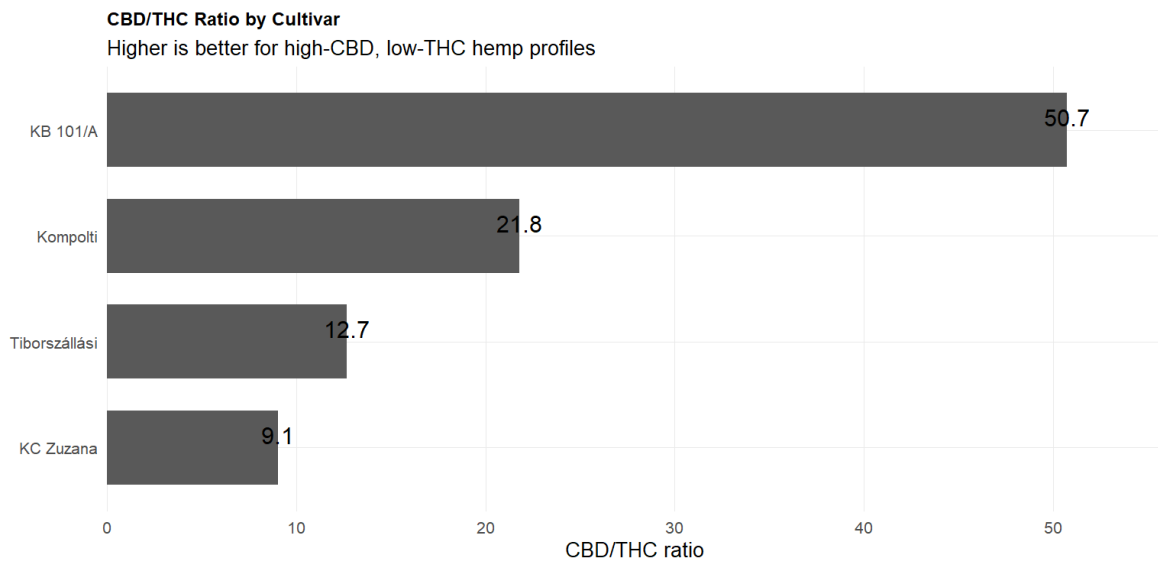


Figure 52. Counted CBD/THC ratio in case of the variety registration trials (NéBiH, 2024)

6. DISCUSSION

The primary objective of this study was to evaluate the utility of an integrated Speed Breeding (SB) platform for the rapid introgression and fixation of recessive traits in dioecious *Cannabis sativa* L. This approach successfully circumvented the primary biological constraint of the species—its photoperiod-sensitive, annual life cycle—by achieving eight generations over two years, an outcome consistent with the potential reported in literature for controlled *Cannabis* environments (Schilling et al., 2023; Somody and Molnár, 2025). The ability to manage the profoundly different flowering times of the parental lines (e.g., the early-maturing *Chamaeleon* and the late-maturing *Eletta Campana*) via photoperiod manipulation was crucial to initiating and sustaining the crossing program.

6.1. Integrating speed breeding into cannabis crossing

The dioecious nature of hemp presents significant challenges for controlled breeding, as many quantitative and qualitative traits cannot be assessed in male plants. Our strategy addressed this by using pollen exclusively from individuals raised from well-defined, selected mother seeds that had surpassed predefined thresholds (cannabinoid profile, seed yield, morphology). This approach, supported by the 90-day SB cycle, ensured a continuous and predictable source of superior male genetic material.

A key finding confirming the system's ability to maintain productivity was the continuous increase in mean seed number per plant over successive cycles (Figure 44). For the early 'B' line, mean seed count rose from 285 in Cycle-2 to over 1,056 in Cycle-5, and for the medium 'E' line, from 286 in Cycle-2 to 891 in Cycle-6. This remarkable increase, coupled with the observed lack of meaningful correlation between seed number and Thousand-Kernel Weight (TKW) (Figure 45), confirms that the intensive selection within the SB environment did not compromise fundamental seed quality or yield potential. Moreover, the maintenance of high final germination capacity across advanced lines (Figure 47) suggests that the accelerated maturation regime does not incur long-term viability penalties.

A crucial selection pressure in this work, consistent across most SB cycles, was the capacity for survival and recovery under extreme thermal conditions, where daily maxima frequently exceeded 40 °C (Table 8 and 9). This inherent pressure, coupled with the thermal stability provided by the greenhouse infrastructure (Füzi and Ladányi, 2022), inadvertently favored heat-

tolerant genotypes, a finding relevant for breeding lines adapted to the increasing frequency of extreme hot days in Central European growing regions.

6.2. Stabilization of the yellow-stem trait

The successful and complete stabilization of the yellow-stem trait by the fifth generation in both the 'B' and 'E' lines validates the efficiency of SB for recessive trait fixation (Table 12 and 15). This trait, when fixed, holds significant industrial and agronomic implications, as the yellow-stem phenotype is recognized in the literature for yielding finer bast fibres and a higher long-fiber proportion (Amarasinghe et al., 2022). This phenotypic stability was subsequently confirmed in the open-field trials in 2023, where advanced generations exhibited 100% yellow-stemmed plants.

However, the segregation patterns observed in the F₂ backcross generation deviated significantly from the expected 3:1 Mendelian ratio (Table 14). The necessity of introducing a 'light green' intermediate class suggests that the trait's inheritance may involve either incomplete dominance at the putative single locus or that the expression of the recessive allele is subject to segregation distortion or viability selection in the resource-constrained SB environment. This complexity was further illustrated in the PCA biplots (Figures 21-34), which showed that while Motherplant identity exerted a statistically significant influence (explaining a small-to-moderate portion of multivariate variation, ranging from 5% to 20%), the heterogeneity within progenies persisted, requiring continuous multi-cycle selection to achieve stability in the targeted yield and morphological traits. This highlights a limitation of relying solely on Mendelian models during rapid advancement, necessitating genotypic confirmation in future work.

The chosen strategy of backcrossing followed by family selection was a deliberate response to the risks posed by the high genetic variability of the starting populations, as outlined in the introduction. The alternative approach—"family breeding" on early F₂ heterozygotes—was strategically avoided because the deficit in homozygous yellow-stemmed female plants would have drastically constrained the number of both seed-bearing mothers and, critically, genetically ideal male pollen donors needed to sustain the accelerated cycle. The chosen backcrossing pathway, though initially slower in terms of single-trait fixation, provided controlled genetic isolation and ensured the continuity of the entire multi-trait process.

6.3. Development of phenotyping methods

The use of Unmanned Aerial Vehicle (UAV)-based phenotyping via the Visible Atmospherically Resistant Index (VARI) proved to be a rapid and cost-effective alternative to manual phenotyping for the yellow-stem trait in field plots (Table 16). The strong correlation observed between VARI and direct SPAD chlorophyll measurements ($r=0.76$, Figure 38), combined with the strong correlation between UAV-derived height estimates and direct measurements ($r = 0.93$, Figure 40), validates this technology for high-throughput field assessment of key agronomic traits (Wang et al., 2018).

The comparative analysis of Growing Degree Days (GDD) between greenhouse and field environments highlighted the difficulty in predicting field performance solely from SB data. Although the total accumulated GDD was comparable between the two field years (2022 and 2023), the time to harvest for the 'E' line differed by over ten days (Table 19). The drastic reduction in the vegetative phase in the SB setting—necessary to control height—made the final height and maturity time of the late-maturing 'E' line harder to predict. The GDD-based thermal model, including the modified GDD calculation, provided no clear advantage in predictive power, supporting the conclusion that while SB is an exceptional tool for accelerating genetic advancement, natural maturation and G×E field validation remain indispensable for final cultivar release (Somody and Molnár, 2025).

6.4. Cannabinoid profiling

The primary constraint of the breeding program was regulatory compliance, mandating strict selection for the low-THC chemotype.

The foundational element of our chemical phenotyping was the use of Thin-Layer Chromatography (TLC) for high-throughput prescreening. The preliminary THC/CBD analysis of the parent cultivars (Figures 10-13, Table 11) showed wide variance, justifying the need for strict culling. While the TLC strategy effectively secured lines compliant with the Hungarian 0.2% THC limit, it introduced a significant methodological trade-off. The tendency of the TLC assay to overestimate THC content (Table 10) led to the premature culling of individuals that might have been high in CBD but technically compliant via official AOAC-validated HPLC analysis. This unintended consequence slowed the potential rate of CBD gain in the advanced lines. However, quantifiable progress was still achieved: the 'E' line demonstrated a clear linear

trend for CBD content across cycles (Figure 49: $r=0.993$), confirming that genetic gain, albeit slow, was achieved under the selective pressure.

Early cross-progenies exhibited pronounced THC content variance (Figure 15). Furthermore, the observation that early-generation heterozygotes derived from the Chamaeleon cross often displayed traits such as lower CBD content and weaker seed yield suggests an unfavorable linkage or poor combining ability between the desired yellow-stem allele and these commercial traits in the F_1 and F_2 generations. This mandated a multi-cycle selection to break the undesirable associations.

The intense focus on the CBD:THC ratio led to the neglect of rare cannabinoids (e.g., CBC), despite their detectable presence in the initial populations (Table 20: Cycle-1-B: 0.143%). Future research should integrate a marker-assisted approach to simultaneously track the inheritance of both major and minor cannabinoids.

6.5. Natural versus accelerated maturation

In controlled environments, flowering time was managed via photoperiod manipulation, which was also necessary to manage final plant height (LED fixtures at 4 m; plants had to remain below this). Longer vegetative phases increased risks of overgrowth and mechanical injury. To better emulate natural July–August irradiance, the system would ideally adjust more than supplemental light alone; in our setup, photoperiod control was anchored to absolute temperature values, which correlated better with growth vigor and expected maximum height—even when temperatures exceeded the optimum.

Each cycle involved transplanting seedlings to the greenhouse, which affects the required vegetative duration. Regeneration is shortest in early spring; rising irradiance accelerates maturation. In August, optimal transplant timing is harder to achieve due to greater heat stress.

In our crosses, the male parent was the early ‘Chamaeleon’ and the female parent the late ‘Eletta Campana’. Field observations allowed selection of mid- to late-maturing lines carrying female-parent-like attributes; most progeny fell into this group. At our latitude (47.8° N), seed set and maturation are secure.

For comparability, we computed GDD to assess how well field traits (height, flowering time) can be predicted from controlled-environment selections. Baseline parameters and expected phenophases aligned well for the early “B” selection. In the mid-to-late “E” line, the

vegetative phase was substantially shortened, making final height and maturity time harder to predict.

6.6. Limitations and challenges

Crossing cultivars with divergent flowering times requires precise environmental control, especially for photoperiod-dependent traits. Ensuring genetic purity necessitated manual interventions (emasculation, controlled pollination) in both greenhouse and field. Field trials expose stands to climatic fluctuations that can affect phenotypes and yield. In the greenhouse, objective assessment of some key traits (natural maximum height, stem diameter and cross-section type, maturity class) is constrained. The trait list studied was targeted and relatively narrow; thus, the method's generalizability to many complex traits cannot yet be judged. Field trials were conducted in two climatically distinct seasons; multi-location testing is ongoing. The efficiency of selection and breeding workflows can be fully assessed only over multiple years. While large-scale, long-term field selection of mother plants remains indispensable for genetic gain and yield stability, speed breeding enables targeted introgression of a few well-defined traits.

6.7. Industrial and agronomic implications

Successful incorporation of the yellow stem, balanced flowering time, and a controllable cannabinoid profile indicates market potential. Yellow-stemmed hemp is clearly distinguishable from drug-type stands; incorporating this trait was also meant to mitigate legal-societal barriers to cultivation while preserving favorable attributes of the founder parents. These advances are directly relevant to textile and pharmaceutical applications (premium fibre, tailored cannabinoid profiles). Adaptation of hemp to higher latitudes and controlled environments improves its agro-ecological viability.

6.8. Future directions

Chemotype inheritance and CBD/THC gene markers are well studied (Cascicini et al., 2019; Toth et al., 2020). Genomic tools should be deployed to clarify the inheritance of critical recessive traits—such as yellow stem—and other quality attributes (seed marbling, seed-coat colour). More accurate climatic models and GDD computations are needed for each maturity group (including humidity and radiation) to better predict field performance of materials selected under accelerated conditions.

In closed production, lighting, heating, and cooling requirements must be defined to meet sustainability and productivity criteria. Extensive, energy-intensive lighting studies are available (Moher et al., 2021; Ahrens et al., 2023). Comprehensive growth analysis is needed to evaluate the sector's carbon footprint and long-term sustainability. For photoperiod-sensitive cultivars, maintaining the vegetative stage does not require a continuous 16-h light period: it suffices to keep the uninterrupted dark phase below 8 h using short light pulses (e.g., 1-h illuminations). Even a one-hour reduction can yield meaningful energy savings, but its impact on vegetative biomass production must be evaluated holistically.

Existing shading systems are low-energy within current infrastructure and merit investigation to reduce cooling/heating loads. Designing optimally controlled environments that serve both growth and sustainability is a key task.

Controlled environments offer substantial automation potential: AI and advanced image analysis can improve phenotyping accuracy, handle large populations, and reduce subjectivity. In UAV-based screening, AI can confer significant advantages: as Radočaj et al. (2023) note, deep learning can rapidly and effectively support individual plant detection, height estimation, assessment of green intensity, and detection of male-flowering plants.

Finally, multi-site testing of stabilized cultivars under diverse climatic conditions is essential to evaluate adaptation and stress tolerance and to deliver varieties suited to conventional agriculture.

Overall, this work represents a significant advance in modern hemp breeding, illustrating how traditional methods and contemporary technologies can reinforce each other to meet industrial demands and regulatory constraints.

7. CONCLUSION

This doctoral research successfully established and validated a novel Speed Breeding (SB) platform tailored for the rapid generation turnover and targeted genetic improvement of industrial hemp (*Cannabis sativa* L.). By precisely controlling photoperiod, temperature, and environment, this system successfully overcame the primary limitations of conventional hemp breeding—the species' dioecious nature and its photoperiod-sensitive, single-generation-per-year life cycle. The platform achieved a consistent seed-to-seed cycle of approximately 90 days, enabling eight selection cycles over two years. This unprecedented acceleration directly addresses the call for faster cultivar development to meet rapidly shifting market and regulatory demands, aligning with recent foundational work demonstrating SB feasibility in hemp (Schilling et al., 2023).

The platform's efficacy was proven through the successful introgression and complete fixation of the yellow-stem phenotype—a recessive trait linked to superior bast fiber quality—into two distinct genetic backgrounds ('B' and 'E' selections) by the fifth generation. This was a critical test of SB's power to stabilize qualitative traits under accelerated conditions, demonstrating its value in transferring specific, desirable industrial characteristics between parents with markedly different flowering times. Crucially, the resulting advanced lines maintained stability in agronomically vital traits, demonstrating high seed yield and Thousand-Kernel Weight (TKW), alongside germination capacity sufficient for robust field multiplication. This success demonstrates that SB, when correctly managed, does not necessitate a trade-off between speed and seed quality.

While achieving rapid generational advance, the study highlighted several inherent genetic and methodological complexities that inform future SB applications:

1. **Genetic Heterogeneity and Linked Traits:** The initial parental population introduced significant challenges. Early-generation heterozygotes derived from the *Chamaeleon* cross often exhibited undesirable traits—specifically, a tendency toward lower CBD content and weaker seed yield, suggesting potential unfavorable linkage or poor combining ability with the yellow-stem allele in the immediate F₁ and F₂ generations.
2. **Accuracy vs. Throughput in Chemical Screening:** The core regulatory success was achieved through rigorous selection using rapid Thin-Layer Chromatography (TLC) pre-screening. While this approach effectively ensured compliance with the stringent

domestic THC threshold of 0.2% (demonstrated by the superior CBD:THC ratios, e.g., >50:1 in the KB 101/A candidate line), the TLC method suffered from a tendency to overestimate THC content. This unintended methodological consequence, while mitigating legal risk by enforcing strict culling, likely led to the premature removal of otherwise high-CBD individuals, consequently slowing the rate of potential CBD gain in the advanced lines.

3. Challenges in Trait Segregation: The stabilization of the yellow-stem trait revealed unexpected genetic complexity, evidenced by the significant deviation from the expected 3:1 Mendelian ratio in early segregating populations (Table 14). The necessity of introducing a 'light green' intermediate class suggests the trait is not strictly monogenic recessive but exhibits characteristics consistent with incomplete dominance or segregation distortion within the controlled environment.

The decision to utilize backcrossing followed by family selection in the SB environment, rather than a more traditional F₂ population advancement (inbreeding early heterozygotes), was strategically justified by these complexities. While family breeding on early heterozygotes might theoretically accelerate initial trait fixation by skipping a backcross generation, this approach was deemed too risky. A pure family breeding strategy would have resulted in far fewer homozygous yellow-stemmed individuals (F₂ segregation), drastically limiting the pool of selected female plants. Furthermore, since the population is dioecious (approximately 50% males), a reduced pool of homozygous lines would have meant the inclusion of fewer potentially ideal male pollen donors in subsequent cycles, which could have stalled the entire breeding process. The chosen pathway successfully mitigated the immediate risks associated with low CBD and reduced yield linked to the *Chamaeleon* background, enabling a controlled, multi-trait advancement.

This research moves beyond proving the concept of *Cannabis* Speed Breeding to demonstrating its practical utility as an integrated, yet critically evaluated, platform for industrial cultivar development. The methodology provides a proven, accelerated pathway to stabilize multiple agronomic and chemical traits simultaneously, significantly shortening the time required to introduce genetically improved, legally compliant hemp varieties into conventional agriculture. The study also validated the application of modern phenotyping techniques, such as UAV-based VARI phenotyping, and demonstrated the selective pressure exerted by the semi-closed system.

8. NOVEL SCIENTIFIC RESULTS OF DOCTORAL RESEARCH

Based on the research conducted, the following results are proposed as novel scientific contributions to the fields of plant breeding, *Cannabis* genetics, and speed breeding methodology:

1. Validation and Optimization of a *Cannabis sativa* Speed Breeding (SB) Platform for Regulatory Compliance:
 - Demonstration and validation of an integrated SB system that overcomes the asynchronous flowering of genetically diverse *Cannabis* parental lines (early-maturing×late-maturing) to successfully achieve eight generational cycles over two years while maintaining seed viability and yield stability.
 - Validation of a high-throughput, low-cost Thin-Layer Chromatography (TLC) pre-screening methodology as a successful tool for regulatory compliance-driven selection within an accelerated program. This approach, despite its confirmed quantitative inaccuracy (TLC overestimation of Δ^9 THC relative to HPLC), proved effective in rapidly identifying and culling non-compliant chemotypes, which secured the regulatory viability of the advanced lines (e.g., KB 101/A with a CBD:THC ratio exceeding 50:1).
 - Quantification of genetic gain in Cannabidiol (CBD) content under severe selection pressure, documenting a clear linear trend ($r = 0.993$) across the accelerated cycles of the 'E' line, confirming that significant chemotype progress can be achieved concurrently with rigorous regulatory culling.
2. Characterization of Unfavorable Genetic Linkage in Industrial Hemp Germplasm:
 - Identification and characterization of an unfavorable genetic association or pleiotropic effect in early-generation heterozygotes derived from the *Chamaeleon* cross, where the desired yellow-stem phenotype was linked to reduced CBD content and weak seed yield. This novel observation highlights a critical genetic constraint for multi-trait breeding strategies involving the industrial yellow-stem trait.

3. Strategic Justification for Dioecious SB Pathway:

- Demonstration of the strategic necessity for backcrossing/family selection over simple F₂ inbreeding (family breeding) in dioecious, photoperiod-sensitive crops to mitigate the risks associated with the above-mentioned genetic constraints. This strategy successfully managed the trade-off between accelerated single-trait fixation and the critical need to preserve the genetic diversity and quantity of the male pollen pool essential for the continuity of the entire multi-trait SB program.

4. Documentation of Minor Cannabinoid Genetic Potential:

- Documentation of the genetic potential for minor cannabinoid biosynthesis (specifically Cannabichromene, CBC) in the early generations of novel industrial hemp lines (e.g., 0.143% CBC in Cycle-1-B), demonstrating the presence of this valuable genetic background despite its subsequent loss due to a breeding focus solely on the major CBD:THC chemotype.

9. PUBLICATIONS

Publications Directly Related to Dissertation Research

- Somody, G., & Molnár, Z. (2025). Flowering Synchronization Using Artificial Light Control for Crossbreeding Hemp (*Cannabis sativa* L.) with Varied Flowering Times. *Plants*, 14(1), 594. <https://doi.org/10.3390/plants14040594>
- Somody, G., & Aranyi, N. R. (2022). The potential impact of flower infecting botrytis bud rot (*Botrytis cinerea* Pers.) on hemp (*Cannabis sativa* L.) selective breeding. *Georgikon for Agriculture: A Multidisciplinary Journal in Agricultural Sciences*, 26(1), 126–137.
- Somody, G., Molnár, Z., & Lakatos, E. (2022). A kender (*Cannabis sativa* L.) domesztikációja, nemesítésének múltja, jelene és jövője. *Acta Agronomica Óváriensis*, 63(2), 158–184.

Other Academic Publications

- Budai, P., Kormos, É., Buda, I., Somody, G., & Lehel, J. (2021). Comparative evaluation of HET-CAM and ICE methods for objective assessment of ocular irritation caused by selected pesticide products. *Toxicology in Vitro*, 74, 105150. <https://doi.org/10.1016/j.tiv.2021.105150>
- Szemerédy, G., Szabó, R., Kormos, É., Somody, G., Somlyay, I. M., Lehel, J., Kormos, É., Somody, G., Buda, I. (2021). Növényvédő szerek szemirritáló hatásának vizsgálatára alkalmas alternatív módszerek összehasonlítása. In S. Bene (Ed.), *XXVII. Ifjúsági Tudományos Fórum* (pp. 117–120). Magyar Agrár- és Élettudományi Egyetem, Georgikon Campus.
- Kormos, É., Buda, I., Somody, G., Major, L., Szabó, R., & Lehel, J. (2020). Növényvédő szerek in vitro szemirritációs hatásának vizsgálata különböző módszerekkel. In S. Bene (Ed.), *XXVI. Ifjúsági Tudományos Fórum* (p. Növénytudományok szekció 3. Előadás). Pannon Egyetem Georgikon Kar.

10. CONFERENCE PRESENTATION

- Somody, G., Molnár, Z., & Lakatos, E. (2024). Possibilities of rapid generation cycling of hemp (*Cannabis sativa L.*) for the stabilization of recessive traits. *Bio Web of Conferences*, 125, 01012. <https://doi.org/10.1051/bioconf/202412501012>

11. ACKNOWLEDGEMENTS

12. REFERENCES

- Adal, A.M., Stout, J.M., et al. (2021). Sex-linked gene expression and evolution of dioecy in *Cannabis sativa*. *Scientific Reports*, 11, 5512. <https://doi.org/10.1038/s41598-021-84985-0>
- Ahrens, A., Llewellyn, D., & Zheng, Y. (2023). Is twelve hours really the optimum photoperiod for promoting flowering in indoor-grown cultivars of *Cannabis sativa*? *Plants*, 12(14), 2605. <https://doi.org/10.3390/plants12142605>
- Ahsan, S. M., Injamum-Ul-Hoque, M., Howlader, N. C., Rahman, M. M., Rahman, M. M., Haque, M. A., & Choi, H. W. (2025). Haploid production in *Cannabis sativa*: Recent updates, prospects, and perspectives. *Biology*, 14(6), 701. <https://doi.org/10.3390/biology14060701> PubMed+1
- Alahmad, S., Dinglasan, E., Leung, K. M., Riaz, A., Derbal, N., Voss-Fels, K. P., et al. (2018). Speed breeding for multiple quantitative traits in durum wheat. *Plant Methods*, 14, 36. <https://doi.org/10.1186/s13007-018-0302-y>
- Alexandrov, O. S., Romanov, D. V., Divashuk, M. G., Razumova, O. V., Ulyanov, D. S., & Karlov, G. I. (2022). Study and physical mapping of the species-specific tandem repeat CS-237 linked with 45S ribosomal DNA intergenic spacer in *Cannabis sativa* L. *Plants*, 11, 1396. <https://doi.org/10.3390/plants11111396>
- Allavena, D. (1967). CS, eine neue Sorte des zweihausigen Hanfes. *Fibra*, 12, 17–24.
- Amaducci, S., Colauzzi, M., Bellocchi, G., & Venturi, G. (2008). Modelling post-emergent hemp phenology (*Cannabis sativa* L.): Theory and evaluation. *European Journal of Agronomy*, 28, 90–102. <https://doi.org/10.1016/j.eja.2007.05.006>
- Amaducci, S., Scordia, D., Liu, F.H., et al. (2008). Key cultivation techniques for hemp in Europe and China. *Industrial Crops and Products*, 28(2), 158–163. <https://doi.org/10.1016/j.indcrop.2008.03.006>
- Amarasinghe, P., Pierre, C., Moussavi, M., & Geremew, A. (2022). The morphological and anatomical variability of the stems of an industrial hemp collection and the properties of its fibres. *Heliyon*. <https://doi.org/10.1016/j.heliyon.2022.e06564>
- Amarasinghe, P., Pierre, C., Moussavi, M., Geremew, A., Woldesenbet, S., & Weerasooriya, A. (2022). The morphological and anatomical variability of the stems of an industrial

- hemp collection and the properties of its fibres. *Heliyon*, 8(4), e09276. <https://doi.org/10.1016/j.heliyon.2022.e09276>. [PMC](#)
- Amarasinghe, P., Pierre, C., Moussavi, M., Geremew, A., Woldesenbet, S., & Weerasooriya, A. (2022). The morphological and anatomical variability of the stems of an industrial hemp collection and the properties of its fibres. *Heliyon*, 8, e09276. <https://doi.org/10.1016/j.heliyon.2022.e09276>
- André, C. M., Larondelle, Y., & Evers, D. (2010). Dietary antioxidants and oxidative stress from a human and plant perspective: A review. *Current Nutrition & Food Science*, 6(1), 2–12.
- Anjum, S. A., Ashraf, U., Zohaib, A., Tanveer, M., Naeem, M., Ali, I., et al. (2017). Growth and developmental responses of crop plants under drought stress: A review. *Zemdirbyste-Agriculture*, 104, 267–276. <https://doi.org/10.13080/z-a.2017.104.034>
- Appendino, G., Gibbons, S., Giana, A., Pagani, A., Grassi, G., Stavri, M., Smith, E., & Rahman, M. M. (2008). Antibacterial cannabinoids from *Cannabis sativa*: A structure–activity study. *Journal of Natural Products*, 71(8), 1427–1430. <https://doi.org/10.1021/np8002673>
- Aydin, N., Demir, B., Akdag, H., Gokmen, S., Sayaslan, A., Bayraç, C., et al. (2024). Accelerated breeding strategies for biochemical marker-assisted backcross breeding and mapping population development in bread wheat (*Triticum aestivum* L.). *Euphytica*, 220, 116. <https://doi.org/10.1007/s10681-024-03370-x>
- Bailey, L. H. (1891). *The nursery-book: A complete guide to the multiplication and pollination of plants*. The Rural Publishing Company. catalog.hathitrust.org+1
- Baloch, A., Shah, N., Idrees, F., Zhou, X., Gan, L., Atem, J. E. C., et al. (2024). Pyramiding of triple clubroot resistance loci conferred superior resistance without negative effects on agronomic traits in *Brassica napus*. *Physiologia Plantarum*, 176, e14414. <https://doi.org/10.1111/ppl.14414>
- Barbieri, R., & Tedeschi, P. (1968). Eletta Campana e T4, nuove cultivar di canapa per l'ambiente campano. *Sementi Elette*, 14, 412–417.
- Bassolino, L., Fulvio, F., Pastore, C., Pasini, F., Gallina Toschi, T., Filippetti, I., & Paris, R. (2023). When *Cannabis sativa* L. turns purple: Biosynthesis and accumulation of anthocyanins. *Antioxidants*, 12, 1393. <https://doi.org/10.3390/antiox12071393>. [MDPI](#)
- Batista, L. A., Bandillo, N., Friskop, A., & Green, A. (2024). Accelerating genetic gain through strategic speed breeding in spring wheat. *Crop Science*, 64, 3311–3322. <https://doi.org/10.1002/csc2.21380>

- Bennett, S. J., Snell, R., & Wright, D. (2006). Effect of variety, seed rate and time of cutting on fibre yield of dew-retted hemp. *Industrial Crops and Products*, 24, 79–86. <https://doi.org/10.1016/j.indcrop.2006.03.010>
- Bermejo C, Gatti I, Cointry E (2016) In vitro embryo culture to shorten the breeding cycle in lentil (*Lens culinaris* Medik). *Plant Cell Tiss Organ Cult* 127:585–590
- Bhatta, M., Sandro, P., Smith, M. R., Delaney, O., Voss-Fels, K. P., Gutierrez, L., et al. (2021). Need for speed: Manipulating plant growth to accelerate breeding cycles. *Current Opinion in Plant Biology*, 60, 101986. <https://doi.org/10.1016/j.pbi.2020.101986>
- Bielecka, M., Kamiński, F., Adams, I., Poulson, H., Sloan, R., Li, Y., Larson, T. R., Winzer, T., & Graham, I. A. (2014). Targeted mutation of $\Delta 12$ and $\Delta 15$ desaturase genes in hemp produce major alterations in seed fatty acid composition including a high oleic hemp oil. *Plant Biotechnology Journal*, 12(5), 613–623. <https://doi.org/10.1111/pbi.12167>
- Blandinières, H., Croci, M., Impollonia, G., Marcone, A., Gay, A., Winters, A., Palmer, S., & Amaducci, S. (2023). Multi-environment assessment of a yellow hemp (*Cannabis sativa* L.) cultivar's eco-physiology and productivity under varying levels of nitrogen fertilisation. *Industrial Crops and Products*, 195, 116360. <https://doi.org/10.1016/j.indcrop.2023.116360>. [ScienceDirect+1](#)
- Blinkov AO, Kroupin PY, Dmitrieva AR, Kocheshkova AA, Karlov GI and Divashuk MG (2025) Speed breeding: protocols, application and achievements. *Front. Plant Sci.* 16:1680955. doi: 10.3389/fpls.2025.1680955
- Blinkov, A. O., Nagamova, V. M., Minkova, Y. V., Svistunova, N., Radzeniece, S., Kocheshkova, A. A., et al. (2025). The reduction of triticale generation time under speed breeding conditions by increasing the amounts of far-red light in the optical radiation. *Vavilov Journal of Genetics and Breeding*, 23. <https://doi.org/10.18699/vjgb-25-96>
- Bócsa, I. (1994). Professor Dr. Ivan Bócsa, the breeder of Kompolti hemp (interview by the JIHA). *Journal of the International Hemp Association*, 1.
- Bócsa, I. (1999). Genetic improvement: conventional approaches. In: *Advances in Hemp Research*. CRC Press.
- Bócsa, I. (2004). *A kender és termesztése*. Agroinform Kiadó.
- Bócsa, I., Karus, M., & Hemptech. (1998). *The cultivation of hemp: Botany, varieties, cultivation and harvesting*. Hemptech.
- Bogatyreva, N. V., Sokolov, A., Moiseeva, Y. M., Gusev, Y. S., & Chumakov, M. I. (2021). Regulatory status of genome-editing plants: Perspectives for Russian Federation. *Ecological Genetics*, 19, 89–101. <https://doi.org/10.17816/ecogen42532>

- Borlaug, N. E. (2007). Sixty-two years of fighting hunger: Personal recollections. *Euphytica*, 157, 287–297. <https://doi.org/10.1007/s10681-007-9480-9>
- Bredemann, G. (1924). Beiträge zur Hanfzüchtung II. Auslese faserreicher Männchen zur Befruchtung durch Faserbestimmung an der lebenden Pflanze vor der Blüte. *Angewandte Botanik*, 6, 348–360.
- Bredemann, G. (1937). Züchtung des Hanfes auf Fasergehalt. *Zeitschrift für Pflanzenzüchtung*, 12, 259–268.
- Bredemann, G. (1953). Verdreifachung des Fasergehalts bei Hanf durch fortgesetzte Männchen- und Weibchenauslese. *Materia Vegetabile*, 2, 167–187.
- Bredemann, G., Garber, K., Huhnke, W., & von Sengbusch, R. (1961). Die Züchtung von monözischen und diözischen, faserertragreichen Hanfsorten Fibrimon und Fibridia. *Zeitschrift für Pflanzenzüchtung*, 46, 235–245.
- Brenneisen, R. (2007). Chemistry and analysis of phytocannabinoids and other *Cannabis* constituents. In M. A. ElSohly (Ed.), *Marijuana and the cannabinoids* (pp. 17–49). Humana Press.
- Bugbee, B., & Koerner, G. (1997). Yield comparisons and unique characteristics of the dwarf wheat cultivar ‘USU-Apogee’. *Advances in Space Research*, 20(10), 1891–1894. [https://doi.org/10.1016/S0273-1177\(97\)00856-9](https://doi.org/10.1016/S0273-1177(97)00856-9)
- Burstein, S. (2015). Cannabidiol (CBD) and its analogs: A review of their effects on inflammation. *Bioorganic & Medicinal Chemistry*, 23(7), 1377–1385. <https://doi.org/10.1016/j.bmc.2015.01.059>
- Campbell, B., Dong, Z., & McKay, J. (2019). Hemp genetics and genomics. In: *Hemp as a modern commodity crop*. Springer.
- Candolle, A. de. (1867). *Lois de la nomenclature botanique*. V. Masson et fils.
- Cascini, F., Farcomeni, A., Migliorini, D., Baldassarri, L., Boschi, I., Martello, S., Amaducci, S., Lucini, L., & Bernardi, J. (2019). Highly predictive genetic markers distinguish drug-type from fiber-type *Cannabis sativa* L. *Plants*, 8, 496. <https://doi.org/10.3390/plants8110496>
- Cazzola, F., Bermejo, C. J., Guindon, M. F., & Cointy, E. (2020). Speed breeding in pea (*Pisum sativum* L.), an efficient and simple system to accelerate breeding programs. *Euphytica*, 216, 178. <https://doi.org/10.1007/s10681-020-02715-6>
- Ceballos, H., Jaramillo, J. J., Salazar, S., Pineda, M. L., Calle, F., Setter, T., et al. (2017). Induction of flowering in cassava through grafting. *Journal of Plant Breeding and Crop Science*, 9, 19–29. <https://doi.org/10.5897/JPBCS2016.0617>

- Ćeran, M., Miladinović, D., Đorđević, V., Trkulja, D., Radanović, A., Glogovac, S., et al. (2024). Genomics-assisted speed breeding for crop improvement: Present and future. *Frontiers in Sustainable Food Systems*, 8. <https://doi.org/10.3389/fsufs.2024.1383302>
- Cha, J.-K., Lee, J.-H., Lee, S.-M., Ko, J.-M., & Shin, D. (2020). Heading date and growth character of Korean wheat cultivars by controlling photoperiod for rapid generation advancement. *Korean Journal of Breeding Science*, 52, 20–24. <https://doi.org/10.9787/KJBS.2020.52.1.20>
- Cha, J.-K., O'Connor, K., Alahmad, S., Lee, J.-H., Dinglasan, E., Park, H., et al. (2022). Speed vernalization to accelerate generation advance in winter cereal crops. *Molecular Plant*, 15, 1300–1309. <https://doi.org/10.1016/j.molp.2022.06.012>
- Cha, J.-K., Park, H., Choi, C., Kwon, Y., Lee, S.-M., Oh, K.-W., et al. (2023). Acceleration of wheat breeding: Enhancing efficiency and practical application of the speed breeding system. *Plant Methods*, 19, 118. <https://doi.org/10.1186/s13007-023-01083-1>
- Cha, J.-K., Park, H., Kwon, Y., Lee, S.-M., Jang, S.-G., Kwon, S.-W., et al. (2024). Synergizing breeding strategies via combining speed breeding, phenotypic selection, and marker-assisted backcrossing for the introgression of *Glu-B1i* in wheat. *Frontiers in Plant Science*, 15. <https://doi.org/10.3389/fpls.2024.1402709>
- Cha, J.-K., Park, M.-R., Shin, D., Kwon, Y., Lee, S.-M., Ko, J.-M., et al. (2021). Growth characteristics of triticale under long-day photoperiod for rapid generation advancement. *Korean Journal of Breeding Science*, 53, 200–205. <https://doi.org/10.9787/KJBS.2021.53.3.200>
- Chandra, S., Lata, H., ElSohly, M. A., Walker, L. A., & Potter, D. (2017). Cannabis cultivation: Methodological issues for obtaining medical-grade product. *Epilepsy & Behavior*, 70, 302–312. <https://doi.org/10.1016/j.yebeh.2016.11.029>
- Chaudhary, N., & Sandhu, R. (2024). A comprehensive review on speed breeding methods and applications. *Euphytica*, 220, 42. <https://doi.org/10.1007/s10681-024-03300-x>
- Chhabra, B., Thrasu, S., Wallace, S., Schoen, A., Shahoveisi, F., Dong, Y., et al. (2024). Evaluation of speed breeding conditions for accelerating *Fusarium* head blight and deoxynivalenol screening in wheat. *Crop Science*, 64, 1586–1594. <https://doi.org/10.1002/csc2.21226>
- Chiurugwi, T., Kemp, S., Powell, W., & Hickey, L. T. (2019). Speed breeding orphan crops. *Theoretical and Applied Genetics*, 132, 607–616. <https://doi.org/10.1007/s00122-018-3202-7>

- Choi, H., Back, S., Kim, G. W., Lee, K., Venkatesh, J., Lee, H. B., et al. (2023). Development of a speed breeding protocol with flowering gene investigation in pepper (*Capsicum annuum*). *Frontiers in Plant Science*, 14. <https://doi.org/10.3389/fpls.2023.1151765>
- Christopher, J., Richard, C., Chenu, K., Christopher, M., Borrell, A., & Hickey, L. (2015). Integrating rapid phenotyping and speed breeding to improve stay-green and root adaptation of wheat in changing, water-limited, Australian environments. *Procedia Environmental Sciences*, 29, 175–176. <https://doi.org/10.1016/j.proenv.2015.07.246>
- Clarke, R. C., & Merlin, M. D. (2013). *Cannabis: Evolution and ethnobotany* (1st ed.). University of California Press.
- Clarke, R. C., & Merlin, M. D. (2016). Cannabis domestication, breeding history, present-day genetic diversity, and future prospects. *Critical Reviews in Plant Sciences*, 35, 293–327. <https://doi.org/10.1080/07352689.2016.1267498>
- Collado, C. E., Hwang, S. J., & Hernández, R. (2024). Supplemental greenhouse lighting increased the water use efficiency, crop growth, and cutting production in *Cannabis sativa*. *Frontiers in Plant Science*, 15, 1371702. <https://doi.org/10.3389/fpls.2024.1371702>
- Collard, B. C. Y., Ismail, A. M., & Hardy, B. (2013). *EIRLSBN: Twenty years of achievements in rice breeding*. International Rice Research Institute.
- Cosentino, S. L., Testa, G., Scordia, D., & Copani, V. (2012). Sowing time and prediction of flowering of different hemp (*Cannabis sativa* L.) genotypes in southern Europe. *Industrial Crops and Products*, 37, 20–33. <https://doi.org/10.1016/j.indcrop.2011.11.017>
- Crini, G., & Lichtfouse, E. (2020). Traditional and new applications of hemp. In *Sustainable Agriculture Reviews*, Springer. https://doi.org/10.1007/978-3-030-41384-2_2
- Croser, J. S., Pazos-Navarro, M., Bennett, R. G., Tschirren, S., Edwards, K., Erskine, W., et al. (2016). Time to flowering of temperate pulses in vivo and generation turnover in vivo–in vitro of narrow-leaf lupin accelerated by low red to far-red ratio and high intensity in the far-red region. *Plant Cell, Tissue and Organ Culture*, 127, 591–599. <https://doi.org/10.1007/s11240-016-1092-4>
- Croser, J., Mao, D., Dron, N., Michelmore, S., McMurray, L., Preston, C., et al. (2021). Evidence for the application of emerging technologies to accelerate crop improvement: A collaborative pipeline to introgress herbicide tolerance into chickpea. *Frontiers in Plant Science*, 12. <https://doi.org/10.3389/fpls.2021.779122>

- Crossa, J., Hernandez, C., Bretting, P., Eberhart, S., & Taba, S. (1993). Statistical genetic considerations for maintaining germ plasm collections. *Theoretical and Applied Genetics*, 86(6), 673–678. <https://doi.org/10.1007/BF00222650>
- D'Angelo, C. J., & Goldman, I. L. (2019). Annualization of the long-day onion breeding cycle through threshold vernalization and dormancy disruption. *Crop Breeding, Genetics and Genomics*, 1, e190009.
- Davis, W. M., & Hatoum, N. S. (1983). Neurobehavioral actions of cannabichromene and interactions with delta-9-tetrahydrocannabinol. *General Pharmacology*, 14(2), 247–252. [https://doi.org/10.1016/0306-3623\(83\)90120-9](https://doi.org/10.1016/0306-3623(83)90120-9)
- de Meijer, E. (2004). The breeding of *Cannabis* cultivars for pharmaceutical end uses. In *Medicinal uses of cannabis and cannabinoids* (pp. 55–70). Pharmaceutical Press.
- de Meijer, E. (2014). The chemical phenotypes (chemotypes) of *Cannabis*. In R. Pertwee (Ed.), *Handbook of cannabis* (Chap. 89). Oxford University Press.
- de Meijer, E. P. (1995). Fibre hemp cultivars: A survey of origin, ancestry, availability and brief agronomic characteristics. *Journal of the International Hemp Association*, 2(2), 66–73.
- de Meijer, E. P. M., Hammond, K. M., & Sutton, A. (2009). The inheritance of chemical phenotype in *Cannabis sativa* L. (IV): Cannabinoid-free plants. *Euphytica*, 168(1), 95–112. <https://doi.org/10.1007/s10681-009-9894-7>
- de Meijer, E. P., Bagatta, M., Carboni, A., Crucitti, P., Moliterni, V. M., Ranalli, P., & Mandolino, G. (2003). The inheritance of chemical phenotype in *Cannabis sativa* L. *Genetics*, 163(1), 335–346. <https://doi.org/10.1093/genetics/163.1.335>
- De Meijer, E.P.M., & Hammond, K.M. (2005). The inheritance of chemical phenotype in *Cannabis sativa* L. (II): Cannabigerol predominant plants. *Euphytica*, 145(1–2), 189–198. <https://doi.org/10.1007/s10681-005-1164-8>
- De Meijer, E.P.M., Hammond, K.M., Micheler, M. (2009). Chemical phenotype variation: Cannabichromene in *Cannabis*. *Euphytica*, 168(1), 95–107. <https://doi.org/10.1007/s10681-008-9787-1>
- de Monet de Lamarck, J. B. P. A., & Poiret, J. L. M. (1808). *Encyclopédie méthodique. Botanique* (Pt. 2, pp. 345–752). Panckoucke.
- De Petrocellis, L., Ligresti, A., Moriello, A. S., Allarà, M., Bisogno, T., Petrosino, S., Stott, C. G., & Di Marzo, V. (2011). Effects of cannabinoids and cannabinoid-enriched *Cannabis* extracts on TRP channels and endocannabinoid metabolic enzymes. *British Journal of Pharmacology*, 163(7), 1479–1494. <https://doi.org/10.1111/j.1476-5381.2010.01166.x>

- DeLong, G. T., Wolf, C. E., Poklis, A., & Lichtman, A. H. (2010). Pharmacological evaluation of the natural constituent of *Cannabis sativa*, cannabichromene and its modulation by Δ^9 -tetrahydrocannabinol. *Drug and Alcohol Dependence*, *112*(1–2), 126–133. <https://doi.org/10.1016/j.drugalcdep.2010.05.019>
- Demotes-Mainard, S., Péron, T., Corot, A., Bertheloot, J., Le Gourrierec, J., Pelleschi-Travier, S., et al. (2016). Plant responses to red and far-red lights: Applications in horticulture. *Environmental and Experimental Botany*, *121*, 4–21. <https://doi.org/10.1016/j.envexpbot.2015.05.010>
- Deng, Y., Yarur-Thys, A., & Baulcombe, D. C. (2024). Virus-induced overexpression of heterologous *FLOWERING LOCUS T* for efficient speed breeding in tomato. *Journal of Experimental Botany*, *75*, 36–44. <https://doi.org/10.1093/jxb/erad369>
- Dewey, L. H. (1927). Hemp varieties of improved type are result of selection. (Kiadói adatok hiányoznak).
- Di Candilo, M., Ranalli, P., Diozzi, M., & Gianpaolo, G. (2002). Attività di miglioramento genetico per la costituzione di nuove varietà di canapa dioiche. *Agroindustria*, *1*, 14–18.
- Di Marzo, V., & Piscitelli, F. (2015). The endocannabinoid system and its modulation by phytocannabinoids. *Neurotherapeutics*, *12*(4), 692–698. <https://doi.org/10.1007/s13311-015-0374-6>
- Dinglasan, E., Godwin, I. D., Mortlock, M. Y., & Hickey, L. T. (2016). Resistance to yellow spot in wheat grown under accelerated growth conditions. *Euphytica*, *209*, 693–707. <https://doi.org/10.1007/s10681-016-1660-z>
- Dong, H., Clark, L. V., Jin, X., Anzoua, K., Bagmet, L., Chebukin, P., Dzyubenko, E., Dzyubenko, N., Ghimire, B. K., Heo, K., ... Sacks, E. J. (2021). Managing flowering time in *Miscanthus* and sugarcane to facilitate intra- and intergeneric crosses. *PLOS ONE*, *16*, e0240390. <https://doi.org/10.1371/journal.pone.0240390>
- Edet, O. U., & Ishii, T. (2022). Cowpea speed breeding using regulated growth chamber conditions and seeds of oven-dried immature pods potentially accommodates eight generations per year. *Plant Methods*, *18*, 106. <https://doi.org/10.1186/s13007-022-00938-3>
- EISohly, H. N., Turner, C. E., Clark, A. M., & ElSohly, M. A. (1982). Synthesis and antimicrobial activities of certain cannabichromene and cannabigerol related compounds. *Journal of Pharmaceutical Sciences*, *71*(12), 1319–1323. <https://doi.org/10.1002/jps.2600711205>

- Englund, A., Stone, J. M., & Morrison, P. D. (2012). Cannabis in the arm: What can we learn from intravenous cannabinoid studies? *Current Pharmaceutical Design*, *18*(32), 4906–4914. <https://doi.org/10.2174/138161212802884683>
- European Parliament and Council of the European Union. (2021). Regulation (EU) 2021/2115 of 2 December 2021 establishing rules on support for CAP Strategic Plans... Official Journal of the European Union, L 435, 1–186. <https://eur-lex.europa.eu/eli/reg/2021/2115/oj>
- Fang, Y., Wang, L., Sapey, E., Fu, S., Wu, T., Zeng, H., Sun, X., Qian, S., Khan, M. A. A., Yuan, S., ... Guo, L. (2021). Speed-breeding system in soybean: Integrating off-site generation advancement, fresh seeding, and marker-assisted selection. *Frontiers in Plant Science*, *12*, 717077. <https://doi.org/10.3389/fpls.2021.717077>
- Faux, A.M., Berhin, A., & Bertin, P. (2016). A comprehensive phenotypic analysis of hemp (*Cannabis sativa* L.) reveals new insights into flowering behavior. *Plant Science*, *253*, 220–234. <https://doi.org/10.1016/j.plantsci.2016.09.001>
- Faux, A.M., Berhin, A., Dauguet, N., & Bertin, P. (2013). Floral development and seed production in monoecious and dioecious hemp. *Euphytica*, *196*(2), 183–197. <https://doi.org/10.1007/s10681-013-1021-4>
- Fellermeier, M., & Zenk, M. H. (1998). Prenylation of olivetolate by a hemp transferase yields cannabigerolic acid, the precursor of tetrahydrocannabinol. *FEBS Letters*, *427*(2), 283–285. [https://doi.org/10.1016/S0014-5793\(98\)00450-5](https://doi.org/10.1016/S0014-5793(98)00450-5)
- Ferwerda, F. P. (1953). Methods to synchronize the flowering time of the components in crossing plots for the production of hybrid seed corn. *Euphytica*, *2*, 127–134. <https://doi.org/10.1007/BF01997049>
- Ficht, A., Bruch, A., Rajcan, I., Pozniak, C., & Lyons, E. M. (2023). Evaluation of the impact of photoperiod and light intensity on decreasing days to maturity in winter wheat. *Crop Science*, *63*, 812–821. <https://doi.org/10.1002/csc2.20886>
- Finch-Savage, W. E., & Leubner-Metzger, G. (2006). Seed dormancy and the control of germination. *New Phytologist*, *171*, 501–523. <https://doi.org/10.1111/j.1469-8137.2006.01787.x>
- Fischedick, J. T., Hazekamp, A., Erkelens, T., Choi, Y. H., & Verpoorte, R. (2010). Metabolic fingerprinting of *Cannabis sativa* L., cannabinoids and terpenoids for chemotaxonomic and drug standardization purposes. *Phytochemistry*, *71*(17–18), 2058–2073. <https://doi.org/10.1016/j.phytochem.2010.10.001>

- Flajšman, M., Slapnik, M., & Murovec, J. (2021). Production of feminized seeds of high CBD *Cannabis sativa* L. by manipulation of sex expression and its application to breeding. *Frontiers in Plant Science*, *12*, 718092. <https://doi.org/10.3389/fpls.2021.718092>
- Fleischmann, R. (1931). Hanf- und Flachskultur in Ungarn. *Faserforschung*, *9*, 143–149.
- Fleischmann, R. (1934). Beiträge zur Hanfzüchtung. *Faserforschung*, *11*, 156–161.
- Flores-Sánchez, I., & Verpoorte, R. (2008). Secondary metabolism in *Cannabis*. *Phytochemistry Reviews*, *7*, 615–639. <https://doi.org/10.1007/s11101-008-9094-4>
- Füzi, T., & Ladányi, M. (2022). Frequency and variability trends of extreme meteorological events in the Moson Plain, Hungary (1961–2018). *Időjárás / Quarterly Journal of the Hungarian Meteorological Service*, *126*, 319–334.
- Gagalova, K. K., et al. (2024). Leaf pigmentation in *Cannabis sativa*: Characterization of anthocyanins and diversity of anthocyanin biosynthesis genes. [Preprint/Article]. (Elérhető összefoglaló és metaadatok). [PMC](https://pubmed.ncbi.nlm.nih.gov/)
- Gamage, D., Thompson, M., Sutherland, M., Hirotsu, N., Makino, A., & Seneweera, S. (2018). New insights into the cellular mechanisms of plant growth at elevated atmospheric carbon dioxide concentrations. *Plant, Cell & Environment*, *41*, 1233–1246. <https://doi.org/10.1111/pce.13206>
- Gangashetty, P. I., Belliappa, S. H., Bomma, N., Kanuganahalli, V., Sajja, S. B., Choudhary, S., et al. (2024). Optimizing speed breeding and seed/pod chip based genotyping techniques in pigeonpea: A way forward for high throughput line development. *Plant Methods*, *20*, 27. <https://doi.org/10.1186/s13007-024-01155-w>
- Gaoua, O., Arslan, M., & Obedgiu, S. (2025). Speed breeding advancements in safflower (*Carthamus tinctorius* L.): A simplified and efficient approach for accelerating breeding programs. *Molecular Breeding*, *45*, 13. <https://doi.org/10.1007/s11032-024-01530-4>
- Ghosh, S., Watson, A., Gonzalez-Navarro, O. E., Ramirez-Gonzalez, R. H., Yanes, L., Mendoza-Suárez, M., Simmonds, J., Wells, R., Rayner, T., Green, P., ... Hickey, L. T. (2018). Speed breeding in growth chambers and glasshouses for crop breeding and model plant research. *Nature Protocols*, *13*, 2944–2963. <https://doi.org/10.1038/s41596-018-0072-z>
- Gimeno-Páez, E., Prohens, J., Moreno-Cerveró, M., De Luis-Margarit, A., Díez, M. J., & Gramazio, P. (2025). Agronomic treatments combined with embryo rescue for rapid generation advancement in tomato speed breeding. *Horticultural Plant Journal*, *11*, 239–250. <https://doi.org/10.1016/j.hpj.2023.06.006>

- Gitelson, A. A., Kaufman, Y. J., Stark, R., & Rundquist, D. (2002). Novel algorithms for remote estimation of vegetation fraction. *Remote Sensing of Environment*, *80*, 76–87. [https://doi.org/10.1016/S0034-4257\(01\)00289-9](https://doi.org/10.1016/S0034-4257(01)00289-9)
- González-Barrios, P., Bhatta, M., Halley, M., Sandro, P., & Gutiérrez, L. (2021). Speed breeding and early panicle harvest accelerates oat (*Avena sativa* L.) breeding cycles. *Crop Science*, *61*, 320–330. <https://doi.org/10.1002/csc2.20269>
- Goulden, C. H. (1939). Problems in plant selection. In *Proceedings of the 7th International Genetics Congress* (pp. 132–133). Cambridge University Press.
- Gray, S. B., & Brady, S. M. (2016). Plant developmental responses to climate change. *Developmental Biology*, *419*, 64–77. <https://doi.org/10.1016/j.ydbio.2016.07.023>
- Gutiérrez, A., & Jose, C. (2005). Chemical characterization of pitch deposits produced in the manufacturing of high-quality paper pulps from hemp fibers. *Bioresource Technology*, *96*(13), 1445–1450. <https://doi.org/10.1016/j.biortech.2004.12.007>
- Haiden, S. R., Johnson, N., & Berkowitz, G. A. (2025). Transcriptomic analysis of CDL-gated photoperiodic flowering mechanisms in cannabis and their responsiveness to red:far-red ratios in controlled environment agriculture. *Scientific Reports*, *15*, 17628. <https://doi.org/10.1038/s41598-025-00430-7>
- Harrison, D., Da Silva, M., Wu, C., De Oliveira, M., Ravelombola, F., Florez-Palacios, L., et al. (2021). Effect of light wavelength on soybean growth and development in a context of speed breeding. *Crop Science*, *61*, 917–928. <https://doi.org/10.1002/csc2.20327>
- Hatfield, J. L., & Prueger, J. H. (2015). Temperature extremes: Effect on plant growth and development. *Weather and Climate Extremes*, *10*, 4–10. <https://doi.org/10.1016/j.wace.2015.08.001>
- Hatfield, J. L., Boote, K. J., Kimball, B. A., Ziska, L. H., Izaurralde, R. C., Ort, D., et al. (2011). Climate impacts on agriculture: Implications for crop production. *Agronomy Journal*, *103*, 351–370. <https://doi.org/10.2134/agronj2010.0303>
- Hatta, M. A. M., Arora, S., Ghosh, S., Matny, O., Smedley, M. A., Yu, G., et al. (2021). The wheat *Sr22*, *Sr33*, *Sr35* and *Sr45* genes confer resistance against stem rust in barley. *Plant Biotechnology Journal*, *19*, 273–284. <https://doi.org/10.1111/pbi.13460>
- Hazekamp, A. (2016). Cannabis: From cultivar to chemovar II—A metabolomics approach to cannabis classification. *Cannabis and Cannabinoid Research*, *1*(1), 202–215. <https://doi.org/10.1089/can.2016.0017>

- He, R., Ju, J., Liu, K., Song, J., Zhang, S., Zhang, M., et al. (2024). Technology of plant factory for vegetable crop speed breeding. *Frontiers in Plant Science*, *15*, 1414860. <https://doi.org/10.3389/fpls.2024.1414860>
- Heikrujam, M., Vashishtha, A., Barupal, T., Kumar, G., Chetri, S. P., Meena, M., et al. (2022). Photoperiod. In *Encyclopedia of Animal Cognition and Behavior* (pp. 5229–5232). Springer.
- Hickey, L. T., Dieters, M. J., DeLacy, I. H., Christopher, M. J., Kravchuk, O. Y., & Banks, P. M. (2010). Screening for grain dormancy in segregating generations of dormant × non-dormant crosses in white-grained wheat (*Triticum aestivum* L.). *Euphytica*, *172*, 183–195. <https://doi.org/10.1007/s10681-009-0028-z>
- Hickey, L. T., Dieters, M. J., DeLacy, I. H., Kravchuk, O. Y., Mares, D. J., & Banks, P. M. (2009). Grain dormancy in fixed lines of white-grained wheat (*Triticum aestivum* L.) grown under controlled environmental conditions. *Euphytica*, *168*, 303–310. <https://doi.org/10.1007/s10681-009-9929-0>
- Hickey, L. T., Germán, S. E., Pereyra, S. A., Diaz, J. E., Ziemis, L. A., Fowler, R. A., Platz, G. J., Franckowiak, J. D., & Dieters, M. J. (2017). Speed breeding for multiple disease resistance in barley. *Euphytica*, *213*, 64. <https://doi.org/10.1007/s10681-016-1803-2>
- Hickey, L. T., Hafeez, N. A., Robinson, H., Jackson, S. A., Leal-Bertioli, S. C. M., Tester, M., et al. (2019). Breeding crops to feed 10 billion. *Nature Biotechnology*, *37*, 744–754. <https://doi.org/10.1038/s41587-019-0152-9>
- Hickey, L. T., Lawson, W., Platz, G. J., Dieters, M., Arief, V. N., Germán, S., et al. (2011). Mapping *Rph20*: A gene conferring adult plant resistance to *Puccinia hordei* in barley. *Theoretical and Applied Genetics*, *123*, 55–68. <https://doi.org/10.1007/s00122-011-1566-z>
- Hickey, L. T., Wilkinson, P. M., Knight, C. R., Godwin, I. D., Kravchuk, O. Y., Aitken, E. A. B., et al. (2012). Rapid phenotyping for adult-plant resistance to stripe rust in wheat. *Plant Breeding*, *131*, 54–61. <https://doi.org/10.1111/j.1439-0523.2011.01925.x>
- Hill, A. J., Williams, C. M., Whalley, B. J., & Stephens, G. J. (2012). Phytocannabinoids as novel therapeutic agents in CNS disorders. *Pharmacology & Therapeutics*, *133*(1), 79–97. <https://doi.org/10.1016/j.pharmthera.2011.09.002>
- Hillig, K. W. (2004). A chemotaxonomic analysis of terpenoid variation in *Cannabis*. *Biochemical Systematics and Ecology*, *32*(10), 875–891. <https://doi.org/10.1016/j.bse.2004.04.004>

- Hillig, K. W. (2005). Genetic evidence for speciation in *Cannabis* (Cannabaceae). *Genetic Resources and Crop Evolution*, 52(2), 161–180. <https://doi.org/10.1007/s10722-003-4452-y>
- Hoffmann, W. (1944). Hanf, *Cannabis sativa* L. In Roemer–Rudorf. Paul Parey.
- Hoffmann, W. (1946). Helle Stengel — eine wertvolle Mutation des Hanfes (*Cannabis sativa* L.). *Der Züchter*, 17, 56–59. <https://doi.org/10.1007/BF00709108>.
- Holmes, J. (2022). Tissue culture and genetic transformation of *Cannabis sativa* L. (Master’s thesis, Simon Fraser University). https://summit.sfu.ca/_flysystem/fedora/2023-01/etd22292.pdf
- Injamum-Ul-Hoque, M., Howlader, N.C., et al. (2025). Haploid production in *Cannabis sativa*. *Biology*, 14(6), 701. <https://www.mdpi.com/2079-7737/14/6/701>
- Iseger, T. A., & Bossong, M. G. (2015). A systematic review of the antipsychotic properties of cannabidiol in humans. *Schizophrenia Research*, 162(1–3), 153–161. <https://doi.org/10.1016/j.schres.2015.01.033>
- Ishida, Y., Hiei, Y., & Komari, T. (2007). *Agrobacterium*-mediated transformation of maize. *Nature Protocols*, 2, 1614–1621. <https://doi.org/10.1038/nprot.2007.241>
- Jackson, S. D. (2009). Plant responses to photoperiod. *New Phytologist*, 181, 517–531. <https://doi.org/10.1111/j.1469-8137.2008.02681.x>
- Jähne, F., Hahn, V., Würschum, T., & Leiser, W. L. (2020). Speed breeding short-day crops by LED-controlled light schemes. *Theoretical and Applied Genetics*, 133, 2335–2342. <https://doi.org/10.1007/s00122-020-03601-4>
- Jamali, S. H., Cockram, J., & Hickey, L. T. (2020). Is plant variety registration keeping pace with speed breeding techniques? *Euphytica*, 216, 131. <https://doi.org/10.1007/s10681-020-02666-y>
- Jang, I. T., Jae, H., Lee, J. H., Shin, E. J., & Nam, S. Y. (2023). Evaluation of growth, flowering, and chlorophyll fluorescence responses of *Viola cornuta* cv. Penny Red Wing according to spectral power distributions. *Journal of People, Plants, and Environment*, 26(3), 335–349. <https://doi.org/10.11628/ksppe.2023.26.3.335>
- Ji, M., Wang, G., Liu, X., Li, X., Xue, Y., Amombo, E., et al. (2022). The extended day length promotes earlier flowering of Bermudagrass. *PeerJ*, 10, e14326. <https://doi.org/10.7717/peerj.14326>
- Jighly, A., Lin, Z., Pembleton, L. W., Cogan, N. O. I., Spangenberg, G. C., Hayes, B. J., & Daetwyler, H. D. (2019). Boosting genetic gain in allogamous crops via speed breeding

- and genomic selection. *Frontiers in Plant Science*, *10*, 1364. <https://doi.org/10.3389/fpls.2019.01364>
- Kabade, P. G., Dixit, S., Singh, U. M., Alam, S., Bhosale, S., Kumar, S., et al. (2024). SpeedFlower: A comprehensive speed breeding protocol for *indica* and *japonica* rice. *Plant Biotechnology Journal*, *22*, 1051–1066. <https://doi.org/10.1111/pbi.14245>
- Kelly, J. (2012). *The graves are walking: The Great Famine and the saga of the Irish people*. Henry Holt and Company.
- Khan, B. A., Warner, P., & Wang, H. (2014). Antibacterial properties of hemp and other natural fibre plants: A review. *BioResources*, *9*(2), 3640–3686.
- Kigoni, M., Choi, M., & Arbelaez, J. D. (2023). Single-Seed-SpeedBulks: A protocol that combines speed breeding with a cost-efficient modified single-seed descent method for rapid-generation-advancement in oat (*Avena sativa* L.). *Plant Methods*, *19*, 92. <https://doi.org/10.1186/s13007-023-01067-1>
- Klein, C., Karanges, E., Spiro, A., Wong, A., Spencer, J., Huynh, T., Gunasekaran, N., Karl, T., Long, L. E., Huang, X.-F., ... & McGregor, I. S. (2011). Cannabidiol potentiates Δ^9 -tetrahydrocannabinol (THC) behavioural effects and alters THC pharmacokinetics during acute and chronic treatment in adolescent rats. *Psychopharmacology*, *218*(2), 443–457. <https://doi.org/10.1007/s00213-011-2342-0>
- Kobayashi, Y., & Weigel, D. (2007). Move on up, it's time for change—Mobile signals controlling photoperiod-dependent flowering. *Genes & Development*, *21*, 2371–2384.
- Koji, T., Iwata, H., Ishimori, M., Takanashi, H., Yamasaki, Y., & Tsujimoto, H. (2023). Genetic dissection of seasonal changes in a greening plant based on time-series multispectral imaging. *Plants*, *12*(20), 3597. <https://doi.org/10.3390/plants12203597>
- Kojoma, M., Seki, H., Yoshida, S., & Muranaka, T. (2006). DNA polymorphisms in the tetrahydrocannabinolic acid (THCA) synthase gene in “drug-type” and “fiber-type” *Cannabis sativa* L. *Forensic Science International*, *159*(2–3), 132–140. <https://doi.org/10.1016/j.forsciint.2005.07.005>
- Kovalchuk, I., Pellino, M., Rigault, P., van Velzen, R., Ebersbach, J., Ashnest, J. R., Mau, M., Schranz, M. E., Alcorn, J., Laprairie, R. B., ... & Sharbel, T. F. (2020). The genomics of *Cannabis* and its close relatives. *Annual Review of Plant Biology*, *71*, 713–739. <https://doi.org/10.1146/annurev-arplant-081519-040203>
- Kuroda, Y., Kuranouchi, T., Okazaki, K., & Takahashi Taguchi, H. K. (2024). Biennial sugar beets capable of flowering without vernalization treatment. *Genetic Resources and Crop Evolution*, *71*, 823–834. <https://doi.org/10.1007/s10722-023-01662-0>

- Lee, D., Han, K., Kim, J. H., Jun, T.-H., & Lee, J. S. (2023). Development of speed-breeding system for Korean soybean varieties (*Glycine max* (L.) Merr.) using LED light source. *Plant Breeding and Biotechnology*, *11*, 49–55. <https://doi.org/10.9787/PBB.2023.11.1.49>
- Li, H., Rasheed, A., Hickey, L. T., & He, Z. (2018). Fast-forwarding genetic gain. *Trends in Plant Science*, *23*, 184–186. <https://doi.org/10.1016/j.tplants.2018.01.007>
- Li, H., Zhu, L., Fan, R., Li, Z., Liu, Y., Shaheen, A., et al. (2024). A platform for whole-genome speed introgression from *Aegilops tauschii* to wheat for breeding future crops. *Nature Protocols*, *19*, 281–312. <https://doi.org/10.1038/s41596-023-00922-8>
- Li, L., Wang, Y., Li, Q., & Sun, G. (2022). Releasing the full potential of Cannabis through genetic modification—Opportunities, bottlenecks and future directions. *Agronomy*, *12*(10), 2439. <https://doi.org/10.3390/agronomy12102439>
- Lisson, S. N., Mendham, N. J., & Carberry, P. S. (2000). Development of a hemp (*Cannabis sativa* L.) simulation model. 4. Model description and validation. *Australian Journal of Experimental Agriculture*, *40*, 425–432. <https://doi.org/10.1071/EA99061>
- Liu, K., He, R., He, X., Tan, J., Chen, Y., Li, Y., et al. (2022). Speed breeding scheme of hot pepper through light environment modification. *Sustainability*, *14*, 12225. <https://doi.org/10.3390/su141912225>
- Lubell, J. D., & Brand, M. H. (2018). Foliar sprays of silver thiosulfate produce male flowers on female hemp plants. *HortTechnology*, *28*(6), 743–747. <https://doi.org/10.21273/HORTTECH04135-18>
- Lulsdorf, M. M., & Banniza, S. (2018). Rapid generation cycling of an F2 population derived from a cross between *Lens culinaris* Medik. and *Lens ervoides* (Brign.) Grande after *Aphanomyces* root rot selection. *Plant Breeding*, *137*, 486–491. <https://doi.org/10.1111/pbr.12612>
- Luo, X., Reiter, M. A., d’Espaux, L., Wong, J., Denby, C. M., Lechner, A., Zhang, Y., Grzybowski, A. T., Harth, S., Lin, W., Lee, H., Yu, C., Shin, J., Deng, K., Benites, V. T., Wang, G., Baidoo, E. E. K., Chen, Y., Dev, I., ... & Keasling, J. D. (2019). Complete biosynthesis of cannabinoids and their unnatural analogues in yeast. *Nature*, *567*(7746), 123–126. <https://doi.org/10.1038/s41586-019-0978-9>
- Ma, X. J., Hou, Y., Yang, S., Zheng, X., Wang, X. M., Cheng, G. X., et al. (2024). Effect of different photoperiods on the period of maturity of hot peppers (*Capsicum annuum* L.) and their changes in color. *Scientia Horticulturae*, *334*, 113337. <https://doi.org/10.1016/j.scienta.2024.113337>

- Magruder, R. (1937). Improvement in the leafy cruciferous vegetables. In *Yearbook of Agriculture* (pp. 283–299).
- Mahmoud, A. E., & Desmond, S. (2005). Chemical constituents of marijuana: The complex mixture of natural cannabinoids. *Life Sciences*, 78(5), 539–548. <https://doi.org/10.1016/j.lfs.2005.09.011>
- Mandolino, G., & Carboni, A. (2004). Potential of marker-assisted selection in hemp genetic improvement. *Euphytica*, 140(1), 107–120. <https://doi.org/10.1007/s10681-004-4759-6>
- Mandolino, G., Bagatta, M., Carboni, A., Ranalli, P., & de Meijer, E. (2003). Qualitative and quantitative aspects of the inheritance of chemical phenotype in *Cannabis*. *Journal of Industrial Hemp*, 8(2), 51–72.
- Mandolino, G., Carboni, A., Forapani, S., Faeti, V., & Ranalli, P. (1999). Identification of DNA markers linked to the male sex in dioecious hemp (*Cannabis sativa* L.). *Theoretical and Applied Genetics*, 98(1), 86–92. <https://doi.org/10.1007/s001220051046>
- Marenkova, A. G., Blinkov, A. O., Radzeniece, S., Kocheshkova, A. A., Karlov, G. I., Lavygina, V. A., et al. (2024). Testing and modification of the protocol for accelerated growth of malting barley under speed breeding conditions. *Nanobiotechnologies Reports*, 19, 808–814. <https://doi.org/10.1134/S2635167624601955>
- McFadden, E. A., & Brookings, S. D. (1917). Wheat–rye hybrids. *Journal of Heredity*, 8, 335. <https://doi.org/10.1093/oxfordjournals.jhered.a111829>
- McKay, J.K. et al. (2019). Hemp genetics and genomics. In: Springer Handbook of Cannabis. Springer.
- McPartland, J. M. (2010). THC synthase in *Cannabis* has undergone accelerated evolution and positive selection pressure. In *Proceedings of the 20th Annual Symposium on the Cannabinoids*. Research Triangle Park, NC.
- McPartland, J. M., & Russo, E. B. (2001). *Cannabis* and *Cannabis* extracts: Greater than the sum of their parts? *Journal of Cannabis Therapeutics*, 1(3–4), 103–132. https://doi.org/10.1300/J175v01n03_08
- McPartland, J. M., Clarke, R. C., & Watson, D. P. (2000). *Hemp diseases and pests: Management and biological control*. CABI.
- Meier, C., & Mediavilla, V. (1998). Factors influencing the yield and the quality of hemp (*Cannabis sativa* L.) essential oil. *Journal of the International Hemp Association*, 5(1), 16–20.

- Mescouto, L. F. L., Piza, M. R., Costa, J. C., Pessoni, L. O., Bruzi, A. T., Pulcinelli, C. E., et al. (2024). Early harvesting: An efficient technique for speed breeding in soybean. *Genetics and Molecular Research*, *23*, gmr19232. <https://doi.org/10.4238/gmr19232>
- Miroshnichenko, D., Klementyeva, A., & Dolgov, S. (2021). The effect of daminozide, dark/light schedule and copper sulphate in tissue culture of *Triticum timopheevii*. *Plants*, *10*, 2620. <https://doi.org/10.3390/plants10122620>
- Miroshnichenko, D., Timerbaev, V., Divashuk, M., Pushin, A., Alekseeva, V., Kroupin, P., et al. (2024). CRISPR/Cas9-mediated multiplexed multi-allelic mutagenesis of genes located on A, B and R subgenomes of hexaploid triticale. *Plant Cell Reports*, *43*, 59. <https://doi.org/10.1007/s00299-023-03139-x>
- Mishchenko, S., Kyrychenko, H., & Laiko, I. (2021). A new multiple-purposes variety of industrial hemp ‘Artemida’ with a high oil content and fiber quality. *Plant Varieties Studying and Protection*, *17*, 43–50. <https://doi.org/10.21498/2518-1017.17.1.2021.228208>
- Mishchenko, S., Laiko, I., & Kyrychenko, H. (2021). Breeding of industrial hemp with a high content of cannabigerol by the case of ‘Vik 2020’ cultivar. *Plant Varieties Studying and Protection*, *17*, 105–112. <https://doi.org/10.21498/2518-1017.17.2.2021.236514>
- Mishchenko, S.V., & Laiko, I.M. (2021). Inheritance of cannabinoid traits by hybrids. Baltija Publishing. <https://www.baltijapublishing.lv/omp/index.php/bp/catalog/view/141/4147/8694-1>
- Mitache, M., Baidani, A., Bencharki, B., & Idrissi, O. (2024a). Exploring the impact of light intensity under speed breeding conditions on the development and growth of lentil and chickpea. *Plant Methods*, *20*, 30. <https://doi.org/10.1186/s13007-024-01156-9>
- Mitache, M., Baidani, A., Houasli, C., Khouakhi, K., Bencharki, B., & Idrissi, O. (2023). Optimization of light/dark cycle in an extended photoperiod-based speed breeding protocol for grain legumes. *Plant Breeding*, *142*, 463–476. <https://doi.org/10.1111/pbr.13112>
- Mitache, M., Baidani, A., Zeroual, A., Bencharki, B., & Idrissi, O. (2024b). Rapid generation advancement through speed breeding in lentil (*Lens culinaris* Medik.). *Crop Breeding and Applied Biotechnology*, *24*, e48632435. <https://doi.org/10.1590/1984-70332024v24n3a30>
- Mobini, S. H., & Warkentin, T. D. (2016). A simple and efficient method of in vivo rapid generation technology in pea (*Pisum sativum* L.). *In Vitro Cellular & Developmental Biology – Plant*, *52*, 530–536. <https://doi.org/10.1007/s11627-016-9772-7>

- Mobini, S. H., Lulsdorf, M., Warkentin, T. D., & Vandenberg, A. (2015). Plant growth regulators improve *in vitro* flowering and rapid generation advancement in lentil and faba bean. *In Vitro Cellular & Developmental Biology – Plant*, *51*, 71–79. <https://doi.org/10.1007/s11627-014-9647-8>
- Mobini, S., Khazaei, H., Warkentin, T. D., & Vandenberg, A. (2020). Shortening the generation cycle in faba bean (*Vicia faba*) by application of cytokinin and cold stress to assist speed breeding. *Plant Breeding*, *139*, 1181–1189. <https://doi.org/10.1111/pbr.12868>
- Moher, M., Jones, M., & Zheng, Y. (2021). Photoperiodic response of *in vitro* *Cannabis sativa* plants. *HortScience*, *56*(1), 108–113. <https://doi.org/10.21273/HORTSCI15452-20>
- Moliterni, V. M. C., Cattivelli, L., Ranalli, P., & Mandolino, G. (2004). The sexual differentiation of *Cannabis sativa* L.: A morphological and molecular study. *Euphytica*, *140*, 95–106. <https://doi.org/10.1007/s10681-004-4758-7>
- Montserrat-de la Paz, S., Marín-Aguilar, F., García-Giménez, M. D., & Fernández-Arche, M. (2014). Hemp (*Cannabis sativa* L.) seed oil: Analytical and phytochemical characterization of the unsaponifiable fraction. *Journal of Agricultural and Food Chemistry*, *62*(5), 1105–1110. <https://doi.org/10.1021/jf404278q>
- Mölleken, H., & Theimer, R. (1997). Survey of minor fatty acids in *Cannabis sativa* L. fruits of various origins. *Journal of the International Hemp Association*, *4*(1), 13–17.
- Musio, S., Müssig, J., & Amaducci, S. (2018). Optimizing hemp fiber production for high-performance composite applications. *Frontiers in Plant Science*, *9*, 1702. <https://doi.org/10.3389/fpls.2018.01702>
- Myles, S., Boyko, A. R., Owens, C. L., Brown, P. J., Grassi, F., Aradhya, M. K., Prins, B., Reynolds, A., Chia, J.-M., Ware, D., Bustamante, C. D., & Buckler, E. S. (2011). Genetic structure and domestication history of the grape. *Proceedings of the National Academy of Sciences*, *108*(9), 3530–3535. <https://doi.org/10.1073/pnas.1009363108>
- Nagatoshi, Y., & Fujita, Y. (2019). Accelerating soybean breeding in a CO₂-supplemented growth chamber. *Plant and Cell Physiology*, *60*, 77–84. <https://doi.org/10.1093/pcp/pcy189>
- Nannuru, V. K. R., Dieseth, J. A., Lillemo, M., & Meuwissen, T. H. E. (2025). Evaluating genomic selection and speed breeding for *Fusarium* head blight resistance in wheat using stochastic simulations. *Molecular Breeding*, *45*, 14. <https://doi.org/10.1007/s11032-024-01527-z>
- O'Connor, D. J., Wright, G. C., Dieters, M. J., George, D. L., Hunter, M. N., Tatnell, J. R., et al. (2013). Development and application of speed breeding technologies in a commercial

- peanut breeding program. *Peanut Science*, *40*, 107–114. <https://doi.org/10.3146/PS12-12.1>
- Ochatt, S. J., Sangwan, R. S., Marget, P., Ndong, Y. A., Rancillac, M., Perney, P., et al. (2002). New approaches towards the shortening of generation cycles for faster breeding of protein legumes. *Plant Breeding*, *121*, 436–440. <https://doi.org/10.1046/j.1439-0523.2002.746803.x>
- Official Journal of the European Communities. (2000, December 28). Commission Regulation (EC) No 2860/2000 of 27 December 2000, Annex VI, Annex XIII (Article 7b(1)). Retrieved from <https://eur-lex.europa.eu/legal-content/EN/TXT/PDF/?uri=CELEX:32000R2860&fm=FR>
- Ortiz, R., Trethowan, R., Ferrara, G. O., Iwanaga, M., Dodds, J. H., Crouch, J. H., et al. (2007). High yield potential, shuttle breeding, genetic diversity, and a new international wheat improvement strategy. *Euphytica*, *157*, 365–384. <https://doi.org/10.1007/s10681-007-9375-9>
- Pacifico, D., Miselli, F., Carboni, A., Moschella, A., & Mandolino, G. (2007). Time course of cannabinoid accumulation and chemotype development during the growth of *Cannabis sativa* L. *Euphytica*, *160*, 231–240. <https://doi.org/10.1007/s10681-007-9543-y>
- Pandey, S., Singh, A., Parida, S. K., & Prasad, M. (2022). Combining speed breeding with traditional and genomics-assisted breeding for crop improvement. *Plant Breeding*, *141*, 301–313. <https://doi.org/10.1111/pbr.13012>
- Park, B. G., Lee, J. H., Shin, E. J., Kim, E. A., & Nam, S. Y. (2024). Light quality influence on growth performance and physiological activity of *Coleus* cultivars. *International Journal of Plant Biology*, *15*, 807–826. <https://doi.org/10.3390/ijpb15030032>
- Parsons, J., Martin, S., James, T., Golenia, G., Boudko, E., & Hepworth, S. (2019). Polyploidization for the genetic improvement of *Cannabis sativa*. *Frontiers in Plant Science*, *10*, 476. <https://doi.org/10.3389/fpls.2019.00476>
- Pazos-Navarro, M., Castello, M., Bennett, R. G., Nichols, P., & Croser, J. (2017). In vitro-assisted single-seed descent for breeding-cycle compression in subterranean clover (*Trifolium subterraneum* L.). *Crop & Pasture Science*, *68*, 958. <https://doi.org/10.1071/CP17067>
- Peterswald, M. C., Eaves, J., Sidhu, H. S., Fisette, S., & Lefsrud, M. (2025). Supplemental far-red light enhances cannabis yield, quality, and water-use efficiency. *Scientific Reports*, *15*, 20710. <https://doi.org/10.1038/s41598-025-22566-6>

- Pipattanawong, R., Yamane, K., Fujishige, N., Bang, S., & Yamaki, Y. (2009). Effects of high temperature on pollen quality, ovule fertilization and development of embryo and achene in ‘Tochiotome’ strawberry. *Journal of the Japanese Society for Horticultural Science*, 78, 300–306. <https://doi.org/10.2503/jjshs1.78.300>
- Popa, L. D., Buburuz, A. A., Isticioaia, S. F., Gauca, C., & Trotuș, C. G. (2019). “Succesiv”— A new monoecious hemp cultivar created at ARDS Secuieni, Neamț County. *Romanian Agricultural Research*, 36, 79–84.
- Popa, L. D., Buburuz, A. A., Trotuș, E., Vlăduț, N. C., Teliban, G. C., Puiu, I. B., Meluca, M., Pintille, P. L., & Matei, G. (2022). Recent progress in monoecious hemp variety for seed, obtained in Romania. *Romanian Agricultural Research*, 39, 1–8.
- Potts, J., Jangra, S., Michael, V. N., & Wu, X. (2023). Speed breeding for crop improvement and food security. *Crops*, 3(4), 276–291. <https://doi.org/10.3390/crops3040025>
- Punja, Z. K., & Ni, L. (2021). The bud rot pathogens infecting cannabis (*Cannabis sativa* L., marijuana) inflorescences: Symptomology, species identification, pathogenicity and biological control. *Canadian Journal of Plant Pathology*. <https://doi.org/10.1080/07060661.2021.1936650>
- Radočaj, D., Rapčan, I., & Jurišić, M. (2023). Indoor plant SPAD prediction based on multispectral indices and soil electroconductivity: A deep learning approach. *Horticulturae*, 9, 1290. <https://doi.org/10.3390/horticulturae9111290>
- Radwan, M. M., ElSohly, M. A., Slade, D., Ahmed, S. A., Khan, I. A., & Ross, S. A. (2009). Biologically active cannabinoids from high-potency *Cannabis sativa*. *Journal of Natural Products*, 72(5), 906–911. <https://doi.org/10.1021/np900067k>
- Rana, M. M., Takamatsu, T., Baslam, M., Kaneko, K., Itoh, K., Harada, N., et al. (2019). Salt tolerance improvement in rice through efficient SNP marker-assisted selection coupled with speed breeding. *International Journal of Molecular Sciences*, 20, 2585. <https://doi.org/10.3390/ijms20102585>
- Ranalli, P. (1998). Hemp. In G. T. S. M. M. A. Pagnotta (Ed.), *Italian contribution to plant genetics and breeding* (pp. 803–811). University of Tuscia.
- Ranalli, P. (2004). Current status and future scenarios of hemp breeding. *Euphytica*, 140(1), 121–131. <https://doi.org/10.1007/s10681-004-4760-0>
- Razumova, O.V., Alexandrov, O.S., Divashuk, M.G., et al. (2016). Genetic mapping and QTL analysis of sex expression in *Cannabis sativa* L. *Russian Journal of Genetics*, 52(2), 132–138. <https://doi.org/10.1134/S1022795416020095>

- Riaz, A., Periyannan, S., Aitken, E., & Hickey, L. (2016). A rapid phenotyping method for adult plant resistance to leaf rust in wheat. *Plant Methods*, *12*, 17. <https://doi.org/10.1186/s13007-016-0117-7>
- Richard, C., Hickey, L. T., Fletcher, S., Jennings, R., Chenu, K., & Christopher, J. T. (2015). High-throughput phenotyping of seminal root traits in wheat. *Plant Methods*, *11*, 13. <https://doi.org/10.1186/s13007-015-0055-9>
- Robert, C. C., & Mark, D. M. (2016). Cannabis domestication, breeding history, present-day genetic diversity, and future prospects. *Critical Reviews in Plant Sciences*, *35*(5–6), 293–327. <https://doi.org/10.1080/07352689.2016.1267498>
- Rogo, U., Fambrini, M., & Pugliesi, C. (2023). Embryo rescue in plant breeding. *Plants*, *12*, 3106. <https://doi.org/10.3390/plants12173106>
- Ross, S. A., ElSohly, M. A., Sultana, G. N., Mehmedic, Z., Hossain, C. F., & Chandra, S. (2005). Flavonoid glycosides and cannabinoids from the pollen of *Cannabis sativa* L. *Phytochemical Analysis*, *16*(1), 45–48. <https://doi.org/10.1002/pca.809>
- Ross, S., Mehmedic, Z., Murphy, T., & ElSohly, M. (2000). GC–MS analysis of the total Δ^9 -THC content of both drug- and fiber-type *Cannabis* seeds. *Journal of Analytical Toxicology*, *24*, 715–717. <https://doi.org/10.1093/jat/24.8.715>
- Rossi, N., Powell, W., Mackay, I. J., Hickey, L., Maurer, A., Pillen, K., et al. (2024). Investigating the genetic control of plant development in spring barley under speed breeding conditions. *Theoretical and Applied Genetics*, *137*, 115. <https://doi.org/10.1007/s00122-024-04618-9>
- Rothschild, M., Bergström, G., & Wängberg, S.-Å. (2005). *Cannabis sativa*: Volatile compounds from pollen and entire male and female plants of two variants, Northern Lights and Hawaiian Indica. *Botanical Journal of the Linnean Society*, *147*(4), 387–397. <https://doi.org/10.1111/j.1095-8339.2005.00379.x>
- Ryu, S., Kim, S., Hong, C., Kim, J., & Kim, S. (2024). A draft haploid genome assembly for *Cannabis sativa* L. *Scientific Data*, *11*, 421. <https://doi.org/10.1038/s41597-024-03104-1>
- Sajja, S., Pranati, J., Shyamala, S., Vinutha, K. S., Reddy, R., Joshi, P., et al. (2025). Rapid Ragi: A speed breeding protocol for finger millet. *Plant Methods*, *21*, 84. <https://doi.org/10.1186/s13007-025-01403-7>
- Salentijn, E. M., Zhang, Q., Amaducci, S., Yang, M., & Trindade, L. M. (2015). New developments in fiber hemp (*Cannabis sativa* L.) breeding. *Industrial Crops and Products*, *68*, 32–41. <https://doi.org/10.1016/j.indcrop.2014.08.011>

- Samineni, S., Sen, M., Sajja, S. B., & Gaur, P. M. (2020). Rapid generation advance (RGA) in chickpea to produce up to seven generations per year and enable speed breeding. *The Crop Journal*, 8, 164–169. <https://doi.org/10.1016/j.cj.2019.08.003>
- Sandhu, N., Singh, J., Pruthi, G., Verma, V. K., Raigar, O. P., Bains, N. S., et al. (2024). SpeedyPaddy: A revolutionized cost-effective protocol for large-scale offseason advancement of rice germplasm. *Plant Methods*, 20, 109. <https://doi.org/10.1186/s13007-024-01235-x>
- Schilling, S., Melzer, R., Dowling, C. A., Shi, J., Muldoon, S., & McCabe, P. F. (2023). A protocol for rapid generation cycling (speed breeding) of hemp (*Cannabis sativa*) for research and agriculture. *The Plant Journal*, 113, 437–445. <https://doi.org/10.1111/tpj.16051>
- Schoen, A., Wallace, S., Holbert, M. F., Brown-Guidera, G., Harrison, S., Murphy, P., et al. (2023). Reducing the generation time in winter wheat cultivars using speed breeding. *Crop Science*, 63, 2079–2090. <https://doi.org/10.1002/csc2.20989>
- Sengbusch, R.V. (1952). A further contribution to the inheritance of sex in hemp as a basis for breeding a monocious hemp. *Zeitschrift fur Pflanzenzuchtung*, 31, 319-38
- Serebriakova, T. I. (1940). Fiber plants. In E. V. Wulff (Ed.), *Flora of cultivated plants*. State Printing Office.
- Sharma, S., Kumar, A., Dhakte, P., Raturi, G., Vishwakarma, G., Barbadikar, K. M., et al. (2023). Speed breeding: Opportunities and challenges for crop improvement. *Journal of Plant Growth Regulation*, 42, 46–59. <https://doi.org/10.1007/s00344-021-10551-8>
- Shimizu-Sato, S., Tsuda, K., Nosaka-Takahashi, M., Suzuki, T., Ono, S., Ta, K. N., et al. (2020). *Agrobacterium*-mediated genetic transformation of wild *Oryza* species using immature embryos. *Rice*, 13, 33. <https://doi.org/10.1186/s12284-020-00394-4>
- Sikora, V., & Koren, A. (2020). Achievements in the improvement of industrial hemp production in the Institute of Field and Vegetable Crops, Novi Sad. *Alternative Crops and Cultivation Practices*, 2, 9–15.
- Singh, V.K., Bhojar, P.I., Sharma, V. (2022). Emerging technologies in plant breeding for fibre crops, cotton, and sunn hemp. Springer.
- Sirikantaramas, S., Taura, F., Tanaka, Y., Ishikawa, Y., Morimoto, S., & Shoyama, Y. (2005). Tetrahydrocannabinolic acid synthase, the enzyme controlling marijuana psychoactivity, is secreted into the storage cavity of the glandular trichomes. *Plant & Cell Physiology*, 46, 1578–1582. <https://doi.org/10.1093/pcp/pci166>

- Slatkin, D. J., Doorenbos, N. J., Harris, L. S., Masoud, A. N., Quimby, M. W., & Schiff, P. L. (1971). Chemical constituents of *Cannabis sativa* L. root. *Journal of Pharmaceutical Sciences*, 60(12), 1891–1892. <https://doi.org/10.1002/jps.2600601234>
- Small, E. (2017). Classification of *Cannabis sativa* L. in relation to agricultural, biotechnological, medical and recreational utilization. In S. Chandra, H. Lata, & M. A. ElSohly (Eds.), *Cannabis sativa L.—Botany and Biotechnology* (pp. 1–62). Springer. https://doi.org/10.1007/978-3-319-54564-6_1
- Small, E., & Cronquist, A. (1976). A practical and natural taxonomy for *Cannabis*. *Taxon*, 25(4), 405–435. <https://doi.org/10.2307/1220524>
- Small, E., & Marcus, D. (2002). Hemp: A new crop with new uses for North America. *Trends in New Crops and New Uses*, 284–326.
- Small, E., & Marcus, D. (2003). Tetrahydrocannabinol levels in hemp (*Cannabis sativa*) germplasm resources. *Economic Botany*, 57(4), 545–558. (DOI/állandó URL: <http://www.jstor.org/stable/4256739>)
- Somody, G & Aranyi, N. (2022): The potential impact of flower infecting *Botrytis* bud rot (*Botrytis cinerea* Pers.) on hemp (*Cannabis sativa* L.) selective breeding. *Georgikon for Agriculture*, 26(1), 126-137.
- Somody, G., & Molnár, Z. (2025). Flowering synchronization using artificial light control for crossbreeding hemp (*Cannabis sativa* L.) with varied flowering times. *Plants*, 14(4), 594. <https://doi.org/10.3390/plants14040594>
- Somody, G., Molnár, Z., & Lakatos, E. (2024). Possibilities of rapid generation cycling of hemp (*Cannabis sativa* L.) for the stabilization of recessive traits. *BIO Web of Conferences*, 125, 1012. <https://doi.org/10.1051/bioconf/202412501012>
- Song, Y., Duan, X., Wang, P., Li, X., Yuan, X., Wang, Z., et al. (2021). Comprehensive speed breeding: A high-throughput and rapid generation system for long-day crops. *Plant Biotechnology Journal*, 20, 13. <https://doi.org/10.1111/pbi.13726>
- Stack, G. M., Toth, J. A., Carlson, C. H., Cala, A. R., Marrero-González, M. I., Wilk, R. L., Gentner, D. R., Crawford, J. L., Philippe, G., Rose, J. K. C., ... Smart, C. D. (2021). Season-long characterization of high-cannabinoid hemp (*Cannabis sativa* L.) reveals variation in cannabinoid accumulation, flowering time, and disease resistance. *GCB Bioenergy*, 13, 546–561.
- Stetter, M. G., Zeitler, L., Steinhaus, A., Kroener, K., Biljecki, M., & Schmid, K. J. (2016). Crossing methods and cultivation conditions for rapid production of segregating

- populations in three grain amaranth species. *Frontiers in Plant Science*, 7, 816. <https://doi.org/10.3389/fpls.2016.00816>
- Stout, J. M., Boubakir, Z., Ambrose, S. J., Purves, R. W., & Page, J. E. (2012). The hexanoyl-CoA precursor for cannabinoid biosynthesis is formed by an acyl-activating enzyme in *Cannabis sativa* trichomes. *The Plant Journal*, 71(3), 353–365. <https://doi.org/10.1111/j.1365-313X.2012.04949.x>
- Taku, M., Saini, M., Kumar, R., Debbarma, P., Rathod, N. K. K., Onteddu, R., et al. (2024). Modified speed breeding approach reduced breeding cycle to less than half in vegetable soybean (*Glycine max* (L.) Merr.). *Physiology and Molecular Biology of Plants*, 30, 1463–1473. <https://doi.org/10.1007/s12298-024-01503-z>
- Taku, M., Saini, M., Kumar, R., Rathod, N. K. K., Reshma, O., Yadav, M., et al. (2025). Rapid development of lipoxygenase-2 free vegetable soybean genotypes (*Glycine max* (L.) Merrill) through molecular breeding under controlled environment. *Plant Breeding*, 144, e13267. <https://doi.org/10.1111/pbr.13267>
- Tanaka, J., Hayashi, T., & Iwata, H. (2016). A practical, rapid generation-advancement system for rice breeding using simplified biotron breeding system. *Breeding Science*, 66, 542–551. <https://doi.org/10.1270/jsbbs.15038>
- Tilkat, E., Hoşer, A., Tilkat, E.A., & Süzerer, V. (2023). Production of industrial hemp: breeding strategies, limitations, economic expectations, and potential applications. *Türk Bilimsel Derlemeler Dergisi*.
- Torres, A. M., Main, D., & Crane, C. F. (2022). High-throughput methods to identify male *Cannabis sativa* using various genotyping methods. *Journal of Cannabis Research*, 4, 52. <https://doi.org/10.1186/s42238-022-00164-7>
- Toth, J. A., Stack, G. M., Cala, A. R., Carlson, C. H., Wilk, R. L., Crawford, J. L., Viands, D. R., Philippe, G., Smart, C. D., Rose, J. K. C., ... Gore, M. A. (2020). Development and validation of genetic markers for sex and cannabinoid chemotype in *Cannabis sativa* L. *GCB Bioenergy*, 12, 213–222. <https://doi.org/10.1111/gcbb.12667>
- Van Amsterdam, J., Brunt, T., & van den Brink, W. (2015). The adverse health effects of synthetic cannabinoids with emphasis on psychosis-like effects. *Journal of Psychopharmacology*, 29(3), 254–263. <https://doi.org/10.1177/0269881114565142>
- Van Bakel, H., Stout, J. M., Cote, A. G., Tallon, C. M., Sharpe, A. G., Hughes, T. R., & Page, J. E. (2011). The draft genome and transcriptome of *Cannabis sativa*. *Genome Biology*, 12(10), R102. <https://doi.org/10.1186/gb-2011-12-10-r102>

- Van Nocker, S., & Gardiner, S. E. (2014). Breeding better cultivars, faster: Applications of new technologies for the rapid deployment of superior horticultural tree crops. *Horticulture Research*, 1, 14022. <https://doi.org/10.1038/hortres.2014.22>
- Vélez, S., Martínez-Peña, R., & Castrillo, D. (2023). Beyond vegetation: A review unveiling additional insights into agriculture and forestry through the application of vegetation indices. *J*, 6(3), 421–436. <https://doi.org/10.3390/j6030028>
- Vikas, V. K., Sivasamy, M., Jayaprakash, P., Vinod, K. K., Geetha, M., Nisha, R., et al. (2021). Customized speed breeding as a potential tool to advance generation in wheat. *Indian Journal of Genetics and Plant Breeding*, 81, 199–207. <https://doi.org/10.31742/IJGPB.81.2.3>
- Volkow, N. D., Baler, R. D., Compton, W. M., & Weiss, S. R. (2014). Adverse health effects of marijuana use. *New England Journal of Medicine*, 370(23), 2219–2227. <https://doi.org/10.1056/NEJMra1402309>
- von Linné, C. (1753). *Species plantarum*.
- Wang, G., Sun, Z., Yang, J., Ma, Q., Wang, X., Ke, H., et al. (2025). The speed breeding technology of five generations per year in cotton. *Theoretical and Applied Genetics*, 138, 79. <https://doi.org/10.1007/s00122-025-04837-8>
- Wang, X., Singh, D., Marla, S., Morris, G., & Poland, J. (2018). Field-based high-throughput phenotyping of plant height in sorghum using different sensing technologies. *Plant Methods*, 14, 53. <https://doi.org/10.1186/s13007-018-0324-5>
- Wanga, M. A., Shimelis, H., Mashilo, J., & Laing, M. D. (2021). Opportunities and challenges of speed breeding: A review. *Plant Breeding*, 140, 185–194. <https://doi.org/10.1111/pbr.12909>
- Watson, A., Ghosh, S., Williams, M. J., Cuddy, W. S., Simmonds, J., Rey, M.-D., Hatta, M. A. M., Hinchliffe, A., Steed, A., Reynolds, D., ... Hickey, L. T. (2018). Speed breeding is a powerful tool to accelerate crop research and breeding. *Nature Plants*, 4, 23–29. <https://doi.org/10.1038/s41477-017-0083-8>
- Watson, A., Hickey, L. T., Christopher, J., Rutkoski, J., Poland, J., & Hayes, B. J. (2019). Multivariate genomic selection and potential of rapid indirect selection with speed breeding in spring wheat. *Crop Science*, 59, 1945–1959. <https://doi.org/10.2135/cropsci2018.12.0757>
- Watson, D. P., & Clarke, R. C. (1997, February). The genetic future of hemp. In *Nova Institute, Bioresource Hemp Symposium Proceedings*. Frankfurt am Main.

- Weiblen, G. D., Wenger, J. P., Craft, K. J., ElSohly, M. A., Mehmedic, Z., Treiber, E. L., & Marks, M. D. (2015). Gene duplication and divergence affecting drug content in *Cannabis sativa*. *New Phytologist*, 208(4), 1241–1250. <https://doi.org/10.1111/nph.13562>
- Weightman, R., & Kindred, D. (2005). *Review and analysis of breeding and regulation of hemp and flax varieties available for growing in the UK* (Project NF0530). Final report for DEFRA. ADAS Centre for Sustainable Crop Management.
- Wellensiek, S. J. (1962). Shortening the breeding cycle. *Euphytica*, 11, 5–10. <https://doi.org/10.1007/BF00044798>
- Wenger, J.P., Dabney, C.J., ElSohly, M.A., et al. (2020). Validating a predictive model of cannabinoid inheritance. *American Journal of Botany*, 107(6), 942–951. <https://doi.org/10.1002/ajb2.1550>
- Woods, P., Campbell, B. J., Nicodemus, T. J., Cahoon, E. B., Mullen, J. L., & McKay, J. K. (2021). Quantitative trait loci controlling agronomic and biochemical traits in *Cannabis sativa*. *Genetics*, 219, iyab099. <https://doi.org/10.1093/genetics/iyab099>
- Wright, M. J., Jr., Vandewater, S. A., & Taffe, M. A. (2013). Cannabidiol attenuates deficits of visuospatial associative memory induced by Δ^9 -tetrahydrocannabinol. *British Journal of Pharmacology*, 170(7), 1365–1373. <https://doi.org/10.1111/bph.12199>
- Yao, Y., Zhang, P., Liu, H., Lu, Z., & Yan, G. (2017). A fully in vitro protocol towards large-scale production of recombinant inbred lines in wheat (*Triticum aestivum* L.). *Plant Cell, Tissue and Organ Culture*, 128, 655–661. <https://doi.org/10.1007/s11240-016-1145-8>
- Yoon, H. I., Lee, S. H., Ryu, D., Choi, H., Park, S. H., Jung, J. H., Kim, H.-Y., & Yang, J.-S. (2024). Non-destructive assessment of cannabis quality during drying process using hyperspectral imaging and machine learning. *Frontiers in Plant Science*, 15, 1365298. <https://doi.org/10.3389/fpls.2024.1365298>
- Zakieh, M., Gaikpa, D. S., Leiva Sandoval, F., Alamrani, M., Henriksson, T., Odilbekov, F., et al. (2021). Characterizing winter wheat germplasm for *Fusarium* head blight resistance under accelerated growth conditions. *Frontiers in Plant Science*, 12. <https://doi.org/10.3389/fpls.2021.705006>
- Zhang, S., Liu, Y., Du, M., Shou, G., Wang, Z., & Xu, G. (2022). Nitrogen as a regulator for flowering time in plants. *Plant and Soil*, 480, 1–29. <https://doi.org/10.1007/s11104-022-05608-w>

- Zhang, X., et al. (2021). Establishment of an Agrobacterium-mediated genetic transformation system for *Cannabis sativa* L. *Plant Biotechnology Journal*, 19, 1978–1980. <https://doi.org/10.1111/pbi.13605>
- Zheljazkov, V.D., Visković, J., Sikora, V., Noller, J. (2023). Industrial Hemp Agronomy and Utilization: A Review. *Agronomy*, 13(3), 931. <https://www.mdpi.com/2073-4395/13/3/931>
- Zheng, Z., Gao, S., Wang, H., & Liu, C. (2023). Shortening generation times for winter cereals by vernalizing seedlings from young embryos at 10 °C. *Plant Breeding*, 142, 202–210. <https://doi.org/10.1111/pbr.13074>